AD_____

Award Number: W81XWH-08-1-0398

TITLE: Coordination of BRCA1/BARD1 - and MRE11/RAD50/NBS1 - Dependent DNA Transactions in Breast Tumor Suppression

PRINCIPAL INVESTIGATOR: Jean Gautier, Ph.D.

CONTRACTING ORGANIZATION: Columbia University
New York, NY 10032

REPORT DATE: July 2011

TYPE OF REPORT: Final

PREPARED FOR: U.S. Army Medical Research and Materiel Command
Fort Detrick, Maryland 21702-5012

REPORT DOCUMENTATION PAGE

Form Approved
OMB No. 0704-0188

1. REPORT DATE *(DD-MM-YYYY)*	2. REPORT TYPE	3. DATES COVERED *(From - To)*
01-07-2011	Final	1 JUL 2008 - 30 JUN 2011

4. TITLE AND SUBTITLE

Coordination of BRCA1/BARD1 - and MRE11/RAD50/NBS1 - Dependent DNA Transactions in Breast Tumor Suppression

5a. CONTRACT NUMBER

5b. GRANT NUMBER
W81XWH-08-1-0398

5c. PROGRAM ELEMENT NUMBER

6. AUTHOR(S)

Jean Gautier, Ph.D.

E-Mail: jg130@columbia.edu

5d. PROJECT NUMBER

5e. TASK NUMBER

5f. WORK UNIT NUMBER

7. PERFORMING ORGANIZATION NAME(S) AND ADDRESS(ES)

Columbia University
New York, NY 10032

8. PERFORMING ORGANIZATION REPORT NUMBER

9. SPONSORING / MONITORING AGENCY NAME(S) AND ADDRESS(ES)

U.S. Army Medical Research and Materiel Command
Fort Detrick, Maryland 21702-5012

10. SPONSOR/MONITOR'S ACRONYM(S)

11. SPONSOR/MONITOR'S REPORT NUMBER(S)

12. DISTRIBUTION / AVAILABILITY STATEMENT

Approved for Public Release; Distribution Unlimited

13. SUPPLEMENTARY NOTES

14. ABSTRACT

The main objective of the proposal is to understand how the Mre11-Rad50-Nbs1 complex and the BRCA1-BARD1 complex interact on DNA and coordinate DNA transactions that are critical for the maintenance of genomic stability and to prevent breast tumor development. We have characterized the behavior of BRCA1/BARD1 on DNA, using a single molecule approach. We have developed new single molecule technologies to study the behavior of BRCA1/BARD1 and MRN complexes. Finally, we have established that MRN-BRAC1/BARD1 interactions are dispensable for MRN/CtIP dependent DNA end resection, the first step of homology-dependent repair of DNA double-strand breaks.

15. SUBJECT TERMS

No subject terms provided.

16. SECURITY CLASSIFICATION OF:			17. LIMITATION OF ABSTRACT	18. NUMBER OF PAGES	19a. NAME OF RESPONSIBLE PERSON
a. REPORT	b. ABSTRACT	c. THIS PAGE			USAMRMC
U	U	U	UU	56	19b. TELEPHONE NUMBER *(include area code)*

Table of Contents

INTRODUCTION

BRCA1/BARD1 and MRE11/RAD50/NBS1 (MRN) play critical roles in preventing the onset of breast tumorigenesis. This is underscored by the fact that mutations in BRCA1 are associated with the most frequent form of hereditary breast cancer (*1*) and women who inherit mutations in the *BRCA1* gene have an estimated lifetime risk of breast and/or ovarian carcinoma as high as 85% (*2*). In addition, mutations in NBS1, RAD50 and Mre11 are associated with increased risk for breast cancer (*3, 4*) or with sporadic breast tumors (*5*). Finally, BRCA1/BARD1 and MRN associate in to form DNA damage-specific complexes, critical for damage checkpoint signaling (*6*). To better understand the functional significances of these interactions, we propose to determine how BRCA1/BARD1 and the MRN complex cooperate in the recognition, signaling and repair of DNA damage during DNA replication and at double-stranded breaks (DSBs) induced by DNA damaging agents. We hypothesize that each protein complex influences the behavior of the other on DNA and that the roles of these proteins in the maintenance of genomic stability are ultimately dictated by their dynamic interactions on DNA. The overall objective of this collaborative effort is to understand precisely how BRCA1/BARD1 breast tumor suppressor complex orchestrates DNA transactions critical for genome stability and how this process interfaces with MRN's diverse roles.

BODY

Significant progress has been made towards Task 1 and Task 2, as outlined in the Statement of Work. This progress was described in the 2009 report. However, the project could not be completed as it was originally anticipated. The project involved the use of highly purified recombinant protein complexes (MRE11-RAD50-NBS1 and BRCA1-BARD1). These complexes are purified by chromatography following expression in baculovirus-infected cells. Our FPLC (to perform chromatography) apparatus broke in the fall of 2009. We made several attempts to fix it but we had to replace it eventually. This has slowed down our progress. Dr. Gautier was able to secure the necessary funds to replace this critical piece of equipment (AKTA purifier 10, $60,000) late in 2010. Accordingly, we had requested a one-year No-Cost Extension for this proposal, which has been granted by the DOD.

In the First Task we proposed to start characterizing BRCA1/BARD1 interactions with DNA by Total Internal Reflection Fluorescent Microscopy (TIRFM).

We have previously reported (2009) our progress in purifying BRCA1/BARD1 protein complexes from baculovirus-infected cells. We purified enough protein complexes to perform the single molecule analysis proposed before our FPLC needed replacement.

We have completed initial characterization of quantum dot(QD)-tagged Brac1/Bard1 interactions with dsDNA using our single molecule DNA curtain imaging technology. We have shown that the QD tagged protein complexes work in our single molecule assays, that the labeling is specific, and that the labeled proteins are well-behaved in our single molecule assays. We have also demonstrated that BRCA1/BARD1 binds double stranded DNA at apparently random locations, and that the protein appears to undergo one-dimensional (1D) diffusion along the DNA in a direction that is biased by buffer flow (see below) before finally stopping at a fixed location (unpublished). We do not yet know the significance of the 1D sliding behavior nor do we know what DNA features influence the binding distributions, but it seems reasonable to expect that these properties reflect mechanistic attributes of BRCA1/BARD1 as it searches for appropriate binding targets. We have also continued to characterize quantum dot(QD)-tagged QD-tagged MRN interactions with dsDNA using our single molecule DNA curtain imaging technology. We have shown that the QD labeling strategy works for this protein complex in our single molecule assays and that the labeling is specific. We have also shown that MRN also slides rapidly along DNA, and that it can bring together two molecules of DNA. This MRN-mediated reaction appears to occur by a zippering mechanism where the molecules first join at

their free end, and then are brought together over regions spanning at 20-30 kilobases (unpublished).

Furthermore, we have also perfected our new approach to making DNA curtains using nanofabricated barriers to lipid diffusion that are now made by electron-beam lithography.(*7*) This process now allows to make highly precise barriers for aligning thousands of molecules of DNA, and we can align them in a variety of configurations, including molecules with defined lateral dispersion,(*8*) molecules anchored by either end (referred to as double-tethered DNA curtains),(*9, 10*) and molecules organized into crisscrossing patterns (unpublished). The double-tethered curtains will be especially relevant to our studies of BRCA1/BARD1 and MRN, as initial characterization of these protein complexes has revealed 1D diffusive motion that is biased in one direction by buffer flow. Continuous buffer flow is an absolute requirement for all of our previous DNA curtain configurations, but our new double-tethered curtains eliminate the need for continuous buffer flow, which will now allow us to probe the exact mechanisms by which BCRA1/BARD1 and MRN travel along DNA.

Finally, in addition to the new DNA Curtain methods, we have established procedures for looking at DNA substrates bound by nucleosomes,(*10, 11*) and for making new dsDNA substrates that have long ssDNA overhangs resembling a processed DSB. These new procedures will be especially poignant for our work on BRCA1/BARD1 and MRN, as we can now study the proteins within the context of DNA substrates engineered to resemble naturally occurring DSBs within the context of chromain.

In the Second Task, we proposed to investigate the interactions between BRCA1/BARD1 and MRN complexes. Analysis by TIRFM and in cell-free extracts.

Progress towards the completion of second task have been impaired by our inability to generate highly purified MRN complexes required for the single molecule studies (see above). Therefore, we have focused our effort on the characterization of the MRN-CtIP interactions with BRCA1/BARD1 in cell-free extracts derived from Xenopus eggs, using the system described in the 2009 report and briefly summarized below.

To better understand the interactions between BRCA1/BARD1 and the MRN complex under physiological conditions, we have designed a system to generate DSBs double-strand breaks in a chromosomal context and to monitor recruitment of signaling and repair proteins at these chromosomal DSBs. To this end, we incubate demembranated sperm nuclei in cell-free extracts derived from *Xenopus* eggs in the presence of PflMI restriction enzyme (0.05 U/µL).

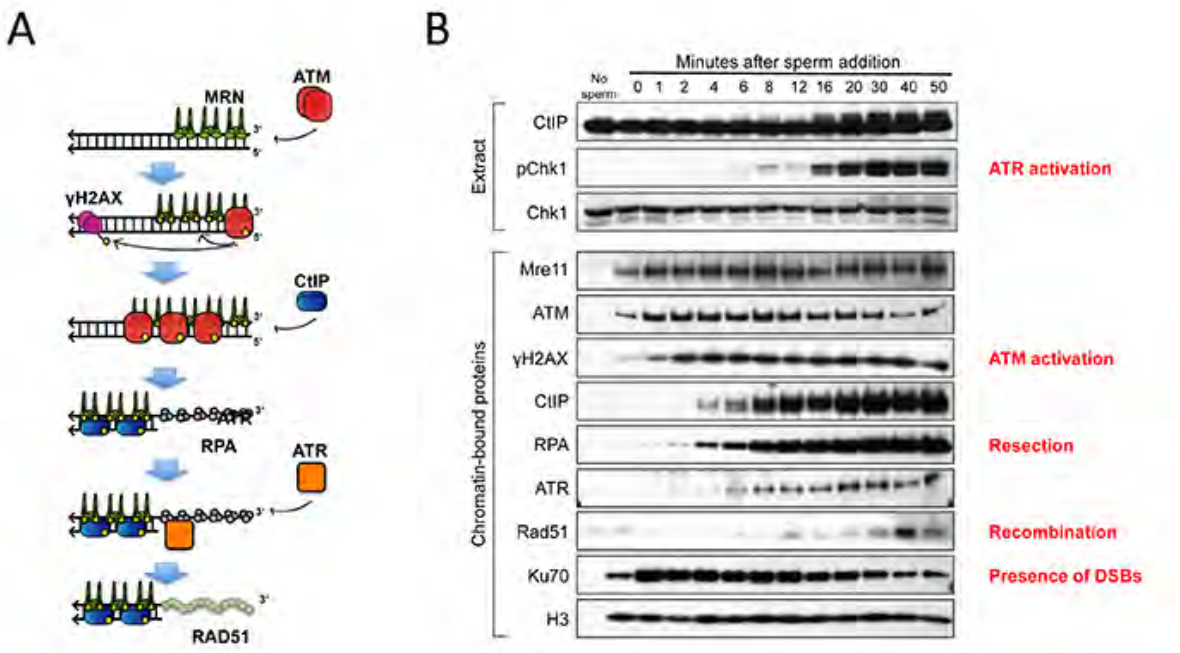

Figure 1: Recruitment of proteins to DSB-containing chromatin:

A: Schematic ordered model of the events occurring at a DSB during HDR.

B: Kinetics of recruitment of DSB-repair proteins. A S-phase extract was pre-incubated with sperm chromatin (5,000 sperm/µL). Aliquots of the sample were taken prior to (0 min) and at the indicated time (minutes) after addition of PflMI restriction endonuclease (0.05 U/ µL). At each time point, 0.5 µL of the sample was removed and processed for Western blotting (extract), and 15 µL of the sample was removed and processed for chromatin-isolation followed by Western blotting with the indicated antibodies ("chromatin-bound proteins"). Biochemical processes at the DSBs are indicated in red.

Following enzyme addition, aliquots of the reaction are diluted and centrifuged through a sucrose cushion. Chromatin pellets are then isolated free of cytosol and processed for electrophoresis and Western blotting (*12*). In contrast to other approaches, this method allows us to monitor the behavior of endogenous, untagged proteins in the absence of cross-linking treatment. We observed that Mre11 was constitutively associated with chromatin but was further recruited and modified upon generation of chromosomal DSBs (Figure 1). Next, ATM was recruited to chromatin and simultaneously activated, as seen by the appearance of γH2AX. CtIP was recruited with slower kinetics than ATM, followed by binding of the ssDNA-binding protein RPA, a read-out of DNA end resection. We found that ATM binding to chromatin peaked early then decreased with time but was never entirely abrogated. Release of ATM from chromatin correlated with RPA (*13*) recruitment on newly resected DNA, consistent with the idea that ATR activation by ssDNA-RPA intermediates participates in ATM down-regulation (*14*). Similar patterns of sequential chromatin recruitment were seen in S-phase and in M-phase (*12*). These

results are consistent with data in yeast and mammalian cells using GFP-tagged proteins or chromatin immunoprecipitation to analyze sequential recruitment of proteins to DSBs *(15-19)*. The experimental system takes advantage of the ability to monitor synchronously the loading of signaling and repair proteins at DNA double-strand breaks (DSBs), including the MRN complex, ATM, CtIP, BRCA1 and RPA, the latter being used as a marker for processing of DSBs. The first event in DSB repair is the generation of single strand DNA (ssDNA). First, we assessed the role of Mre11-Rad50-Nbs1 complex (MRN) in resection using this new assay. We find that depletion of the MRN complex completely abrogates DNA end resection in M-phase extract (Figure 2, middle panel). Moreover, we show that CtiP depletion likewise abrogates resection in M-phase (Figure 2, right panel).

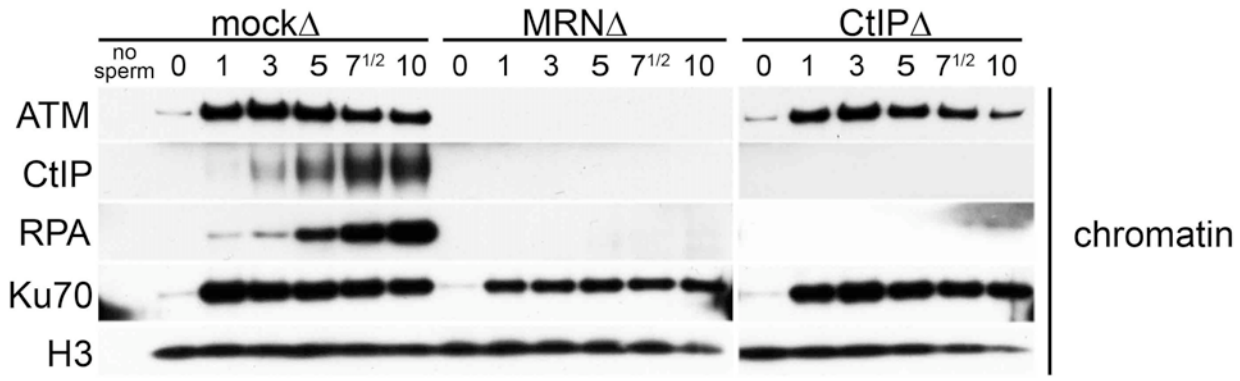

Figure 2. MRN and CtIP are absolutely required for DNA end resection in M-phase.
Kinetics of recruitment of proteins to DSB-containing chromatin in in Mock-depleted, Mre11-depleted, and CtIP-depleted M-phase extracts. M-phase extract (meiotic, CSF-arrested) was pre-incubated with sperm chromatin (5,000 sperm/µL). Aliquots of the sample (15 µL) were taken prior to (0 min) and at the indicated time (minutes) after addition of PflMI restriction endonuclease (0.05 U/ µL) and processed for chromatin-isolation followed by Western blotting with the indicated antibodies. Ku70 is a marker of DSBs generation following restriction digest. RPA is a ssDNA binding protein and is a marker for DNA end resection. Histone H3 (H3) is used as loading control.

It has been proposed that BRCA1 played a critical role in this early step of DSB repair (*20*). However, this point has been controversial and different results have been reported (*21, 22*). Using this cell-free system, we started to evaluate the potential role of BRCA1 in DNA end resection, as seen by the accumulation of RPA on chromatin. To test the role of BRCA1 in this system, we generated antibodies against xBRCA1 and depleted BRCA1 from our extracts. We observed that BRCA1 depletion co-depleted CtIP. In contrast, CtIP depletion did not significantly decrease in BRCA1 levels, we therefore hypothesized that CtIP co-depletion might be due to non-specific association with immuno-complexes. Therefore, to evaluate the impact of BRCA1

loss on DNA resection, we supplemented BRCA1-depleted extracts with recombinant xCtIP protein. We found that BRCA1 depletion did not affect CtIP recruitment to damaged chromatin or DNA resection in S-phase or in M-phase. We conclude that BRCA1 is dispensable for MRN-dependent DNA end resection at a nuclease-generated DSB.

Our work shows unambiguously that MRN/CtIP is required for this first step of DNA resection together with CtIP (Figure 2 and (*12*)). CtIP is one of the few bona fide BRCA1-interacting protein with BACH1 and Abraxas. Phosphorylated CtIP interacts specifically with the BRCT tandem repeat of BRCA1 (*13*). CtIP-BRCA1 interactions have been proposed to be required for DNA resection in mammalian cells (*23*). In contrast, loss of CtIP-BRCA1interaction in chicken DT40 cells did not inhibit resection. Mutation of the phosphorylated serine to a non-phosphorylatable alanine, abrogates BRCA1-CtIP interaction in both chicken and mammalian cells. To evaluate the impact of BRCA1-CtIP interactions on CtIP-dependent resection, we generated and purified a non-phosphorylatable version of Xenopus CtIP (xCtIP-S328A). First, we established that substitution of S328 to a non-phosphorylatable alanine abrogated BRCA1-CtIP interactions (*12*). We then monitored resection in cell-free extracts depleted from endogenous xCtIP and supplemented with either wild type or mutant recombinant xCtIP.

Figure 3. BRCA1-CtIP/MRN interactions are dispensable for MRN-dependent DNA end resection. Sperm chromatin was incubated in S-phase extract that was mock-depleted, CtIP-depleted, or CtIP-depleted supplemented with 75 nM wildtype or S328A xCtIP, and was treated with buffer (-) or PflMI (+) for 30 minutes. Samples were processed for chromatin-isolation and Western blotting as indicated. A. Control extract

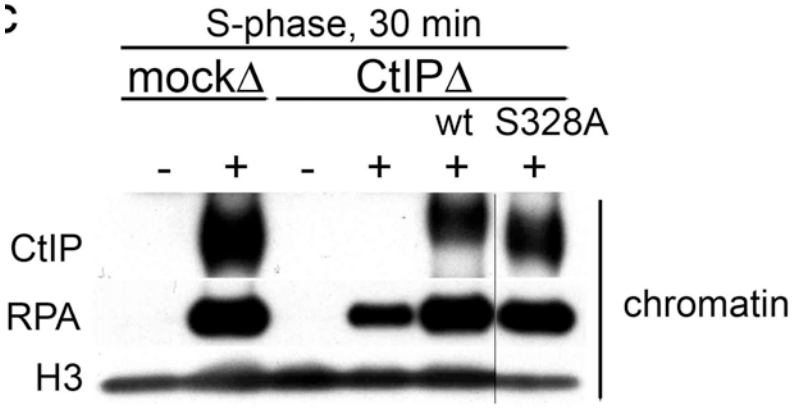

As anticipated, depletion of CtIP from M-phase extracts abolished resection as seen by the lack of RPA bond to chromatin (Figure 3). Addition of wild type recombiannt xCtIP protein restored resection to control levels. Notably, addition of mutant CtIP (xCtIP-S328A) unable to bind to BRCA1 also restored CtIP-dependent resection to control levels (Figure 3). This established that BRCA1-CtIP interactions are not required for the initial step of DSB processing generated

by restriction endonucleases.

KEY RESEARCH ACCOMPLISHMENTS

- Characterized the behavior of BRAC1/BARD1 on DNA, using a single molecule approach.
- Developed new single molecule technologies to study the behavior of BRCA1/BARD1 and MRN complexes.
- Established that MRN-BRAC1/BARD1 interactions are dispensable for MRN/CtIP dependent DNA end resection, the first step of homology-dependent repair.

REPORTABLE OUTCOME

Most of the results presented in this report have been published:

- Visnapuu, M.; Greene, E. *Nat Struct Mol Biol* **2009,** 16, (10), 1056 - 62.
- Greene, E.; Wind, S.; Fazio, T.; Gorman, J.; Visnapuu, M. *Methods Enzymol* **2010,** 472, 293 - 315.
- Visnapuu, M.; Fazio, T.; Wind, S.; Greene, E. *Langmuir* **2008,** 24, (19), 11293 - 9.
- Gorman, J.; Fazio, T.; Wang, F.; Wind, S.; Greene, E. *Langmuir* **2010,** 26, (2), 1372 - 9.
- Symington L. and Gautier J. *Annual Review of Genetics*. **2011** In press.
- Peterson S., Li Y., Chait B., Baer R., Gottesman M. and Gautier J. *J. Cell Biol.* **2011** 194: 705-720.

The personnel involved in this research project:

- Dr. Jean Gautier
- Dr. Eric Greene
- Dr. Shaun Peterson
- Dr. Jason Gorman

CONCLUSION

Our experiments in cell-free extracts have allowed us to separate the functions of the BRCA1/BARD1 and MRN/CtIP complex in performing the DNA transactions that initiate double-strand breaks repair. Because both complexes have been associated with the development of breast tumors, we hypothesize that their common role in checkpoint signaling might be critical to prevent breast tumor development. Our finding that BRCA1 and BRCA1-CtIP interactions are not needed to initiate DSB repair was not anticipated. It might in part reflect the fact that our method for generating DNA double-strand breaks is restriction endonuclease. This is also the method of choice in yeast (HO endonuclase) and mammalian cells studies (I-SceI). It is therefore tempting to speculate that BRCA1/BARD1, which are unambiguously involved in DSB repair, might be dispensable in presence of simple restriction nuclease-generated DNA ends. In contrast, this complex might be required to process more complex DNA ends, which harbor damaged bases, modified ends of protein-DNA adducts.

REFERENCES

1. Hodgson, S. V., Morrison, P. J., and Irving, M. (2004) Breast cancer genetics: unsolved questions and open perspectives in an expanding clinical practice, *Am J Med Genet C Semin Med Genet 129*, 56-64.
2. King, M. C., Marks, J. H., and Mandell, J. B. (2003) Breast and ovarian cancer risks due to inherited mutations in BRCA1 and BRCA2, *Science 302*, 643-646.
3. Heikkinen, K., Rapakko, K., Karppinen, S. M., Erkko, H., Knuutila, S., Lundan, T., Mannermaa, A., Borresen-Dale, A. L., Borg, A., Barkardottir, R. B., Petrini, J., and Winqvist, R. (2006) RAD50 and NBS1 are breast cancer susceptibility genes associated with genomic instability, *Carcinogenesis 27*, 1593-1599.
4. Steffen, J., Nowakowska, D., Niwinska, A., Czapczak, D., Kluska, A., Piatkowska, M., Wisniewska, A., and Paszko, Z. (2006) Germline mutations 657del5 of the NBS1 gene contribute significantly to the incidence of breast cancer in Central Poland, *Int J Cancer 119*, 472-475.
5. Sjoblom, T., Jones, S., Wood, L. D., Parsons, D. W., Lin, J., Barber, T. D., Mandelker, D., Leary, R. J., Ptak, J., Silliman, N., Szabo, S., Buckhaults, P., Farrell, C., Meeh, P., Markowitz, S. D., Willis, J., Dawson, D., Willson, J. K., Gazdar, A. F., Hartigan, J., Wu, L., Liu, C., Parmigiani, G., Park, B. H., Bachman, K. E., Papadopoulos, N., Vogelstein, B., Kinzler, K. W., and Velculescu, V. E. (2006) The consensus coding sequences of human breast and colorectal cancers, *Science 314*, 268-274.
6. Greenberg, R. A., Sobhian, B., Pathania, S., Cantor, S. B., Nakatani, Y., and Livingston, D. M. (2006) Multifactorial contributions to an acute DNA damage response by BRCA1/BARD1-containing complexes, *Genes Dev 20*, 34-46.
7. Greene, E., Wind, S., Fazio, T., Gorman, J., and Visnapuu, M. (2010) DNA curtains for high-throughput single-molecule optical imaging, *Methods Enzymol 472*, 293 - 315.
8. Visnapuu, M., Fazio, T., Wind, S., and Greene, E. (2008) Parallel arrays of geometric nanowells for assembling curtains of DNA with controlled lateral dispersion, *Langmuir 24*, 11293 - 11299.
9. Gorman, J., Fazio, T., Wang, F., Wind, S., and Greene, E. (2010) Nanofabricated racks of aligned and anchored DNA substrates for single-molecule imaging, *Langmuir 26*, 1372 - 1379.
10. Gorman, J., Plys, A., Visnapuu, M., Alani, E., and Greene, E. (2010) Visualizing one-dimensional diffusion of eukaryotic DNA repair factors along a chromatin lattice, *Nat Struct Mol Biol 17*, 932 - 938.
11. Visnapuu, M., and Greene, E. (2009) Single-molecule imaging of DNA curtains reveals intrinsic energy landscapes for nucleosome deposition, *Nat Struct Mol Biol 16*, 1056 - 1062.
12. Peterson, S. E., Li, Y., Chait, B. T., Gottesman, M. E., Baer, R., and Gautier, J. (2011) Cdk1 uncouples CtIP-dependent resection and Rad51 filament formation during M-phase double-strand break repair, *J Cell Biol 194*, 705-720.
13. Yu, X., Wu, L. C., Bowcock, A. M., Aronheim, A., and Baer, R. (1998) The C-terminal (BRCT) domains of BRCA1 interact in vivo with CtIP, a protein implicated in the CtBP pathway of transcriptional repression, *J Biol Chem 273*, 25388-25392.
14. Shiotani, B., and Zou, L. (2009) Single-stranded DNA orchestrates an ATM-to-ATR switch at DNA breaks, *Mol Cell 33*, 547-558.
15. Lisby, M., Barlow, J. H., Burgess, R. C., and Rothstein, R. (2004) Choreography of the DNA damage response: spatiotemporal relationships among checkpoint and repair proteins, *Cell 118*, 699-713.
16. Symington, L. S., and Gautier, J. (2011) Double-Strand Break End Resection and Repair Pathway Choice, *Annu Rev Genet*.

17. Bekker-Jensen, S., Lukas, C., Kitagawa, R., Melander, F., Kastan, M. B., Bartek, J., and Lukas, J. (2006) Spatial organization of the mammalian genome surveillance machinery in response to DNA strand breaks, *J Cell Biol 173*, 195-206.
18. Rodrigue, A., Lafrance, M., Gauthier, M. C., McDonald, D., Hendzel, M., West, S. C., Jasin, M., and Masson, J. Y. (2006) Interplay between human DNA repair proteins at a unique double-strand break in vivo, *EMBO J 25*, 222-231.
19. Berkovich, E., Monnat, R. J., Jr., and Kastan, M. B. (2008) Assessment of protein dynamics and DNA repair following generation of DNA double-strand breaks at defined genomic sites, *Nat Protoc 3*, 915-922.
20. Jasin, M. (2002) Homologous repair of DNA damage and tumorigenesis: the BRCA connection, *Oncogene 21*, 8981-8993.
21. Nakamura, K., Kogame, T., Oshiumi, H., Shinohara, A., Sumitomo, Y., Agama, K., Pommier, Y., Tsutsui, K. M., Tsutsui, K., Hartsuiker, E., Ogi, T., Takeda, S., and Taniguchi, Y. (2010) Collaborative action of Brca1 and CtIP in elimination of covalent modifications from double-strand breaks to facilitate subsequent break repair, *PLoS Genet 6*, e1000828.
22. Yun, M. H., and Hiom, K. (2009) CtIP-BRCA1 modulates the choice of DNA double-strand-break repair pathway throughout the cell cycle, *Nature 459*, 460-463.
23. Chen, L., Nievera, C. J., Lee, A. Y., and Wu, X. (2008) Cell cycle-dependent complex formation of BRCA1.CtIP.MRN is important for DNA double-strand break repair, *J Biol Chem 283*, 7713-7720.
24. Yu, X., Fu, S., Lai, M., Baer, R., and Chen, J. (2006) BRCA1 ubiquitinates its phosphorylation-dependent binding partner CtIP, *Genes Dev 20*, 1721-1726.

Review in Advance first posted online on September 9, 2011. (Changes may still occur before final publication online and in print.)

Double-Strand Break End Resection and Repair Pathway Choice

Lorraine S. Symington[1] and Jean Gautier[2]

[1]Department of Microbiology & Immunology, Columbia University Medical Center, New York, New York 10032; email: lss5@columbia.edu

[2]Department of Genetics & Development and Institute for Cancer Genetics, Columbia University Medical Center, New York, New York 10032; email: jg130@columbia.edu

Annu. Rev. Genet. 2011. 45:247–71

The *Annual Review of Genetics* is online at genet.annualreviews.org

This article's doi: 10.1146/annurev-genet-110410-132435

0066-4197/11/1201-0247$20.00

Keywords

homologous recombination, MRX/N, Sae2/CtIP/Ctp1, Ku, checkpoint, nonhomologous end joining

Abstract

DNA double-strand breaks (DSBs) are cytotoxic lesions that can result in mutagenic events or cell death if left unrepaired or repaired inappropriately. Cells use two major pathways for DSB repair: nonhomologous end joining (NHEJ) and homologous recombination (HR). The choice between these pathways depends on the phase of the cell cycle and the nature of the DSB ends. A critical determinant of repair pathway choice is the initiation of 5′-3′ resection of DNA ends, which commits cells to homology-dependent repair, and prevents repair by classical NHEJ. Here, we review the components of the end resection machinery, the role of end structure, and the cell-cycle phase on resection and the interplay of end processing with NHEJ.

INTRODUCTION

Double-strand break (DSB): DNA damage that results in both strands of DNA being broken

Nonhomologous end joining (NHEJ): a pathway to repair DSBs by direct ligation without the need for a homologous template

DNA double-strand breaks (DSBs) are one of the most cytotoxic forms of DNA damage, and their repair is critical for cell survival and the maintenance of genome integrity. DSBs can occur accidentally during normal cell metabolism and by exposure of cells to exogenous agents, such as ionizing radiation (IR) or some classes of chemotherapeutic drugs. In addition, DSBs are essential intermediates during programmed recombination events, such as meiosis, budding yeast mating-type interconversion, and lymphocyte development (120, 143). Classically, two pathways of DSB repair have been defined: nonhomologous end joining (NHEJ) and homologous recombination (HR). As their names imply, NHEJ involves direct ligation of the broken ends, whereas HR requires an undamaged homologous sequence to serve as a template for repair of both broken strands (**Figure 1**). Recently, a third modality of repair, microhomology-mediated end joining (MMEJ), has come to be appreciated. MMEJ utilizes annealing of short homologous sequences (microhomologies) revealed by the end-resection machinery to align ends

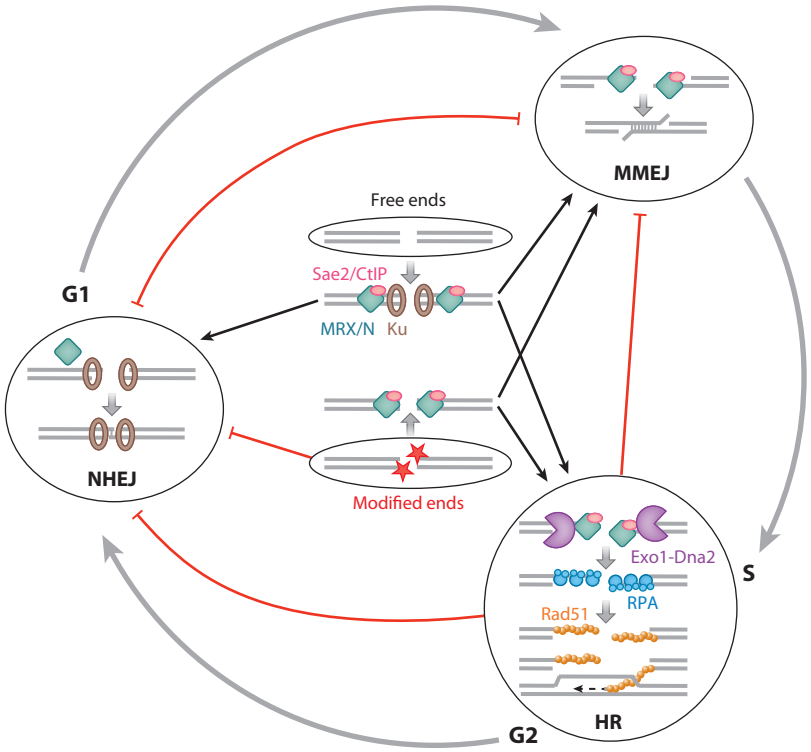

Figure 1

Regulation of repair pathway choice. The three major modes of DSB repair are outlined. Chemically modified or damaged ends (*stars*) cannot be repaired by nonhomologous end joining (NHEJ) and require processing (137), whereas free ends can be processed by any pathway. Once initiated, NHEJ inhibits end processing via Ku and prevents microhomology-mediated end joining (MMEJ) or homologous recombination (HR). Conversely, MRN/X-Sae2/CtIP-dependent resection displaces Ku and inhibits NHEJ. Extensive resection results in Rad51 filament formation and inhibition of MMEJ. NHEJ is used primarily in the G1 phase of the cell cycle, and HR is used primarily in the S and G2 phases, following replication of the genome. MMEJ is active throughout the cell cycle. Negative interactions are shown by red lines, positive interactions by black arrows, and cell cycle transitions by grey arrows.

prior to ligation. The choice among these pathways depends on the structure of the DNA ends and the phase of the cell cycle.

NHEJ represents the simplest mechanism to heal DSBs and restore chromosome integrity (39, 83). The Ku70 and Ku80 proteins form a heterodimer (hereafter referred to as Ku) with high affinity for DNA ends (44). Binding of Ku to ends protects them from degradation and is required for the recruitment of DNA ligase IV (encoded by *DNL4* in yeast) and the ligase accessory proteins Lif1/Xrcc4 and Nej1/Xlf (168, 179).

The budding yeast *Saccharomyces cerevisiae* does not have an end processing nuclease among its NHEJ proteins, so NHEJ only works efficiently and with high fidelity in repair of DSBs with compatible ends, such as those generated by restriction endonucleases, and is a minor pathway for repair of IR-induced damage (21, 102). If the ends are incompatible or lack 3′-hydroxyl or 5′-phosphate groups, then processing is required, and this can result in mutagenic deletions or insertions at the break site (39, 83).

All mechanisms of homology-dependent and microhomology-mediated DSB repair initiate by nucleolytic degradation of the 5′ strands to yield 3′ single-stranded DNA (ssDNA) tails, a process referred to as 5′-3′ resection (120). Replication protein A (RPA) binds to the ssDNA thus exposed and is then displaced by Rad51 to form a nucleoprotein filament that catalyzes homologous pairing and strand invasion (70). Details of the downstream events following Rad51-dependent strand invasion can be found in recent reviews (98, 132). RPA-bound ssDNA also activates the ATR (ATM and Rad3-related kinase)/Mec1/Rad3 DNA damage checkpoint (187). Thus, resection is an essential step for HR and the ATR-mediated checkpoint response to DSBs.

In *S. cerevisiae*, end resection is initiated by the conserved Mre11-Rad50-Xrs2/Nbs1 (MRX/N) complex, which together with Sae2/CtIP/Ctp1 can remove oligonucleotides from the 5′ strand, resulting in limited end processing (103, 184). In addition, the MRX complex is required to recruit Dna2, Exo1, and Sgs1 to the break site (138). More extensive resection is carried out by the 5′-3′ exonuclease, Exo1, or by the combined activities of the Sgs1-Top3-Rmi1 complex (hereafter referred to as STR) and Dna2 (104). In the absence of MRX-Sae2, Exo1, and Sgs1, no processing of DNA ends is detected, and this results in a complete block to homology-directed repair (103, 184).

The initiation of resection is a critical determinant for repair pathway choice (60, 181). Once resection has initiated, the DNA ends become poor substrates for binding by Ku and cells are committed to HR (**Figure 1**). Not surprisingly, resection is regulated during the cell cycle to ensure commitment to HR is coordinated with DNA replication, and occurs primarily in S and G2 phases of cell cycle when a sister chromatid is available as a repair template (6, 9, 60, 63).

Here, we review the components of the end resection machinery, the role of resection in DNA damage signaling, how the structure of DNA ends influences resection, and the regulation of these activities during the cell cycle. This review focuses on the budding yeast *S. cerevisiae* because the molecular details of resection are best understood in this system, with reference to other organisms where appropriate.

INITIATION OF END RESECTION BY THE MRX/N COMPLEX AND SAE2/CTIP/CTP1

Structural and Biochemical Properties of the MRX/N Complex and Sae2/CtIP/Ctp1

The *MRE11*, *RAD50*, and *XRS2* genes were originally identified by their requirement for the repair of IR-induced DNA damage and for meiotic recombination in *S. cerevisiae* (70). Mre11 and Rad50 are conserved in prokaryotes, archeae, and eukaryotes, whereas Xrs2/Nbs1 is found only in eukaryotes and functions to signal DSBs via the PI3K-like kinase (PIKK), Tel1/ATM (ataxia telangiectasia mutated) (136, 147). The three proteins interact to form a heterohexameric DNA binding complex,

Homologous recombination (HR): a DNA repair mechanism that relies on a homologous sequence as the template for repair

Microhomology-mediated end joining (MMEJ): repair of DSBs by end resection to expose short sequence homologies used to anneal the two ends prior to ligation

Ku: Ku70-Ku80 heterodimer

RPA: replication protein A

ATR: ATM and Rad3-related kinase

Checkpoint: a signal transduction pathway that coordinately regulates DNA repair, cell-cycle progression, and cell death following DNA damage

End resection: 5′-3′ nucleolytic degradation of DSB ends

MRX/N: Mre11-Rad50-Xrs2/Nbs1 complex

STR: Sgs1-Top3-Rmi1 complex

PIKK: PI3K-like kinase

ATM: ataxia telangiectasia mutated

containing dimers of each subunit (158, 163). The MRX/N complex has several functions in chromosome break metabolism; it is a sensor of DSBs, tethers DNA ends, promotes NHEJ repair, controls 5′-3′ resection and is required for telomere maintenance (147). Loss of these functions is tolerated by yeast, but all three genes are essential for cell proliferation in vertebrates (147).

Mre11 belongs to the lambda phosphatase family of phosphoesterases and exhibits manganese-dependent nuclease activities in vitro, including 3′-5′ dsDNA exonuclease activity and an ssDNA endonuclease activity that acts on ssDNA/double-stranded DNA (dsDNA) transitions and hairpin loops (121, 152). Conserved residues within the phosphoesterase motifs, for example, Asp 16, Asp 56, His 125 and His 213 of ScMre11, are required for endo- and exonuclease activities in vitro (24, 51, 106, 157, 166). His 52 of *Pyrococcus furiosus* Mre11 [equivalent to ScMre11 His 59 and *Schizosaccharomyces pombe* (Sp) Mre11 His 68] is required for the 3′-5′ exonuclease, but not the endonuclease activity, and is the only mutation characterized to date that separates the nuclease activities (166). Both Rad50 and Xrs2/Nbs1 enhance the nuclease activity of Mre11 in vitro (121, 122, 152). The C-terminal region of Mre11 has two DNA binding sites, the most C-terminal of which is required for meiotic DSB formation is *S. cerevisiae*, and a Rad50 interaction site (51, 157, 164).

The 153 kDa ScRad50 protein belongs to the structural maintenance of chromosomes (SMC) family of proteins characterized by coiled-coil domains formed by intramolecular folding to bring the N-terminal Walker A and the C-terminal Walker B ATPase motifs in close proximity (4, 40, 57). To date, however, there is no evidence that MRX/N assembles into ring-like structures around DNA as SMC complexes do. Rad50 exhibits ATPase activity in vitro, which is required for DNA repair and meiosis (3, 57). The *rad50S* alleles carry point mutations near the conserved ATPase motifs and are characterized by proficiency for mitotic DSBR, but are defective in processing Spo11-induced DSBs during meiosis (see below) (3). This phenotype is similar to *mre11* nuclease defective and *sae2*Δ mutants. The apex of the Rad50 coiled coil contains a conserved Cys-X-X-Cys motif that dimerizes with a second hook domain via cysteine-mediated zinc ion coordination (56). Crystallographic and scanning EM studies have shown hook-mediated dimerization between two MR complexes to tether DNA molecules (40). Dimerization of Rad50 is required for all functions of the Mre11 complex, suggesting tethering of DNA ends or sister chromatids is critical for repair (167). Mre11 binds to the base of the Rad50 coiled coils forming a head region comprised of the Mre11 nuclease and Rad50 ATPase domain that together provide DNA binding and end-processing activities (163). ATP binding by Rad50 induces a closed configuration of the Mre11-Rad50 head domain and inhibition of the Mre11 nuclease, whereas ATP hydrolysis results in a large conformational change to an open structure unmasking the Mre11 nuclease active site (73, 85, 164).

Xrs2/Nbs1 is the least conserved member of the MRX/N complex and is thought to act as a regulatory and protein recruitment module (147). Human Nbs1/Nibrin contains FHA (forkhead associated) and BRCT (BRCA1 C terminus) domains in the N-terminal region separated from the Mre11 and ATM DNA binding domains by a flexible tether (90, 165). The FHA domain of *S. pombe* Nbs1 interacts with phosphorylated Ctp1, and this is important to recruit Ctp1 to DSBs in vivo and for their subsequent repair (90, 165). Tethering of Ctp1/CtIP to the MRN complex could help restrict DNA resection to the proximity of DSBs, where MRN localizes. The BRCT domains of Nbs1 interact with the checkpoint adaptor MDC1, which in turn binds to phosphorylated H2AX, to amplify and/or maintain the DNA damage checkpoint (147).

Sae2 is even more divergent than Xrs2 and residues conserved with the apparent orthologs, SpCtp1 and HsCtIP, are restricted to the C-terminal region and a dimerization domain near the N-terminus (2, 86, 99, 124, 133). Sae2 forms

dimers or oligomers, and exhibits endonuclease activity in vitro at ssDNA/dsDNA transitions that is stimulated by the MRX complex and an adjacent DNA hairpin loop (79). No obvious nuclease domains are present in Sae2. Nuclease activity has not been reported for CtIP, but the CtIP-MRN complex exhibits more robust endonuclease activity than MRN alone (133). Although direct interaction between MRX and Sae2 has not been detected by immunoprecipitation, the proteins form a higher order complex on DNA (79).

Initiation of Resection

The requirement for MRX and Sae2 in end resection is highly dependent on the nature of the DNA ends (**Figure 2**). Here, we consider three types of DNA ends: those produced by restriction endonucleases, damage generated by IR, and DSBs with a protein covalently bound to the 5′ end. The ends produced by endonucleases have 3′ hydroxyl and a 5′ phosphate groups and are considered to be clean because they require no further processing to be ligated or extended by DNA polymerases. IR produces double- and single-strand breaks, base and sugar damage, and DNA-protein crosslinks (8, 54), thus, the ends are considered complex or dirty. Topoisomerases are transiently bound to the 5′ or 3′ ends of DNA during the catalytic cycle, and some chemotherapeutic agents, for example, camptothecin (CPT), extend the half

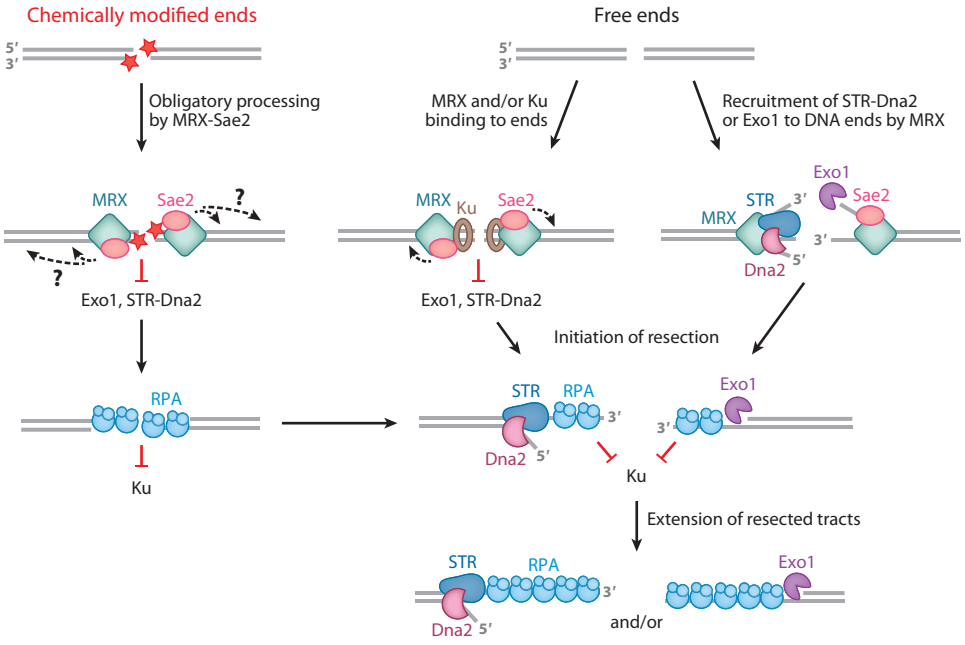

Figure 2

Model of how distinct pathways resect modified and free DNA ends. Endonucleolytic clipping of the ends (*shown as dashed black arrows*) by the MRX complex and Sae2 is mandatory to release covalent modifications, such as the tyrosyl-DNA bond formed by Spo11 (*left panel*). This processing could occur close to the end to remove a short oligonucleotide, or it could occur several hundred nucleotides from the end followed by bidirectional exonucleolytic processing. Partial resection inhibits Ku binding, enabling these intermediates to undergo extensive resection by either STR-Dna2 or Exo1. Free ends are bound by Ku and/or MRX/N; clipping by MRX/N and Sae2/CtIP removes Ku or creates substrates that are no longer bound by Ku, and can be further processed by Exo1 or STR-Dna2. Alternatively, MRX/N recruits Exo1 or STR-Dna2 to free ends to directly initiate resection directly, but this reaction is most efficient in the absence of Ku. Exo1 can also process ends independently of MRX in the absence of Ku (*not shown*).

life of the cleavage complex. Spo11, a member of the TopVI family, is required for the initiation of meiotic recombination and cleaves DNA by a topoisomerase-like transesterase mechanism forming a stable covalent linkage between both subunits of a Spo11 dimer and the 5′ ends of DNA (15, 67).

Resection of free DNA ends can occur in the absence of MRX and Sae2, but resection of modified ends depends on these factors. The nature of the modification determines the extent of dependence. The most extreme case is exemplified by ends bound to Spo11, which forms a covalent bond between a tyrosine on the enzyme and a 5'-phosphate in the DNA. Such ends are not processed in *sae2*Δ or *rad50S* mutants, or in the absence of the Mre11 endonuclease (3, 51, 99, 106, 124, 153, 157). In *S. pombe*, where MRN is not required for Spo11 to generate DSBs, *mre11*Δ/*rad32*Δ and *rad50*Δ mutants accumulate unprocessed meiotic DSBs (174). The requirement for MRX in meiotic DSB formation in budding yeast may be due to the larger number of DSBs, necessitating greater coordination between DSB formation and end processing.

Spo11 is released from DNA ends covalently coupled to an oligonucleotide of 12 to 34 nucleotides, consistent with the view that MRX and Sae2 incise the DNA at a short distance from the Spo11-bound end (53, 101, 113, 131). Release of Spo11-oligonucleotides could occur directly by endonucleolytic cleavage 12 to 34 nts from the ends, or result from Mre11 3′-5′ exonucleolytic degradation from a more distant MRX-Sae2 directed nick. In the absence of Exo1, the length of ssDNA tails is around 270 nt, suggesting multiple rounds of MRX-Sae2 cleavage from ends, or a single endonucleolytic event distant from the break, followed by bidirectional exonucleolytic processing (177). To date, no in vitro studies have shown MRX-Sae2 can nick dsDNA at a distance from a protein-bound end. However, short oligonucleotides are released from DNA ends at chromatin breaks in an MRN-dependent manner in Xenopus extracts, consistent with an endonucleolytic clipping mechanism (62).

The *mre11*Δ, *rad50*Δ, and *xrs2*Δ mutants show much higher sensitivity to IR than *sae2*Δ or *mre11* nuclease-defective mutants (24, 69, 105). However, the fission yeast *ctp1*Δ and *mre11-H134S* (nuclease defective) mutants exhibit similar IR sensitivity as the *mre11*Δ mutant (86, 166). The endonuclease activity of Mre11 appears to be the critical determinant of IR sensitivity in *S. pombe* because the exonuclease-defective *mre11-H68S* mutant is IR resistant (166). The IR sensitivity of *mre11*Δ and *rad50*Δ mutants can be suppressed by overexpression of Exo1, indicating that Exo1 is able to process IR-induced DSBs independently of MRX (80, 107, 154). Partial resistance to IR can be restored in the *mre11*Δ mutant by elimination of Ku, provided that Exo1 is present. This is consistent with the view that Ku is a barrier to Exo1-catalyzed resection (105, 150, 166). The IR resistance of the *mre11*Δ *yku70*Δ mutant is independent of Sgs1, suggesting that MRX is more important for recruitment of Sgs1-Dna2 to ends than it is for Exo1 (105).

Direct analysis of ssDNA intermediates resulting from resection of IR-induced breaks is not possible because these breaks occur at random locations and are not amenable to physical methods, such as restriction endonuclease and Southern blot analysis. However, localization of RPA to discrete subnuclear sites (foci) can be used as an indirect measure of resection (9, 88). The recruitment of RPA to IR-induced DSBs still occurs in the absence of MRX, suggesting that resection can be initiated by Exo1 or possibly STR-Dna2. Recently, a pulsed field gel electrophoresis method was developed to detect linearization and processing of a circular chromosome in IR-treated cells (162). The linearized chromosome was rapidly resected in wild-type cells, as well as *rad51*Δ and *rad52*Δ mutants, but there was a significant delay and reduction in the extent of end processing in a *rad50*Δ mutant. This delay was also seen for an HO (homothallic) endonuclease-induced DSB but was more pronounced for IR-induced DNA damage. The *sae2*Δ and *mre11-H125N* mutants have yet to be tested in this system.

DSBs generated by rare-cutting endonucleases (HO or *I-Sce*I) and their subsequent processing can be analyzed directly by physical methods. DSB ends are more stable in *mre11*Δ, *rad50*Δ, and *xrs2*Δ mutants than in wild-type cells, but approximately 80% are eventually processed (61, 103, 153, 184). In a *rad50*Δ mutant, there is a delay in initiation of resection, but once resection initiates, the rate is similar to that in wild-type cells, around 4 kb hr^{-1} (184). There is less of a delay in resection initiation in the *sae2*Δ or *tel1*Δ mutants compared with a *rad50*Δ mutant or a *mre11*Δ mutant, and no obvious defect in processing one, or even multiple, HO-induced DSBs in the *mre11-H125N* mutant (36, 89). Although these findings have led to some confusion over the role of the Sae2 and the Mre11 nucleases in resection, the initiation function is perhaps best understood in the context of how well the long-range resection mechanisms are able to access and process ends. The more severe defect conferred by loss of the MRX complex is most likely due to reduced recruitment of Sgs1, Dna2, and Exo1 to DSBs rather than a specific requirement for MRX to initiate resection at clean ends. In contrast, Sgs1 and Dna2 are still recruited in a *sae2*Δ mutant and in Mre11 nuclease defective mutants, and the synergistic defect in end processing and IR sensitivity observed for the *mre11-H125N sgs1*Δ and *mre11-H125N dna2* mutants could be interpreted as a bypass of the Mre11-Sae2 nuclease initiation function by Sgs1-Dna2 (25, 105, 138). These results suggest that initiation and extensive resection should not necessarily be considered as distinct phases, and there is likely to be cooperation between them (**Figure 2**). In the case of Spo11-induced DSBs, Exo1 and/or Sgs1-Dna2 cannot compensate for MRX and Sae2 in initiation of resection, presumably because the large 5′ adduct prevents binding and/or endonucleolytic clipping by Dna2 or Exo1.

Hairpin capped ends formed at DNA palindromes are inaccessible to the Dna2 and Exo1 nucleases, which both require a free end for degradation (7, 75); therefore, hairpin processing is also completely dependent on MRX-Sae2 (91, 129).

In wild-type *exo1*Δ or *sgs1*Δ cells, no intermediates of processing a single endonuclease-induced DSB are detected; but in an *exo1*Δ *sgs1*Δ double mutant, slow MRX-Sae2-dependent processing occurs by incremental removal of approximately 100 nt from the ends, resulting in discrete species with faster mobility than the cut fragments (103, 184). It is unclear whether this processing occurs in wild-type cells but is not detected because the resection tracts are rapidly extended by Exo1 or Sgs1-Dna2 or if MRX-Sae2 processing only occurs in the absence of the other mechanisms or when end-blocking adducts are present.

Direct measurement of ssDNA formed by resection of an endonuclease-induced DSB has primarily been reported for *S. cerevisiae*. Methods used in other systems include in vivo labeling genomic DNA with bromodeoxyuridine, which can be detected by indirect immunofluorescence when the DNA becomes single stranded, or by association of RPA or Rad51 close to HO- or IR-induced DSBs. In contrast to budding yeast, *S. pombe ctp1*Δ and *mre11-H134S* mutants show greatly reduced RPA binding to sequences adjacent to the HO cut site after DSB formation, comparable to the *mre11*Δ mutant (86, 166). Both CtIP and the Mre11 nuclease are essential for viability of mammalian cells, and their roles in end resection have been assessed using siRNA or conditional knockout mouse embryonic fibroblasts, respectively. Similar to *S. pombe*, CtIP and the Mre11 nuclease activity are required for RPA recruitment to IR or UV microirradiation–induced DNA damage in mammalian cells and for the recruitment of Rad51 to IR-induced damage in DT40 cells (26, 110, 133). It is possible that the downstream resection mechanisms are less able to access DNA ends in organisms other than *S. cerevisiae*. The IR and CPT sensitivity of *mre11*Δ, *ctp1*Δ, and *mre11-H134S* mutants is effectively suppressed by elimination of Ku and this suppression requires Exo1; thus, Ku might be more of a barrier to Exo1 resection in *S. pombe* than in

budding yeast (86, 150, 166). Furthermore, the role of Rqh1/Sgs1 and Dna2 in resection of IR- or endonuclease-induced DSBs has yet to be reported in *S. pombe*, and it is possible this pathway has a more limited role in end resection.

EXTENSIVE RESECTION BY EXO1 OR STR-DNA2

Exo1

Exo1 is a member of the Rad2/XPG family of nucleases that possesses 5′-3′ dsDNA specific exonuclease and 5′-flap endonuclease activities in vitro (151). Exo1 expression is induced during meiosis, suggesting a role in meiotic DSB resection (149). Studies in the *dmc1*Δ mutant, which exhibits hyper-resected meiotic DSBs, demonstrated decreased processing in the absence of Exo1 and indicated a minor role for Sgs1 in meiotic resection (95, 154). Several recent studies have addressed the roles of Exo1 and Sgs1 for processing meiotic DSBs under physiological conditions (strand invasion proficient cells) (55, 66, 177). In wild-type cells, resection tracts average 850 nt in length and are reduced to 270 nt in *exo1*Δ and nuclease-defective *exo1-D173A* mutant cells. Surprisingly, the length of ssDNA tracts in wild-type cells or the *exo1*Δ mutant is not altered by mutation of *SGS1*, indicating that the pathways that promote extensive resection are not redundant in meiosis (177). In both wild-type and *exo1*Δ mutant cells, the extent of resection is fairly constant at different times after DSB formation, suggesting that initial processing and Exo1-dependent resection are tightly coupled. This is consistent with in vitro studies showing stimulation of Exo1 activity by MRX-Sae2 (114, 115). As described above, the resection tracts formed in an *exo1*Δ mutant are due to the activity of MRX and Sae2 in Spo11 removal, indicating that the initial phase of resection removes substantially greater sequence than the few dozen nucleotides that can be recovered covalently bound to Spo11.

Initiation of resection at endonuclease-induced DSBs occurs normally in the *exo1*Δ mutant, but extensive processing is reduced (37, 89, 103, 184). Furthermore, Exo1 is required for normal levels of RPA recruitment following irradiation of mouse embryonic fibroblasts and human cells (19, 134). This subtle resection defect does not impair repair dependent upon gene conversion or survival in response to IR in budding yeast. Initiation and extensive resection are reduced in the *S. cerevisiae exo1*Δ *mre11*Δ double mutant compared with the *mre11*Δ single mutant, resulting in decreased resistance to IR and methyl methanesulfonate (MMS). In *S. pombe*, radiation-induced Rad51 foci are not detected in the *exo1*Δ *rad50*Δ double mutant, suggesting the single-strand tails are absent or very short (150). Although the IR resistance of the *sae2*Δ and *mre11-H125N* mutants is decreased by the *exo1*Δ mutation, the double mutants are considerably more resistant than the *mre11*Δ single mutant, presumably because MRX recruits Sgs1-Dna2 to initiate resection (105, 107). The residual resection of the *exo1*Δ *mre11*Δ mutant suggests there must be a low level of Sgs1-Dna2 recruitment independent of MRX. The importance of end resection for cell proliferation is highlighed by evidence that *exo1*Δ *mre11*Δ *sgs1*Δ, *exo1*Δ *mre11-H125N sgs1*Δ, and *exo1*Δ *sae*Δ *sgs1*Δ triple mutants are inviable (103).

Reconstitution of the Exo1 resection mechanism in vitro revealed a stimulation of both nuclease activities of Exo1 by MRX and Sae2 (114, 115). At high Exo1 concentration, the MRX-Sae2 stimulatory effect was lessened, consistent with genetic studies showing that Exo1 can process ends independently of MRX when overexpressed (77, 107, 114). MRX recruits Exo1 to DNA ends, but unlike Sgs1-Dna2 recruitment, no stable protein-protein interactions could be detected between MRX or Sae2 and Exo1 in solution. However, MRX, Sae2, and Exo1 formed complexes in the context of DNA, as evidenced by the cooperative binding to oligonucleotide substrates when all proteins were present (114). Therefore, MRX-Sae2 most likely enables recruitment of Exo1 to the DNA end by creating a specific DNA structure that allows higher affinity binding of Exo1. Prior incubation of a

linear DNA substrate with MRX-Sae2 resulted in more efficient resection by Exo1, suggesting that limited 5′ strand processing contributes to the enhancement of Exo1-mediated resection, but the reaction was most efficient with all components present at the same time (114).

HsMRN can increase the processivity of Exo1-mediated resection, indicating that stimulation of Exo1 by MRX/N is not restricted to the initiation step (115). In vivo, the recruitment of Exo1 to DSBs requires MRX, but the role of Sae2/CtIP appears to differ between organisms. Sae2 was reported to be dispensable for Exo1 recruitment in budding yeast, but in human cells CtIP is required and the two proteins directly interact (45, 138).

The STR-Dna2 Resection Mechanism

Sgs1 is a member of the highly conserved RecQ family of 3′-5′ DNA helicases that are required for genome integrity (16). Sgs1 physically interacts with the type I topoisomerase Top3, which in turn interacts with the oligonucleotide/oligosaccharide-binding (OB)-fold containing protein, Rmi1 (16). Conservation of these interactions indicates that Sgs1 is the ortholog of the human gene mutated in Bloom's syndrome (BLM). The STR complex (BLM-Top3α-RMI1-RMI2 in human) dissolves double Holliday junction intermediates in vitro and suppresses mitotic crossovers (16). The unanticipated role for Sgs1 in end resection was identified by its function in long-range resection (>10 kb from the DSB) and the functional redundancy with Exo1 (52, 103, 184). *sgs1*Δ, *top3*Δ, and *rmi1*Δ mutants display equivalent resection defects, but in contrast to dHJ dissolution, resection does not require the Top3 active site tyrosine, indicating that Top3-Rmi1 plays a structural rather than a catalytic role (117, 184). The ssDNA formed by Sgs1 unwinding is degraded by the bipolar endonuclease/helicase Dna2 (184). Resection is independent of the Dna2 helicase activity, indicating that Sgs1 is the helicase that unwinds from ends and Dna2 provides the nuclease activity (52, 103, 184).

Three recent studies reported that purified Sgs1/BLM, Dna2, and RPA constitute the minimal components of the STR/BTR-Dna2 resection mechanism (28, 115, 117). *Escherichia coli* single-stranded DNA binding protein (SSB) poorly substituted for RPA in stimulation of the Sgs1 helicase, suggesting that a species-specific interaction between the Sgs1 and RPA is required for efficient unwinding of linear dsDNA, in addition to sequestration of the unwound ssDNA by RPA. The role for RPA was further demonstrated in Xenopus cell-free extracts, where RPA is required to support WRN (the product of the gene mutated in Werner's syndrome)- and Dna2-dependent resection (171). Dna2 can degrade 3′ or 5′ flaps in vitro, raising the question of how strand discrimination occurs during resection. Interestingly, RPA was shown to stimulate the 5′ endonuclease activity of Dna2 on model Y-shaped substrates and to inhibit the 3′ flap endonuclease, thus targeting degradation to only the 5′ strand in vitro (28, 117). In contrast, RPA is not required for Exo1-catalyzed resection in vitro but has been shown to stimulate the HsExo1 nuclease (114, 115). Top3 and Rmi1 stimulate resection by recruiting Sgs1 to the substrate, but are not essential for resection (28, 117). Similarly, MRX is not required for resection by Sgs1-Dna2-RPA in vitro but interacts directly with Sgs1 and stimulates unwinding, particularly at low Sgs1 concentration (28, 30, 117). Use of dsDNA substrates with a 3′ overhang bypassed the requirement for MRX, suggesting that MRX creates a favorable substrate for Sgs1-Dna2, such as unwound or recessed 5′ ends (117).

Mammals have five RecQ proteins, raising the question as to which of these participates in end resection. Experiments with purified recombinant proteins showed that WRN, RecQ4, or RecQ5 could not substitute for BLM in the Dna2-catalyzed resection reaction (115). Furthermore, BLM is rapidly recruited to laser-induced chromatin damage in mammalian cells, and a defect in RPA recruitment in $Blm^{-/-}$ cells is observed in the absence of Exo1 (52, 64). However, resection of a linear dsDNA template is carried out by the WRN

helicase and Dna2 in Xenopus egg extracts (82). Although the Exo1 and Sgs1 resection pathways appear to be independent in budding yeast, BLM was shown to stimulate resection by human Exo1 by recruiting it to DNA ends via a direct protein interaction (115, 116).

What is the Purpose of Extensive Resection?

The rate of resection is estimated to be approximately 4 kb hr^{-1} in budding yeast, and resection can degrade thousands of nucleotides in the absence of a homologous donor or the Rad51 or Dmc1 recombinases (17, 148, 184). In HR-proficient cells, the resected ssDNA tracts vary in length depending on the availability and location of the homologous template and correlate with the kinetics of repair. In meiotic cells, the average length of ssDNA formed is 850 nt, whereas 2–4 kb ssDNA tails are formed during mitotic repair between chromosome homologs (32, 177). Resection tracts in cycling cells were measured following constitutive expression of HO, which cuts both sister chromatids, precluding repair by the favored sister chromatid template and forcing inefficient repair from the homolog or an ectopic sequence. This is likely to result in more extensive resection during the extended homology search phase of HR. The extent of resection during sister-chromatid recombination has yet to be determined. Long ssDNA tracts are required, however, to activate the DNA damage checkpoint and it has been suggested that extensive resection serves to ensure fidelity by preventing repair between short dispersed repeats (32, 52, 184).

In the absence of Exo1 and Sgs1-Dna2, the short 3′ ssDNA tails of around 100–700 nt resulting from MRX-Sae2 dependent cleavage can be utilized for Rad51-dependent recombination, but if there is heterology adjacent to the DSB then the efficiency of repair is reduced (52, 103, 184). Heterology adjacent to the DSB also results in a greatly increased frequency of telomere addition at DSBs in an *exo1*Δ *sgs1*Δ mutant (32, 93). These events are extremely rare in wild-type cells, and their increased incidence in the *exo1*Δ *sgs1*Δ mutant could be due to inability to engage in HR due to lack of sufficient resection to expose homology and/or increased retention of MRX/Tel1 at DSBs and subsequent recruitment of telomerase. The absence of extensive resection in the *exo1*Δ *sgs1*Δ mutant results in stabilization of transformed linear DNA and more efficient gene targeting or break-induced replication from short linear substrates (32, 96).

DNA RESECTION AND CHECKPOINT ACTIVATION

Checkpoints are signal transduction pathways that coordinate DNA damage sensing with signaling, DNA repair, and cell-cycle progression. Two PIKKs, ATM/Tel1 and ATR/Mec1, are critical upstream regulators of checkpoint signaling. ATM is activated primarily by DSBs, whereas both stalled replication forks and DSBs activate ATR (34, 63). Thus, the activities of ATM and ATR are directly tied to the detection and nucleolytic processing of DSBs (63). DNA-PK, a third member of the PIKK family, is also activated by DSB damage. In contrast to ATM and ATR, the role of DNA-PK is restricted to NHEJ repair. All three PIKKs are recruited to DNA damage via a small conserved C-terminal motif that facilitates interactions with Nbs1 (ATM), ATRIP (ATR), and Ku (DNA-PK) (48). PIKKs can regulate resection by phosphorylating several key proteins of the resection apparatus.

ATM is specifically recruited to DSBs by Nbs1. Cells defective in any component of the MRN complex are deficient in ATM activation and localization to DSBs (147). The initial recruitment and activation of ATM at sites of damage is followed by modifications of the surrounding chromatin—phosphorylation of H2AX—which in turns facilitates the recruitment of ubiquitin ligases that modify chromatin to assemble multiprotein complexes (33). This second recruitment step enhances the ATM-dependent response to DSBs and could help maintain signaling once the MRN complex dissociates from DSBs.

When DSBs occur during the S or G2 phases of the cell cycle, MRN recruits CtIP to initiate resection, and the resulting ssDNA 3′ overhang becomes coated by RPA. This ssDNA-RPA intermediate interacts with ATRIP, leading to ATRIP recruitment and subsequent ATR activation (38, 187). Therefore, the resection-dependent conversion of DSBs into ssDNA is critical for the sequential activation of ATM and ATR (**Figure 3**). Notably, resection requires ATM activity and ultimately leads to ATM inactivation, which is independent of ATR activation (139), thus setting up a very efficient switch. It remains to be determined whether MRX/N-dependent resection is sufficient to downregulate ATM activity in vivo, or whether Exo1- or Dna2-dependent long-range resection is required.

Phosphorylation and protein-protein interactions also regulate the ATM-to-ATR switch. ATM signaling is required for efficient ATR recruitment and activation. In addition to ssDNA-RPA complexes, ATR recruitment and activation by ATRIP requires TopBP1, the 9-1-1 complex and possibly the MRN complex itself. ATM-dependent phosphorylation of TopBP1 at S1131 is mediated by MRN and is required for ATR activation (71, 172). This introduces a second layer of regulation in the sequential activation of ATM and ATR: Both MRN-ATM dependent resection and ATM kinase activity are required for ATR activation.

Different organisms exhibit notable differences in the respective roles of ATM and ATR

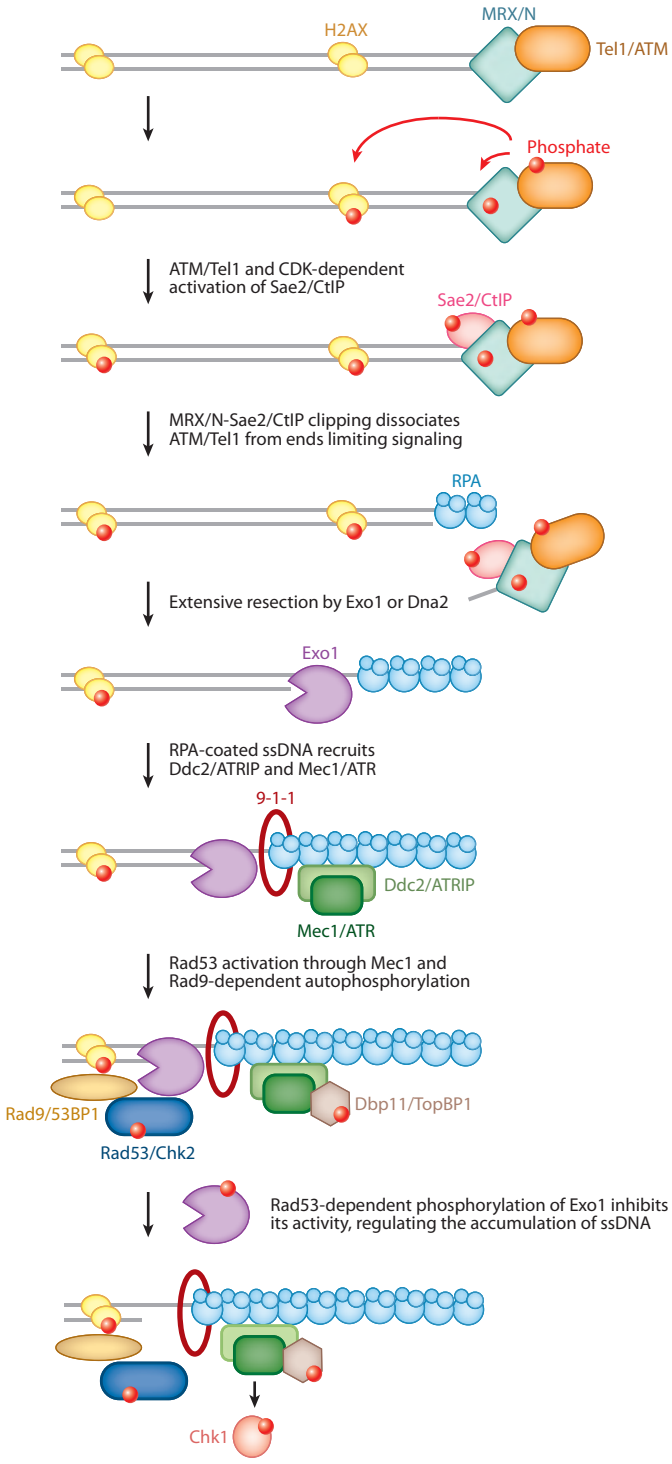

Figure 3

Model for activation of the DNA damage checkpoint. MRX/N recruits ATM/Tel1 to DSBs and activates ATM/Tel1 to phosphorylate MRX/N and other targets. Resection initiation dissociates MRX/N from ends and provides an ssDNA tail for RPA binding. Multiple rounds of MRX/N clipping could occur, or extensive resection by Exo1 or Sgs1/BLM-Dna2. RPA-ssDNA recruits ATRIP-ATR/Ddc2-Mec1 and subsequently activates Rad53/Chk2 and/or Chk1. Rad53 phosphorylation of Exo1 inhibits its activity, regulating the accumulation of ssDNA.

orthologs in checkpoint activation. The nuclease activity of the MRN/X complex is required for resection and radio resistance in fission yeast and in mammalian cells but not in budding yeast (26, 81, 89, 166). Furthermore, *sae2*Δ mutants are not especially radiosensitive, whereas in *S. pombe* and mammals the Sae2 functional homologs (Ctp1 and CtIP) are required for survival after IR (2, 79, 86, 133). Finally, unlike ATM in mammals, which is required for Chk2 activation, yeast Tel1 plays a very minor role in Rad53/Chk2 activation in wild-type cells.

How do these interspecies differences impact checkpoint activation? Budding yeast *sae2*Δ mutants or *mre11* nuclease-deficient mutants are not defective in checkpoint signaling from an irreparable HO-induced DSB; rather, these cells are unable to turn off the checkpoint signal. Conversely, overexpression of Sae2/CtIP inhibits Rad53/Chk2 activation (37). In contrast, nuclease-deficient *mre11* mutants in fission yeast are deficient in Chk1 activation (87). Strikingly, deletion of *SAE2* reveals a cryptic checkpoint pathway in which Tel1 activates Rad53/Chk2 (37, 156). A similar Tel1 to Chk1 signaling is revealed upon *ctp1* deletion in fission yeast (87). In both cases, signaling from Tel1 requires MRX/N. Upon Sae2/Ctp1 depletion, the MRX/N complex is stabilized at DSBs, which could promote sustained Tel1 signaling via interaction with Xrs2/Nbs1 (37, 87, 88). In this context, limited resection by the MRX/N complex would have two distinct consequences: (*a*) the generation of short ssDNA that could recruit a downstream regulator of Chk1 activation, such as the 9-1-1 complex; and (*b*) the displacement of MRX/N, possibly because of RPA loading (139). This model would therefore explain a smooth transition from ATM to ATR signaling in which ATM/Tel1 could overlap with ATR/Mec1 role in the early steps of checkpoint activation (87).

How the extent of resection in vivo affects checkpoint activation is not fully understood. Stable binding of RPA to ssDNA requires approximately 30 nucleotides, and in vitro recruitment of ATRIP to ssDNA-RPA requires at least 2 RPA complexes (187). Moreover, in a reconstituted in vitro system, ATR activation by ssDNA-RPA, ATRIP, and TopBP1 is inefficient when ssDNA is less than 200 nt and greatly enhanced with ssDNA length greater than 1,000 nt (31). These in vitro data suggest that ATR signaling should be proportional to the length of resected DNA. However, these studies did not analyze the role of the 9-1-1 complex, which loads at the ssDNA-dsDNA junction, independently of resection length.

Supporting the hypothesis that long ssDNA tracts are required to activate Mec1/ATR, the *S. cerevisiae exo1*Δ *sgs1*Δ mutant is defective for Ddc2/ATRIP recruitment and subsequent Rad53 activation (52, 184). In Xenopus, depletion of Dna2 reduces resection but does not prevent Chk1 phosphorylation (a readout for ATR activation), suggesting that enough ssDNA-RPA is generated in the absence of Dna2 to elicit the ATR-Chk1 checkpoint (160).

Proteomic studies in yeast and mammalian cells show that ATM and ATR phosphorylate multiple components of the resection machinery, including Sae2/CtIP, Exo1, Mre11, Nbs1, and Rad50, following induction of DSBs (97, 109, 141). Exo1 is phosphorylated at several sites following hydroxyurea (HU) treatment (46), including a PIKK consensus site that is also phosphorylated following IR (97). MRN/CtIP dependent resection is sensitive to ATM inhibition in Xenopus extracts suggesting that one or more of these proteins are activated by ATM phosphorylation at DSBs (173). BLM is phosphorylated at PIKK consensus sites following HU or IR treatments. Mutations at these sites results in a deficient DNA damage response; however, the effect on resection was not specifically tested (12, 127).

It is thought that resection should be limited to prevent the generation of long single-stranded regions in the genome. In mammalian cells, phosphorylation of Exo1 triggers its ubiquitylation and subsequent degradation following fork stalling (47). It would be important to determine if a similar mechanism operates to regulate Exo1 activity at DSBs and participates in a negative feedback loop to prevent excessive resection. In budding yeast, Exo1 is

phosphorylated by Rad53 in a Rad9-dependent manner following extensive generation of ssDNA, and this phosphorylation might inhibit its activity (108). Rad9 inhibits ssDNA accumulation at DSBs, thus limiting the amount of ssDNA generated during the DNA damage response (74). However, the increased resection in *rad9* mutants is Rad50 rather than Exo1 dependent, suggesting it is due to MRX/N or Sgs1-Dna2. In budding yeast Tel1/ATM and Mec1/ATR may attenuate checkpoint signaling by phosphorylating Sae2/CtIP, which inhibits MRX/N signaling (10, 37). Xenopus Mre11 becomes hyperphosphorylated in the presence of DSBs. This phosphorylation is in part ATM- and ATR dependent and phosphorylation at PIKK putative sites regulates MRN binding to DNA; hyperphosphorylation of Mre11 triggers the dissociation of MRN from chromatin, and this could also be part of a negative feedback loop to prevent excessive resection (41).

DNA RESECTION AND REPAIR PATHWAY CHOICE

Cell-Cycle Regulation of End Resection

An important factor governing the choice between the HR and NHEJ repair pathways is the phase of the cell cycle. HR is generally restricted to the S and G2 phases when DNA has replicated and the sister chromatid is available as a repair template. On the other hand, NHEJ operates throughout the cell cycle but seems to be more prevalent in the G1 phase (**Figure 1**). Resection of DSBs induced in G1 phase cells is greatly reduced compared with cycling or G2-arrested cells (6, 9, 35, 60, 63, 186). A DSB present during DNA replication (S phase) is more efficiently processed than during G2, and this most likely accounts for the increased resection observed in cycling compared with G2 cells (186). Interestingly, resection in G2 phase is more dependent on MRX than in cycling cells, suggesting replication forks could serve to recruit Exo1 and/or STR-Dna2 in lieu of the MRX complex.

The reduced resection of G1 phase cells is due to both NHEJ and low cyclin–dependent protein kinase (Cdc28/CDK) activity (6, 35, 60, 63). G1 phase cells deficient for Ku show greater recruitment of Mre11 to an endonuclease-induced DSB and increased resection of sequences up to 5 kb from the break site (break proximal) (9, 35). Overexpression of Exo1 is also able to overcome the inhibition to resection in G1 phase cells, which is consistent with other studies showing Ku is a barrier to Exo1-mediated end resection (35, 86, 105, 138, 150). The inhibitory effect of NHEJ was observed to a lesser extent in the *dnl4*Δ mutant, suggesting the end binding function of Ku and ligation both contribute to protecting ends from degradation in G1 (6, 35, 186). Although Ku does not inhibit resection in G2 cells, overexpression of Ku results in a significant decrease in Mre11 recruitment and resection (35).

Inhibition of CDK by using an analog-sensitive allele of the *CDC28* kinase or by overexpression of Sic1, an inhibitor of Cdc28, results in greatly reduced end resection (6, 35, 60). Interestingly, inhibition of CDK in G2 phase *ku80* cells fails to block resection of break-proximal sequences, similar to the situation in G1 phase *ku80* cells, and activation of CDK in G1 phase by overexpression of Clb2 restores both initiation and extensive resection (35). Together, these results suggest that Ku (and to a lesser extent ligation by Dnl4) is the primary rate-limiting factor for the initiation of end resection in G1 by competing with MRX and Exo1 for end binding. On the other hand, extensive resection appears to be regulated by CDK independently of Ku.

The block to end resection in G1 phase cells could be due to the requirement for a CDK target to counteract the inhibitory effect of Ku and/or to function directly in resection. Sae2, which is phosphorylated on Ser 267 by CDK, has emerged as a likely candidate to fulfill this role. Mutation of this site to a non-phosphorylatable residue, S267A, phenocopies *sae2*Δ, including hypersensitivity to CPT, defective sporulation, reduced hairpin-induced recombination, impaired DSB processing,

and persistent Mre11 foci (58). Similarly, a mutation at the equivalent CDK site in human CtIP (T847A) impairs resection in human cells, whereas Ctp1 is regulated transcriptionally during the cell cycle (59, 86). It was originally reported that an *sae2-S267E* mutation, which behaves as a phosphomimic to confer constitutive activation, complements *sae2*Δ and overcomes the requirement for CDK activity for DSB resection (58). However, a similar mutation (*sae2-S267D*) was reported to be not fully wild type in phenotype and still defective for G1 resection (20). The DNA damage sensitivity of the *sae2*Δ mutant is completely suppressed by elimination of Ku, and this suppression requires both Exo1 and Sgs1, suggesting CDK activation of Sae2 serves to remove Ku from DNA ends to allow direct access to Exo1 or STR-Dna2 to restore resection (105). It is possible that Ku is removed from ends by MRX-Sae2 clipping, similar to Spo11, or that a dynamic equilibrium exists between MRX-Sae2 and Ku binding, and that once MRX-Sae2 initiate resection, the preferred substrate for Ku binding is no longer available (**Figure 2**). Alternatively, a nuclease-independent function of Sae2 might be required to restrict Ku binding to DNA ends in G2 phase cells. It should be noted, however, that Sae2 is still required for meiosis and hairpin cleavage in the absence of Ku, indicating an essential role for Sae2 nuclease, or activation of the Mre11 endonuclease by Sae2, to process these ends (105, 129).

Two other components of the resection apparatus, RPA and Dna2, are also CDK targets (43, 155). Dna2 has a bipartite nuclear localization sequence overlapping a CDK phosphorylation site, and mutation of that site prevents nuclear entry during S-phase (68); thus, the long-range resection defect of *ku80* G1 cells could be due to insufficient nuclear Dna2. The role of RPA phosphorylation in end resection has yet to be determined. Loss of Rad9 can partially bypass the CDK requirement for resection, suggesting that Rad9 could also be a target of the CDK-dependent regulation of resection (74).

Nonhomologous End Joining and Homologous Recombination Interplay at Double-Strand Breaks

As described above, the initiation of resection commits cells to repair DSBs by HR or MMEJ because Ku binds poorly to long ssDNA overhangs, and additional processing factors would be required to trim the ends for ligation (44). The efficiency of HR increases in the absence of Ku, but the reverse is not the case, suggesting that cells attempt to join ends by NHEJ before the initiation of resection (5, 50, 123, 181). Thus, it appears cells favor repair of DSBs by NHEJ if the ends are compatible for joining, and if this fails resection initiates to prepare substrates for HR. As described above, Ku protects ends from degradation; thus, the increase in HR observed in the absence of Ku is probably due to creating substrates favorable for HR. Reduced resection appears to be the major impediment to HR in G1 cells as *ku70* mutants exhibit increased HR between ectopic repeats when arrested in G1 (6, 181).

Microhomology-Mediated End Joining: From Backup System to Bona Fide Repair Pathway

MMEJ is a DSB repair pathway that uses microhomologies to align broken ends before ligation. Inhibition of classical NHEJ (C-NHEJ) by use of Ku or Lig IV deficient cells revealed a robust end-joining activity (118, 178). This reflects an alternative mode of repair, alternative NHEJ (A-NHEJ), that probably comprises several pathways. Of these, only MMEJ requires DNA end resection and will be discussed here (reviewed in 100). MMEJ was first thought to be a backup repair pathway operating only in the absence of C-NHEJ; however, recent studies indicate that MMEJ works even when C-NHEJ is functional (78, 180).

Unlike C-NHEJ, MMEJ requires limited resection and always results in deletions flanking the original breaks (100). The genes required for MMEJ in budding yeast include *Mre11*, *Rad50*, *Xrs2*, *Sae2*, and *TEL1*, indicating that resection initiation is an essential

step (76, 94). Consistent with the yeast studies, the MRN-CtIP pathway promotes MMEJ in mammalian cells. Following the development of chromosomal reporters for DSB-induced HR [Direct repeat–green fluorescent protein (DR-GFP)]), all repair pathways requiring end resection could be monitored in rodent and human cells: homology-dependent repair, single-strand annealing, and MMEJ (13, 14, 49, 128, 169). Downregulation of Mre11 via siRNA or inhibition with the small molecule mirin resulted in a decrease in end-joining capacity in *Xrcc4*$^{-/-}$ cells defective in C-NHEJ, indicating that Mre11 is required for MMEJ (128, 169). Likewise, using a different reporter specific for MMEJ, inactivation of Nbs1 or CtIP decreased MMEJ (13, 14). Overexpression of wild-type Mre11, but not of a nuclease-deficient Mre11 mutant, was shown to increase DNA end resection and MMEJ (128). Together, these data suggest that resection by the MRN/CtIP pathway generates single-strand overhangs that anneal during MMEJ.

The role of ATM was recently evaluated using a plasmid-based reporter for MMEJ (126). This study confirmed the role of Mre11 and showed that MMEJ was increased in A-T cells, confirming previous observations that ATM represses DNA degradation (125, 126). On the other hand, ATM is required for CtIP-dependent resection in Xenopus extracts, as seen by the reduced accumulation of ssDNA-RPA intermediates upon treatment with KU55933 (173). This suggests that ATM could play antagonistic roles in resection by stimulating some reactions while inhibiting others, thus placing it in a critical position to determine repair pathway choice.

Fanconi Anemia Proteins and Repair Pathway Choice

Fanconi anemia (FA) is genomic instability syndrome characterized by bone marrow failure, increased cancer incidence, and sensitivity to crosslinking drugs at the cellular level (reviewed in 65, 159). FA is caused by mutations in at least 13 genes, eight of which encode for a large core protein complex responsible for the ubiquitylation of the FANCD2/FANCI (FA proteins D2/I) heterodimer. In addition, three FA proteins associated with breast cancer susceptibility (FANCD1/BRCA2, FANCJ/BACH1, and FANCN/PALB2) function downstream of the other FA components in the pathway. Recent studies indicate that the FA pathway is another critical determinant of repair pathway choice. Chromatin replicated in Xenopus extracts depleted of FA proteins accumulates DSBs (142). Work in *Caenorhabditis elegans*, DT40 chicken cells, and mammalian cells now shows that the cellular defects associated with mutations in the FA pathway can be rescued by elimination of C-NHEJ factors: Ku in DT40 cells, or Lig IV or Ku in mammalian cells (1, 119). These observations indicate that the FA pathway channels DSB repair during DNA replication toward the accurate HR pathway and suppresses error-prone NHEJ. It also suggests that in the absence of the FA pathway, DSBs generated during DNA replication could be repaired by NHEJ to generate chromosome rearrangements. As whole genome sequencing turns into a powerful method to evaluate the impact of DNA repair on chromosome rearrangements (see below), it will be critical to determine whether the chromosomal aberrations associated with FA harbor a specific signature (MMEJ or C-NHEJ) at repair junctions. FA mutants have only a mild defect in HR when assayed in the context of a DR-GFP reporter but display a profound HR repair defect in the context of interstrand crosslink (ICL) repair (111, 112). It is tempting to speculate that the FA pathway could influence pathway choice by participating directly in DNA end processing, an idea that is supported by the fact that FANCD2 harbors exonuclease activity. FANCD2 could facilitate resection of context-specific DSBs (such as ICL-associated breaks). Consistent with the idea that the FA could facilitate resection, FA cells show reduced alternative NHEJ repair of DSBs (92).

BRCA1 and Repair Pathway Choice

Recent in vivo studies indicate that BRCA1 (Breast Cancer 1, Early Onset) plays a critical

role in the competition between HR and NHEJ. Chromosomal abnormalities and tumorigenesis associated with BRCA1 loss are rescued by deleting 53BP1, a factor implicated in NHEJ (22, 27). The mechanistic bases of this competition are not entirely clear.

BRCA1 regulates an early step of DSB repair to promote HR; however, the involvement of BRCA1 in DSB resection has not been clearly established (29, 110, 135, 144, 176). Using RPA foci to monitor resection following IR, some studies show that ssDNA formation is BRCA1-independent (182), whereas other studies suggest it is BRCA1-dependent (135). These differences could be due to distinct genetic backgrounds in the cell lines used or might reflect the limitation of using RPA foci as the sole readout for DNA resection. Studies that correlate the formation of RPA foci with a direct measure of the extent of DNA resection might help resolve some of these issues in mammalian cells.

BRCA1 associates with phosphorylated CtIP via its BRCT tandem repeat (175). Phosphorylation of CtIP at S332 in chicken DT40 cells is required for BRCA1 interaction but is dispensable for DSB resection or HR, suggesting that CtIP-dependent resection does not require interaction with BRCA1 (110). However, another study using DT40 lymphoblastoid cells showed that phosphorylation of CtIP S332 is critical for HR (176). Of note, in this latter study, CtIP inactivation is compatible with cell growth, suggesting that these cells have acquired a mechanism to bypass the CtIP requirement for cell proliferation.

Conflicting results have been obtained in testing the role of BRCA1 in episomal-based rejoining assays (11, 183, 185). Using a specific reporter integrated in a chromosome, Benardo et al. show that *Brca1*$^{-/-}$ cells display a defect in end joining that might be attributed to a defect in the rejoining of cohesive ends (14). Further studies with this assay should clarify the role of BRCA1 in the different modes of DSB repair.

Pathological Consequences of Pathway Choice: Resection and Chromosome Translocations

Alternative NHEJ/MMEJ is emerging as a repair pathway responsible for chromosome translocations. Recurrent chromosome translocations are the hallmark of some hematological malignancies such as Burkitt's lymphoma and chronic myelogenous leukemia. Recurrent translocations are also found in epithelial tumors, yet at a lower frequency, possibly because the complex chromosome rearrangements associated with these tumors could mask such translocations. Nonetheless, recurrent translocations have been described in papillary thyroid carcinomas, prostate cancers, and, more recently, nonsmall-cell lung cancers (reviewed in 23, 72, 84, 118, 178). Novel sequencing strategies are also revealing that solid tumors have more complex rearrangements than previously appreciated, including intrachromosomal translocations, which in the case of breast tumors are not occuring at recurrent sites (145, 146).

The extent of DNA end resection appears to be a critical factor in generating these tumorigenic rearrangements. Analysis of DNA sequences at translocation breakpoints indicate that translocations rarely occur at homologous sequences (145, 146, 161). Indeed, translocations are suppressed by homology-dependent repair requiring extensive DNA resection (130). The classical NHEJ pathway also suppresses translocations. Elimination of Ku, Lig IV, or both, which favors DSB repair without resection, promotes translocations (18, 42, 49, 140, 170). In an experimental model for interchromosomal translocations, downregulation of CtIP dramatically reduced translocation frequency and microhomology usage in the remaining rearrangements (180). Notably, the remaining C-NHEJ-dependent translocations were not affected by CtIP depletion. This shows that in this system, translocations arise predominantly through MMEJ. During normal class switch recombination (CSR), CtIP is required for switching events in

C-NHEJ proficient cells, where it is recruited to switch regions in an AID-dependent manner (78).

Maintaining the proper balance of DNA resection is therefore critical to prevent toxic chromosome rearrangements. Because MMEJ is active throughout the cell cycle, it could promote translocations when any of the following aberrancies occur: (*a*) inhibition of C-NHEJ; (*b*) stimulation of short-range (MRX/N-CtIP-dependent) resection in G1 phase; (*c*) inhibition of HR, or (*d*) inhibition of long-range (Exo1/Dna2-dependent) resection in S/G2 phase.

SUMMARY POINTS

1. Initiation of DSB end resection prevents NHEJ and promotes HR or MMEJ, depending on the extent of resection.
2. MRX/N and Sae2/CtIP/Ctp1 are necessary to initiate resection of covalently modified DNA ends, but the Mre11 and Sae2 nucleases are dispensable for resection of unmodified ends.
3. MRX/N recruits Dna2, Exo1, and Sgs1 to DSBs to initiate resection of unmodified ends directly and to carry out extensive resection. Extensive resection by Exo1 or STR-Dna2 improves the efficiency and fidelity of HR.
4. Ku binding to DNA ends prevents resection initiation in G1 phase cells; activation of CDK overcomes the Ku-mediated inhibition to resection and promotes extensive resection of DNA ends.
5. MRX/N recruits Tel1/ATM to DSBs to signal DNA damage. Activation of resection removes MRX/N and Tel1/ATM from ends and promotes recruitment of ATRIP-ATR to RPA-coated ssDNA tails.
6. Initiation of resection is required for MMEJ to reveal short sequence homologies internal to the ends for annealing. MMEJ is emerging as the major mechanism for chromosome translocations, and possibly other rearrangements, in mammalian cells.

FUTURE ISSUES

1. Are Sae2/CtIP and Dna2 the only CDK-regulated resection factors?
2. How do PIKKs influence resection?
3. How is resection limited?
4. Do the HR and MMEJ repair pathways compete?
5. Are the extensive resection pathways fully redundant in mitotic cells?

DISCLOSURE STATEMENT

The authors are not aware of any affiliations, memberships, funding, or financial holdings that might be perceived as affecting the objectivity of this review.

LITERATURE CITED

1. Adamo A, Collis SJ, Adelman CA, Silva N, Horejsi Z, et al. 2010. Preventing nonhomologous end joining suppresses DNA repair defects of Fanconi anemia. *Mol. Cell* 39:25–35
2. Akamatsu Y, Murayama Y, Yamada T, Nakazaki T, Tsutsui Y, et al. 2008. Molecular characterization of the role of the *Schizosaccharomyces pombe* nip1+/ctp1 +gene in DNA double-strand break repair in association with the Mre11-Rad50-Nbs1 complex. *Mol. Cell. Biol.* 28:3639–51
3. Alani E, Padmore R, Kleckner N. 1990. Analysis of wild-type and rad50 mutants of yeast suggests an intimate relationship between meiotic chromosome synapsis and recombination. *Cell* 61:419–36
4. Alani E, Subbiah S, Kleckner N. 1989. The yeast RAD50 gene encodes a predicted 153-kD protein containing a purine nucleotide-binding domain and two large heptad-repeat regions. *Genetics* 122:47–57
5. Allen C, Kurimasa A, Brenneman MA, Chen DJ, Nickoloff JA. 2002. DNA-dependent protein kinase suppresses double-strand break–induced and spontaneous homologous recombination. *Proc. Natl. Acad. Sci. USA* 99:3758–63
6. Aylon Y, Liefshitz B, Kupiec M. 2004. The CDK regulates repair of double-strand breaks by homologous recombination during the cell cycle. *EMBO J.* 23:4868–75
7. Balakrishnan L, Polaczek P, Pokharel S, Campbell JL, Bambara RA. 2010. Dna2 exhibits a unique strand end–dependent helicase function. *J. Biol. Chem.* 285:38861–68
8. Barker S, Weinfeld M, Zheng J, Li L, Murray D. 2005. Identification of mammalian proteins cross-linked to DNA by ionizing radiation. *J. Biol. Chem.* 280:33826–38
9. Barlow JH, Lisby M, Rothstein R. 2008. Differential regulation of the cellular response to DNA double-strand breaks in G1. *Mol. Cell* 30:73–85
10. Baroni E, Viscardi V, Cartagena-Lirola H, Lucchini G, Longhese MP. 2004. The functions of budding yeast Sae2 in the DNA damage response require Mec1- and Tel1-dependent phosphorylation. *Mol. Cell. Biol.* 24:4151–65
11. Bau DT, Fu YP, Chen ST, Cheng TC, Yu JC, et al. 2004. Breast cancer risk and the DNA double-strand break end-joining capacity of nonhomologous end-joining genes are affected by BRCA1. *Cancer Res.* 64:5013–19
12. Beamish H, Kedar P, Kaneko H, Chen P, Fukao T, et al. 2002. Functional link between BLM defective in Bloom's syndrome and the ataxia-telangiectasia-mutated protein, ATM. *J. Biol. Chem.* 277:30515–23
13. Bennardo N, Cheng A, Huang N, Stark JM. 2008. Alternative-NHEJ is a mechanistically distinct pathway of mammalian chromosome break repair. *PLoS Genet.* 4:e1000110
14. Bennardo N, Gunn A, Cheng A, Hasty P, Stark JM. 2009. Limiting the persistence of a chromosome break diminishes its mutagenic potential. *PLoS Genet.* 5:e1000683
15. Bergerat A, de Massy B, Gadelle D, Varoutas PC, Nicolas A, Forterre P. 1997. An atypical topoisomerase II from Archaea with implications for meiotic recombination. *Nature* 386:414–17
16. Bernstein KA, Gangloff S, Rothstein R. 2010. The RecQ DNA helicases in DNA repair. *Annu. Rev. Genet.* 44:393–417
17. Bishop DK, Park D, Xu L, Kleckner N. 1992. DMC1: a meiosis-specific yeast homolog of *E. coli* recA required for recombination, synaptonemal complex formation, and cell cycle progression. *Cell* 69:439–56
18. Boboila C, Jankovic M, Yan CT, Wang JH, Wesemann DR, et al. 2010. Alternative end-joining catalyzes robust IgH locus deletions and translocations in the combined absence of ligase 4 and Ku70. *Proc. Natl. Acad. Sci. USA* 107:3034–39
19. Bolderson E, Tomimatsu N, Richard DJ, Boucher D, Kumar R, et al. 2010. Phosphorylation of Exo1 modulates homologous recombination repair of DNA double-strand breaks. *Nucleic Acids Res.* 38:1821–31

20. Bonetti D, Martina M, Clerici M, Lucchini G, Longhese MP. 2009. Multiple pathways regulate 3′ overhang generation at *S. cerevisiae* telomeres. *Mol. Cell* 35:70–81
21. Boulton SJ, Jackson SP. 1996. *Saccharomyces cerevisiae* Ku70 potentiates illegitimate DNA double-strand break repair and serves as a barrier to error-prone DNA repair pathways. *EMBO J.* 15:5093–103
22. Bouwman P, Aly A, Escandell JM, Pieterse M, Bartkova J, et al. 2010. 53BP1 loss rescues BRCA1 deficiency and is associated with triple-negative and BRCA-mutated breast cancers. *Nat. Struct. Mol. Biol.* 17:688–95
23. Brenner JC, Chinnaiyan AM. 2009. Translocations in epithelial cancers. *Biochim. Biophys. Acta* 1796:201–15
24. Bressan DA, Olivares HA, Nelms BE, Petrini JH. 1998. Alteration of N-terminal phosphoesterase signature motifs inactivates *Saccharomyces cerevisiae* Mre11. *Genetics* 150:591–600
25. Budd ME, Campbell JL. 2009. Interplay of Mre11 nuclease with Dna2 plus Sgs1 in Rad51-dependent recombinational repair. *PLoS ONE* 4:e4267
26. Buis J, Wu Y, Deng Y, Leddon J, Westfield G, et al. 2008. Mre11 nuclease activity has essential roles in DNA repair and genomic stability distinct from ATM activation. *Cell* 135:85–96
27. Bunting SF, Callen E, Wong N, Chen HT, Polato F, et al. 2010. 53BP1 inhibits homologous recombination in Brca1-deficient cells by blocking resection of DNA breaks. *Cell* 141:243–54
28. Cejka P, Cannavo E, Polaczek P, Masuda-Sasa T, Pokharel S, et al. 2010. DNA end resection by Dna2-Sgs1-RPA and its stimulation by Top3-Rmi1 and Mre11-Rad50-Xrs2. *Nature* 467:112–16
29. Chen L, Nievera CJ, Lee AY, Wu X. 2008. Cell cycle–dependent complex formation of BRCA1.CtIP.MRN is important for DNA double-strand break repair. *J. Biol. Chem.* 283:7713–20
30. Chiolo I, Carotenuto W, Maffioletti G, Petrini JH, Foiani M, Liberi G. 2005. Srs2 and Sgs1 DNA helicases associate with Mre11 in different subcomplexes following checkpoint activation and CDK1-mediated Srs2 phosphorylation. *Mol. Cell. Biol.* 25:5738–51
31. Choi JH, Lindsey-Boltz LA, Kemp M, Mason AC, Wold MS, Sancar A. 2010. Reconstitution of RPA-covered single-stranded DNA-activated ATR-Chk1 signaling. *Proc. Natl. Acad. Sci. USA* 107:13660–65
32. Chung WH, Zhu Z, Papusha A, Malkova A, Ira G. 2010. Defective resection at DNA double-strand breaks leads to de novo telomere formation and enhances gene targeting. *PLoS Genet.* 6:e1000948
33. Ciccia A, Elledge SJ. 2010. The DNA damage response: making it safe to play with knives. *Mol. Cell* 40:179–204
34. Cimprich KA, Cortez D. 2008. ATR: an essential regulator of genome integrity. *Nat. Rev. Mol. Cell. Biol.* 9:616–27
35. Clerici M, Mantiero D, Guerini I, Lucchini G, Longhese MP. 2008. The Yku70-Yku80 complex contributes to regulate double-strand break processing and checkpoint activation during the cell cycle. *EMBO Rep.* 9:810–18
36. Clerici M, Mantiero D, Lucchini G, Longhese MP. 2005. The Saccharomyces cerevisiae Sae2 protein promotes resection and bridging of double strand break ends. *J. Biol. Chem.* 280:38631–38
37. Clerici M, Mantiero D, Lucchini G, Longhese MP. 2006. The Saccharomyces cerevisiae Sae2 protein negatively regulates DNA damage checkpoint signalling. *EMBO Rep.* 7:212–18
38. Costanzo V, Robertson K, Bibikova M, Kim E, Grieco D, et al. 2001. Mre11 protein complex prevents double-strand break accumulation during chromosomal DNA replication. *Mol. Cell* 8:137–47
39. Daley JM, Palmbos PL, Wu D, Wilson TE. 2005. Nonhomologous end joining in yeast. *Annu. Rev. Genet.* 39:431–51
40. de Jager M, van Noort J, van Gent DC, Dekker C, Kanaar R, Wyman C. 2001. Human Rad50/Mre11 is a flexible complex that can tether DNA ends. *Mol. Cell* 8:1129–35
41. Di Virgilio M, Ying CY, Gautier J. 2009. PIKK-dependent phosphorylation of Mre11 induces MRN complex inactivation by disassembly from chromatin. *DNA Repair (Amst.)* 8:1311–20
42. Difilippantonio MJ, Zhu J, Chen HT, Meffre E, Nussenzweig MC, et al. 2000. DNA repair protein Ku80 suppresses chromosomal aberrations and malignant transformation. *Nature* 404:510–14
43. Din S, Brill SJ, Fairman MP, Stillman B. 1990. Cell-cycle-regulated phosphorylation of DNA replication factor A from human and yeast cells. *Genes Dev.* 4:968–77
44. Dynan WS, Yoo S. 1998. Interaction of Ku protein and DNA-dependent protein kinase catalytic subunit with nucleic acids. *Nucleic Acids Res.* 26:1551–59

45. Eid W, Steger M, El-Shemerly M, Ferretti LP, Pena-Diaz J, et al. 2010. DNA end resection by CtIP and exonuclease 1 prevents genomic instability. *EMBO Rep.* 11:962–68
46. El-Shemerly M, Hess D, Pyakurel AK, Moselhy S, Ferrari S. 2008. ATR-dependent pathways control hEXO1 stability in response to stalled forks. *Nucleic Acids Res.* 36:511–19
47. El-Shemerly M, Janscak P, Hess D, Jiricny J, Ferrari S. 2005. Degradation of human exonuclease 1b upon DNA synthesis inhibition. *Cancer Res.* 65:3604–9
48. Falck J, Coates J, Jackson SP. 2005. Conserved modes of recruitment of ATM, ATR and DNA-PKcs to sites of DNA damage. *Nature* 434:605–11
49. Fattah F, Lee EH, Weisensel N, Wang Y, Lichter N, Hendrickson EA. 2010. Ku regulates the non-homologous end joining pathway choice of DNA double-strand break repair in human somatic cells. *PLoS Genet.* 6:e1000855
50. Frank-Vaillant M, Marcand S. 2002. Transient stability of DNA ends allows nonhomologous end joining to precede homologous recombination. *Mol. Cell* 10:1189–99
51. Furuse M, Nagase Y, Tsubouchi H, Murakami-Murofushi K, Shibata T, Ohta K. 1998. Distinct roles of two separable in vitro activities of yeast Mre11 in mitotic and meiotic recombination. *EMBO J.* 17:6412–25
52. Gravel S, Chapman JR, Magill C, Jackson SP. 2008. DNA helicases Sgs1 and BLM promote DNA double-strand break resection. *Genes Dev.* 22:2767–72
53. Hartsuiker E, Mizuno K, Molnar M, Kohli J, Ohta K, Carr AM. 2009. Ctp1CtIP and Rad32Mre11 nuclease activity are required for Rec12Spo11 removal, but Rec12Spo11 removal is dispensable for other MRN-dependent meiotic functions. *Mol. Cell. Biol.* 29:1671–81
54. Henner WD, Rodriguez LO, Hecht SM, Haseltine WA. 1983. Gamma ray induced deoxyribonucleic acid strand breaks. 3′ glycolate termini. *J. Biol. Chem.* 258:711–13
55. Hodgson A, Terentyev Y, Johnson RA, Bishop-Bailey A, Angevin T, et al. 2011. Mre11 and Exo1 contribute to the initiation and processivity of resection at meiotic double-strand breaks made independently of Spo11. *DNA Repair (Amst.)* 10:138–48
56. Hopfner KP, Craig L, Moncalian G, Zinkel RA, Usui T, et al. 2002. The Rad50 zinc-hook is a structure joining Mre11 complexes in DNA recombination and repair. *Nature* 418:562–66
57. Hopfner KP, Karcher A, Shin DS, Craig L, Arthur LM, et al. 2000. Structural biology of Rad50 ATPase: ATP-driven conformational control in DNA double-strand break repair and the ABC-ATPase superfamily. *Cell* 101:789–800
58. Huertas P, Cortes-Ledesma F, Sartori AA, Aguilera A, Jackson SP. 2008. CDK targets Sae2 to control DNA-end resection and homologous recombination. *Nature* 455:689–92
59. Huertas P, Jackson SP. 2009. Human CtIP mediates cell cycle control of DNA end resection and double strand break repair. *J. Biol. Chem.* 284:9558–65
60. Ira G, Pellicioli A, Balijja A, Wang X, Fiorani S, et al. 2004. DNA end resection, homologous recombination and DNA damage checkpoint activation require CDK1. *Nature* 431:1011–17
61. Ivanov EL, Sugawara N, White CI, Fabre F, Haber JE. 1994. Mutations in XRS2 and RAD50 delay but do not prevent mating-type switching in *Saccharomyces cerevisiae*. *Mol. Cell. Biol.* 14:3414–25
62. Jazayeri A, Balestrini A, Garner E, Haber JE, Costanzo V. 2008. Mre11-Rad50-Nbs1-dependent processing of DNA breaks generates oligonucleotides that stimulate ATM activity. *EMBO J.* 27:1953–62
63. Jazayeri A, Falck J, Lukas C, Bartek J, Smith GC, et al. 2006. ATM- and cell cycle-dependent regulation of ATR in response to DNA double-strand breaks. *Nat. Cell Biol.* 8:37–45
64. Karmakar P, Seki M, Kanamori M, Hashiguchi K, Ohtsuki M, et al. 2006. BLM is an early responder to DNA double-strand breaks. *Biochem. Biophys. Res. Commun.* 348:62–69
65. Kee Y, D'Andrea AD. 2010. Expanded roles of the Fanconi anemia pathway in preserving genomic stability. *Genes Dev.* 24:1680–94
66. Keelagher RE, Cotton VE, Goldman AS, Borts RH. 2011. Separable roles for exonuclease I in meiotic DNA double-strand break repair. *DNA Repair (Amst.)* 10:126–37
67. Keeney S, Giroux CN, Kleckner N. 1997. Meiosis-specific DNA double-strand breaks are catalyzed by Spo11, a member of a widely conserved protein family. *Cell* 88:375–84

68. Kosugi S, Hasebe M, Tomita M, Yanagawa H. 2009. Systematic identification of cell cycle–dependent yeast nucleocytoplasmic shuttling proteins by prediction of composite motifs. *Proc. Natl. Acad. Sci. USA* 106:10171–76
69. Krogh BO, Llorente B, Lam A, Symington LS. 2005. Mutations in Mre11 phosphoesterase motif I that impair *Saccharomyces cerevisiae* Mre11-Rad50-Xrs2 complex stability in addition to nuclease activity. *Genetics* 171:1561–70
70. Krogh BO, Symington LS. 2004. Recombination proteins in yeast. *Annu. Rev. Genet.* 38:233–71
71. Kumagai A, Lee J, Yoo HY, Dunphy WG. 2006. TopBP1 activates the ATR-ATRIP complex. *Cell* 124:943–55
72. Kuppers R, Dalla-Favera R. 2001. Mechanisms of chromosomal translocations in B cell lymphomas. *Oncogene* 20:5580–94
73. Lammens K, Bemeleit DJ, Mockel C, Clausing E, Schele A, et al. 2011. The Mre11:Rad50 structure shows an ATP-dependent molecular clamp in DNA double-strand break repair. *Cell* 145:54–66
74. Lazzaro F, Sapountzi V, Granata M, Pellicioli A, Vaze M, et al. 2008. Histone methyltransferase Dot1 and Rad9 inhibit single-stranded DNA accumulation at DSBs and uncapped telomeres. *EMBO J.* 27:1502–12
75. Lee Bi BI, Nguyen LH, Barsky D, Fernandes M, Wilson DM 3rd. 2002. Molecular interactions of human Exo1 with DNA. *Nucleic Acids Res.* 30:942–49
76. Lee K, Lee SE. 2007. *Saccharomyces cerevisiae* Sae2- and Tel1-dependent single-strand DNA formation at DNA break promotes microhomology-mediated end joining. *Genetics* 176:2003–14
77. Lee SE, Bressan DA, Petrini JH, Haber JE. 2002. Complementation between N-terminal *Saccharomyces cerevisiae* mre11 alleles in DNA repair and telomere length maintenance. *DNA Repair (Amst.)* 1:27–40
78. Lee-Theilen M, Matthews AJ, Kelly D, Zheng S, Chaudhuri J. 2011. CtIP promotes microhomology-mediated alternative end joining during class-switch recombination. *Nat. Struct. Mol. Biol.* 18:75–79
79. Lengsfeld BM, Rattray AJ, Bhaskara V, Ghirlando R, Paull TT. 2007. Sae2 is an endonuclease that processes hairpin DNA cooperatively with the Mre11/Rad50/Xrs2 complex. *Mol. Cell* 28:638–51
80. Lewis LK, Karthikeyan G, Westmoreland JW, Resnick MA. 2002. Differential suppression of DNA repair deficiencies of yeast rad50, mre11 and xrs2 mutants by EXO1 and TLC1 (the RNA component of telomerase). *Genetics* 160:49–62
81. Lewis LK, Storici F, Van Komen S, Calero S, Sung P, Resnick MA. 2004. Role of the nuclease activity of *Saccharomyces cerevisiae* Mre11 in repair of DNA double-strand breaks in mitotic cells. *Genetics* 166:1701–13
82. Liao S, Toczylowski T, Yan H. 2008. Identification of the Xenopus DNA2 protein as a major nuclease for the 5′->3′ strand-specific processing of DNA ends. *Nucleic Acids Res.* 36:6091–100
83. Lieber MR. 2010. The mechanism of double-strand DNA break repair by the nonhomologous DNA end-joining pathway. *Annu. Rev. Biochem.* 79:181–211
84. Lieber MR, Yu K, Raghavan SC. 2006. Roles of nonhomologous DNA end joining, V(D)J recombination, and class switch recombination in chromosomal translocations. *DNA Repair (Amst.)* 5:1234–45
85. Lim HS, Kim JS, Park YB, Gwon GH, Cho Y. 2011. Crystal structure of the Mre11-Rad50-ATPγS complex: understanding the interplay between Mre11 and Rad50. *Genes Dev.* 25:1091–104
86. Limbo O, Chahwan C, Yamada Y, de Bruin RA, Wittenberg C, Russell P. 2007. Ctp1 is a cell-cycle-regulated protein that functions with Mre11 complex to control double-strand break repair by homologous recombination. *Mol. Cell* 28:134–46
87. Limbo O, Porter-Goff ME, Rhind N, Russell P. 2011. Mre11 nuclease activity and Ctp1 regulate Chk1 activation by Rad3ATR and Tel1ATM checkpoint kinases at double-strand breaks. *Mol. Cell. Biol.* 31:573–83
88. Lisby M, Barlow JH, Burgess RC, Rothstein R. 2004. Choreography of the DNA damage response: spatiotemporal relationships among checkpoint and repair proteins. *Cell* 118:699–713
89. Llorente B, Symington LS. 2004. The Mre11 nuclease is not required for 5′ to 3′ resection at multiple HO-induced double-strand breaks. *Mol. Cell. Biol.* 24:9682–94
90. Lloyd J, Chapman JR, Clapperton JA, Haire LF, Hartsuiker E, et al. 2009. A supramodular FHA/BRCT-repeat architecture mediates Nbs1 adaptor function in response to DNA damage. *Cell* 139:100–11
91. Lobachev KS, Gordenin DA, Resnick MA. 2002. The Mre11 complex is required for repair of hairpin-capped double-strand breaks and prevention of chromosome rearrangements. *Cell* 108:183–93

92. Lundberg R, Mavinakere M, Campbell C. 2001. Deficient DNA end joining activity in extracts from Fanconi anemia fibroblasts. *J. Biol. Chem.* 276:9543–49
93. Lydeard JR, Lipkin-Moore Z, Jain S, Eapen VV, Haber JE. 2010. Sgs1 and exo1 redundantly inhibit break-induced replication and de novo telomere addition at broken chromosome ends. *PLoS Genet.* 6:e1000973
94. Ma JL, Kim EM, Haber JE, Lee SE. 2003. Yeast Mre11 and Rad1 proteins define a Ku-independent mechanism to repair double-strand breaks lacking overlapping end sequences. *Mol. Cell. Biol.* 23:8820–28
95. Manfrini N, Guerini I, Citterio A, Lucchini G, Longhese MP. 2010. Processing of meiotic DNA double strand breaks requires cyclin-dependent kinase and multiple nucleases. *J. Biol. Chem.* 285:11628–37
96. Marrero VA, Symington LS. 2010. Extensive DNA end processing by exo1 and sgs1 inhibits break-induced replication. *PLoS Genet.* 6:e1001007
97. Matsuoka S, Ballif BA, Smogorzewska A, McDonald ER 3rd, Hurov KE, et al. 2007. ATM and ATR substrate analysis reveals extensive protein networks responsive to DNA damage. *Science* 316:1160–66
98. Mazon G, Mimitou EP, Symington LS. 2010. SnapShot: homologous recombination in DNA double-strand break repair. *Cell* 142:646, e1
99. McKee AH, Kleckner N. 1997. A general method for identifying recessive diploid-specific mutations in *Saccharomyces cerevisiae*, its application to the isolation of mutants blocked at intermediate stages of meiotic prophase and characterization of a new gene SAE2. *Genetics* 146:797–816
100. McVey M, Lee SE. 2008. MMEJ repair of double-strand breaks (director's cut): deleted sequences and alternative endings. *Trends Genet.* 24:529–38
101. Milman N, Higuchi E, Smith GR. 2009. Meiotic DNA double-strand break repair requires two nucleases, MRN and Ctp1, to produce a single size class of Rec12 (Spo11)-oligonucleotide complexes. *Mol. Cell. Biol.* 29:5998–6005
102. Milne GT, Jin S, Shannon KB, Weaver DT. 1996. Mutations in two Ku homologs define a DNA end-joining repair pathway in *Saccharomyces cerevisiae*. *Mol. Cell. Biol.* 16:4189–98
103. Mimitou EP, Symington LS. 2008. Sae2, Exo1 and Sgs1 collaborate in DNA double-strand break processing. *Nature* 455:770–74
104. Mimitou EP, Symington LS. 2009. DNA end resection: many nucleases make light work. *DNA Repair (Amst.)* 8:983–95
105. Mimitou EP, Symington LS. 2010. Ku prevents Exo1 and Sgs1-dependent resection of DNA ends in the absence of a functional MRX complex or Sae2. *EMBO J.* 29:3358–69
106. Moreau S, Ferguson JR, Symington LS. 1999. The nuclease activity of Mre11 is required for meiosis but not for mating type switching, end joining, or telomere maintenance. *Mol. Cell. Biol.* 19:556–66
107. Moreau S, Morgan EA, Symington LS. 2001. Overlapping functions of the *Saccharomyces cerevisiae* Mre11, Exo1 and Rad27 nucleases in DNA metabolism. *Genetics* 159:1423–33
108. Morin I, Ngo HP, Greenall A, Zubko MK, Morrice N, Lydall D. 2008. Checkpoint-dependent phosphorylation of Exo1 modulates the DNA damage response. *EMBO J.* 27:240–41
109. Mu JJ, Wang Y, Luo H, Leng M, Zhang J, et al. 2007. A proteomic analysis of ataxia telangiectasia-mutated (ATM)/ATM-Rad3-related (ATR) substrates identifies the ubiquitin-proteasome system as a regulator for DNA damage checkpoints. *J. Biol. Chem.* 282:17330–34
110. Nakamura K, Kogame T, Oshiumi H, Shinohara A, Sumitomo Y, et al. 2010. Collaborative action of Brca1 and CtIP in elimination of covalent modifications from double-strand breaks to facilitate subsequent break repair. *PLoS Genet.* 6:e1000828
111. Nakanishi K, Cavallo F, Perrouault L, Giovannangeli C, Moynahan ME, et al. 2011. Homology-directed Fanconi anemia pathway cross-link repair is dependent on DNA replication. *Nat. Struct. Mol. Biol.* 18:500–3
112. Nakanishi K, Yang YG, Pierce AJ, Taniguchi T, Digweed M, et al. 2005. Human Fanconi anemia monoubiquitination pathway promotes homologous DNA repair. *Proc. Natl. Acad. Sci. USA* 102:1110–15
113. Neale MJ, Pan J, Keeney S. 2005. Endonucleolytic processing of covalent protein-linked DNA double-strand breaks. *Nature* 436:1053–57
114. Nicolette ML, Lee K, Guo Z, Rani M, Chow JM, et al. 2010. Mre11-Rad50-Xrs2 and Sae2 promote 5′ strand resection of DNA double-strand breaks. *Nat. Struct. Mol. Biol.* 17:1478–85

115. Nimonkar AV, Genschel J, Kinoshita E, Polaczek P, Campbell JL, et al. 2011. BLM-DNA2-RPA-MRN and EXO1-BLM-RPA-MRN constitute two DNA end resection machineries for human DNA break repair. *Genes Dev.* 25:350–62
116. Nimonkar AV, Ozsoy AZ, Genschel J, Modrich P, Kowalczykowski SC. 2008. Human exonuclease 1 and BLM helicase interact to resect DNA and initiate DNA repair. *Proc. Natl. Acad. Sci. USA* 105:16906–11
117. Niu H, Chung WH, Zhu Z, Kwon Y, Zhao W, et al. 2010. Mechanism of the ATP-dependent DNA end-resection machinery from *Saccharomyces cerevisiae*. *Nature* 467:108–11
118. Nussenzweig A, Nussenzweig MC. 2010. Origin of chromosomal translocations in lymphoid cancer. *Cell* 141:27–38
119. Pace P, Mosedale G, Hodskinson MR, Rosado IV, Sivasubramaniam M, Patel KJ. 2010. Ku70 corrupts DNA repair in the absence of the Fanconi anemia pathway. *Science* 329:219–23
120. Paques F, Haber JE. 1999. Multiple pathways of recombination induced by double-strand breaks in *Saccharomyces cerevisiae*. *Microbiol. Mol. Biol. Rev.* 63:349–404
121. Paull TT, Gellert M. 1998. The 3′ to 5′ exonuclease activity of Mre 11 facilitates repair of DNA double-strand breaks. *Mol. Cell* 1:969–79
122. Paull TT, Gellert M. 1999. Nbs1 potentiates ATP-driven DNA unwinding and endonuclease cleavage by the Mre11/Rad50 complex. *Genes Dev.* 13:1276–88
123. Pierce AJ, Hu P, Han M, Ellis N, Jasin M. 2001. Ku DNA end-binding protein modulates homologous repair of double-strand breaks in mammalian cells. *Genes Dev.* 15:3237–42
124. Prinz S, Amon A, Klein F. 1997. Isolation of COM1, a new gene required to complete meiotic double-strand break-induced recombination in *Saccharomyces cerevisiae*. *Genetics* 146:781–95
125. Rahal EA, Henricksen LA, Li Y, Turchi JJ, Pawelczak KS, Dixon K. 2008. ATM mediates repression of DNA end-degradation in an ATP-dependent manner. *DNA Repair (Amst.)* 7:464–75
126. Rahal EA, Henricksen LA, Li Y, Williams RS, Tainer JA, Dixon K. 2010. ATM regulates Mre11-dependent DNA end-degradation and microhomology-mediated end joining. *Cell Cycle* 9:2866–77
127. Rao VA, Fan AM, Meng L, Doe CF, North PS, et al. 2005. Phosphorylation of BLM, dissociation from topoisomerase IIIalpha, and colocalization with gamma-H2AX after topoisomerase I–induced replication damage. *Mol. Cell. Biol.* 25:8925–37
128. Rass E, Grabarz A, Plo I, Gautier J, Bertrand P, Lopez BS. 2009. Role of Mre11 in chromosomal nonhomologous end joining in mammalian cells. *Nat. Struct. Mol. Biol.* 16:819–24
129. Rattray AJ, Shafer BK, Neelam B, Strathern JN. 2005. A mechanism of palindromic gene amplification in *Saccharomyces cerevisiae*. *Genes Dev.* 19:1390–99
130. Richardson C, Moynahan ME, Jasin M. 1998. Double-strand break repair by interchromosomal recombination: suppression of chromosomal translocations. *Genes Dev.* 12:3831–42
131. Rothenberg M, Kohli J, Ludin K. 2009. Ctp1 and the MRN-complex are required for endonucleolytic Rec12 removal with release of a single class of oligonucleotides in fission yeast. *PLoS Genet.* 5:e1000722
132. San Filippo J, Sung P, Klein H. 2008. Mechanism of eukaryotic homologous recombination. *Annu. Rev. Biochem.* 77:229–57
133. Sartori AA, Lukas C, Coates J, Mistrik M, Fu S, et al. 2007. Human CtIP promotes DNA end resection. *Nature* 450:509–14
134. Schaetzlein S, Kodandaramireddy NR, Ju Z, Lechel A, Stepczynska A, et al. 2007. Exonuclease-1 deletion impairs DNA damage signaling and prolongs lifespan of telomere-dysfunctional mice. *Cell* 130:863–77
135. Schlegel BP, Jodelka FM, Nunez R. 2006. BRCA1 promotes induction of ssDNA by ionizing radiation. *Cancer Res.* 66:5181–89
136. Sharples GJ, Leach DR. 1995. Structural and functional similarities between the SbcCD proteins of *Escherichia coli* and the RAD50 and MRE11 (RAD32) recombination and repair proteins of yeast. *Mol. Microbiol.* 17:1215–17
137. Shibata A, Conrad S, Birraux J, Geuting V, Barton O, et al. 2011. Factors determining DNA double-strand break repair pathway choice in G2 phase. *EMBO J.* 30:1079–92
138. Shim EY, Chung WH, Nicolette ML, Zhang Y, Davis M, et al. 2010. *Saccharomyces cerevisiae* Mre11/Rad50/Xrs2 and Ku proteins regulate association of Exo1 and Dna2 with DNA breaks. *EMBO J.* 29:3370–80

139. Shiotani B, Zou L. 2009. Single-stranded DNA orchestrates an ATM-to-ATR switch at DNA breaks. *Mol. Cell* 33:547–58
140. Simsek D, Jasin M. 2010. Alternative end-joining is suppressed by the canonical NHEJ component Xrcc4-ligase IV during chromosomal translocation formation. *Nat. Struct. Mol. Biol.* 17:410–16
141. Smolka MB, Albuquerque CP, Chen SH, Zhou H. 2007. Proteome-wide identification of in vivo targets of DNA damage checkpoint kinases. *Proc. Natl. Acad. Sci. USA* 104:10364–69
142. Sobeck A, Stone S, Costanzo V, de Graaf B, Reuter T, et al. 2006. Fanconi anemia proteins are required to prevent accumulation of replication-associated DNA double-strand breaks. *Mol. Cell. Biol.* 26:425–37
143. Soulas-Sprauel P, Rivera-Munoz P, Malivert L, Le Guyader G, Abramowski V, et al. 2007. V(D)J and immunoglobulin class switch recombinations: a paradigm to study the regulation of DNA end-joining. *Oncogene* 26:7780–91
144. Stark JM, Pierce AJ, Oh J, Pastink A, Jasin M. 2004. Genetic steps of mammalian homologous repair with distinct mutagenic consequences. *Mol. Cell. Biol.* 24:9305–16
145. Stephens PJ, Greenman CD, Fu B, Yang F, Bignell GR, et al. 2011. Massive genomic rearrangement acquired in a single catastrophic event during cancer development. *Cell* 144:27–40
146. Stephens PJ, McBride DJ, Lin ML, Varela I, Pleasance ED, et al. 2009. Complex landscapes of somatic rearrangement in human breast cancer genomes. *Nature* 462:1005–10
147. Stracker TH, Petrini JH. 2011. The MRE11 complex: starting from the ends. *Nat. Rev Mol. Cell Biol.* 12:90–103
148. Sugawara N, Ivanov EL, Fishman-Lobell J, Ray BL, Wu X, Haber JE. 1995. DNA structure-dependent requirements for yeast RAD genes in gene conversion. *Nature* 373:84–86
149. Szankasi P, Smith GR. 1992. A DNA exonuclease induced during meiosis of *Schizosaccharomyces pombe*. *J. Biol. Chem.* 267:3014–23
150. Tomita K, Matsuura A, Caspari T, Carr AM, Akamatsu Y, et al. 2003. Competition between the Rad50 complex and the Ku heterodimer reveals a role for Exo1 in processing double-strand breaks but not telomeres. *Mol. Cell. Biol.* 23:5186–97
151. Tran PT, Erdeniz N, Symington LS, Liskay RM. 2004. EXO1-A multi-tasking eukaryotic nuclease. *DNA Repair (Amst.)* 3:1549–59
152. Trujillo KM, Yuan SS, Lee EY, Sung P. 1998. Nuclease activities in a complex of human recombination and DNA repair factors Rad50, Mre11, and p95. *J. Biol. Chem.* 273:21447–50
153. Tsubouchi H, Ogawa H. 1998. A novel mre11 mutation impairs processing of double-strand breaks of DNA during both mitosis and meiosis. *Mol. Cell. Biol.* 18:260–68
154. Tsubouchi H, Ogawa H. 2000. Exo1 roles for repair of DNA double-strand breaks and meiotic crossing over in *Saccharomyces cerevisiae*. *Mol. Biol. Cell* 11:2221–33
155. Ubersax JA, Woodbury EL, Quang PN, Paraz M, Blethrow JD, et al. 2003. Targets of the cyclin-dependent kinase Cdk1. *Nature* 425:859–64
156. Usui T, Ogawa H, Petrini JH. 2001. A DNA damage response pathway controlled by Tel1 and the Mre11 complex. *Mol. Cell* 7:1255–66
157. Usui T, Ohta T, Oshiumi H, Tomizawa J, Ogawa H, Ogawa T. 1998. Complex formation and functional versatility of Mre11 of budding yeast in recombination. *Cell* 95:705–16
158. van der Linden E, Sanchez H, Kinoshita E, Kanaar R, Wyman C. 2009. RAD50 and NBS1 form a stable complex functional in DNA binding and tethering. *Nucleic Acids Res.* 37:1580–88
159. Wang LC, Gautier J. 2010. The Fanconi anemia pathway and ICL repair: implications for cancer therapy. *Crit. Rev. Biochem. Mol. Biol.* 45:424–39
160. Wawrousek KE, Fortini BK, Polaczek P, Chen L, Liu Q, et al. 2010. Xenopus DNA2 is a helicase/nuclease that is found in complexes with replication proteins And-1/Ctf4 and Mcm10 and DSB response proteins Nbs1 and ATM. *Cell Cycle* 9:1156–66
161. Weinstock DM, Elliott B, Jasin M. 2006. A model of oncogenic rearrangements: differences between chromosomal translocation mechanisms and simple double-strand break repair. *Blood* 107:777–80
162. Westmoreland J, Ma W, Yan Y, Van Hulle K, Malkova A, Resnick MA. 2009. RAD50 is required for efficient initiation of resection and recombinational repair at random, gamma-induced double-strand break ends. *PLoS Genet.* 5:e1000656

163. Williams GJ, Lees-Miller SP, Tainer JA. 2010. Mre11-Rad50-Nbs1 conformations and the control of sensing, signaling, and effector responses at DNA double-strand breaks. *DNA Repair (Amst.)* 9:1299–306
164. Williams GJ, Williams RS, Williams JS, Moncalian G, Arvai AS, et al. 2011. ABC ATPase signature helices in Rad50 link nucleotide state to Mre11 interface for DNA repair. *Nat. Struct. Mol. Biol.* 18:423–31
165. Williams RS, Dodson GE, Limbo O, Yamada Y, Williams JS, et al. 2009. Nbs1 flexibly tethers Ctp1 and Mre11-Rad50 to coordinate DNA double-strand break processing and repair. *Cell* 139:87–99
166. Williams RS, Moncalian G, Williams JS, Yamada Y, Limbo O, et al. 2008. Mre11 dimers coordinate DNA end bridging and nuclease processing in double-strand-break repair. *Cell* 135:97–109
167. Wiltzius JJ, Hohl M, Fleming JC, Petrini JH. 2005. The Rad50 hook domain is a critical determinant of Mre11 complex functions. *Nat. Struct. Mol. Biol.* 12:403–7
168. Wu W, Wang M, Singh SK, Mussfeldt T, Iliakis G. 2008. Repair of radiation induced DNA double strand breaks by backup NHEJ is enhanced in G2. *DNA Repair (Amst.)* 7:329–38
169. Xie A, Kwok A, Scully R. 2009. Role of mammalian Mre11 in classical and alternative nonhomologous end joining. *Nat. Struct. Mol. Biol.* 16:814–18
170. Yan CT, Boboila C, Souza EK, Franco S, Hickernell TR, et al. 2007. IgH class switching and translocations use a robust non-classical end-joining pathway. *Nature* 449:478–82
171. Yan H, Toczylowski T, McCane J, Chen C, Liao S. 2011. Replication protein A promotes 5′–>3′ end processing during homology-dependent DNA double-strand break repair. *J. Cell Biol.* 192:251–61
172. Yoo HY, Kumagai A, Shevchenko A, Dunphy WG. 2009. The Mre11-Rad50-Nbs1 complex mediates activation of TopBP1 by ATM. *Mol. Biol. Cell* 20:2351–60
173. You Z, Shi LZ, Zhu Q, Wu P, Zhang YW, et al. 2009. CtIP links DNA double-strand break sensing to resection. *Mol. Cell* 36:954–69
174. Young JA, Hyppa RW, Smith GR. 2004. Conserved and nonconserved proteins for meiotic DNA breakage and repair in yeasts. *Genetics* 167:593–605
175. Yu X, Chen J. 2004. DNA damage-induced cell cycle checkpoint control requires CtIP, a phosphorylation-dependent binding partner of BRCA1 C-terminal domains. *Mol. Cell. Biol.* 24:9478–86
176. Yun MH, Hiom K. 2009. CtIP-BRCA1 modulates the choice of DNA double-strand-break repair pathway throughout the cell cycle. *Nature* 459:460–63
177. Zakharyevich K, Ma Y, Tang S, Hwang PY, Boiteux S, Hunter N. 2010. Temporally and biochemically distinct activities of Exo1 during meiosis: double-strand break resection and resolution of double Holliday junctions. *Mol. Cell* 40:1001–15
178. Zhang Y, Gostissa M, Hildebrand DG, Becker MS, Boboila C, et al. 2010. The role of mechanistic factors in promoting chromosomal translocations found in lymphoid and other cancers. *Adv. Immunol.* 106:93–133
179. Zhang Y, Hefferin ML, Chen L, Shim EY, Tseng HM, et al. 2007. Role of Dnl4-Lif1 in nonhomologous end-joining repair complex assembly and suppression of homologous recombination. *Nat. Struct. Mol. Biol.* 14:639–46
180. Zhang Y, Jasin M. 2011. An essential role for CtIP in chromosomal translocation formation through an alternative end-joining pathway. *Nat. Struct. Mol. Biol.* 18:80–84
181. Zhang Y, Shim EY, Davis M, Lee SE. 2009. Regulation of repair choice: Cdk1 suppresses recruitment of end joining factors at DNA breaks. *DNA Repair (Amst.)* 8:1235–41
182. Zhao GY, Sonoda E, Barber LJ, Oka H, Murakawa Y, et al. 2007. A critical role for the ubiquitin-conjugating enzyme Ubc13 in initiating homologous recombination. *Mol. Cell* 25:663–75
183. Zhong Q, Boyer TG, Chen PL, Lee WH. 2002. Deficient nonhomologous end-joining activity in cell-free extracts from Brca1-null fibroblasts. *Cancer Res.* 62:3966–70
184. Zhu Z, Chung WH, Shim EY, Lee SE, Ira G. 2008. Sgs1 helicase and two nucleases, Dna2 and Exo1, resect DNA double-strand break ends. *Cell* 134:981–94
185. Zhuang J, Zhang J, Willers H, Wang H, Chung JH, et al. 2006. Checkpoint kinase 2-mediated phosphorylation of BRCA1 regulates the fidelity of nonhomologous end-joining. *Cancer Res.* 66:1401–8
186. Zierhut C, Diffley JF. 2008. Break dosage, cell cycle stage and DNA replication influence DNA double strand break response. *EMBO J.* 27:1875–85
187. Zou L, Elledge SJ. 2003. Sensing DNA damage through ATRIP recognition of RPA-ssDNA complexes. *Science* 300:1542–48

Cdk1 uncouples CtIP-dependent resection and Rad51 filament formation during M-phase double-strand break repair

Shaun E. Peterson,[1,2] Yinyin Li,[7] Brian T. Chait,[7] Max E. Gottesman,[4,5] Richard Baer,[1,6] and Jean Gautier[1,3]

[1]Institute for Cancer Genetics, [2]Department of Biological Sciences, [3]Department of Genetics and Development, [4]Institute of Cancer Research, [5]Department of Biochemistry and Molecular Biophysics, and [6]Department of Pathology and Cell Biology, Columbia University Medical Center, New York, NY 10032
[7]Laboratory of Mass Spectrometry and Gaseous Ion Chemistry, The Rockefeller University, New York, NY 10065

DNA double-strand break (DSB) resection, which results in RPA-bound single-stranded DNA (ssDNA), is activated in S phase by Cdk2. RPA-ssDNA activates the ATR-dependent checkpoint and homology-directed repair (HDR) via Rad51-dependent mechanisms. On the other hand, the fate of DSBs sustained during vertebrate M phase is largely unknown. We use cell-free *Xenopus laevis* egg extracts to examine the recruitment of proteins to chromatin after DSB formation. We find that S-phase extract recapitulates a two-step resection mechanism. M-phase chromosomes are also resected in cell-free extracts and cultured human cells. In contrast to the events in S phase, M-phase resection is solely dependent on MRN-CtIP. Despite generation of RPA-ssDNA, M-phase resection does not lead to ATR activation or Rad51 chromatin association. Remarkably, we find that Cdk1 permits resection by phosphorylation of CtIP but also prevents Rad51 binding to the resected ends. We have thus identified Cdk1 as a critical regulator of DSB repair in M phase. Cdk1 induces persistent ssDNA-RPA overhangs in M phase, thereby preventing both classical NHEJ and Rad51-dependent HDR.

Introduction

DNA double-strand breaks (DSBs) are potentially the most harmful form of DNA damage. DSBs are repaired by classical nonhomologous end joining (C-NHEJ), alternative nonhomologous end joining (Alt-NHEJ/microhomology-mediated end joining), or homology-directed repair (HDR). HDR and Alt-NHEJ pathways are initiated by degradation of the 5′ strand of the DSB to yield a 3′ single-stranded DNA (ssDNA) overhang, a process called DNA end resection (Symington, 2002). Resection allows RPA loading onto the ssDNA and subsequent repair by high-fidelity HDR pathways, which require Rad51 nucleoprotein filament formation and strand invasion into a homologous sequence. Resection in the absence of strand invasion may lead to mutagenic Alt-NHEJ, a source of chromosomal translocations (Zhang et al., 2010; Lee-Theilen et al., 2011; Zhang and Jasin, 2011).

At least two mechanistically distinct stages of DNA resection have been observed. Resection is initiated by the MRN (Mre11–Rad50–Nbs1) complex (Xrs2 is the budding yeast orthologue of Nbs1), which binds to DSB ends and facilitates activation of the ATM protein kinase. CtIP (Sae2 in budding yeast) is then recruited to the DSB-MRN complex (Lisby et al., 2004; Limbo et al., 2007), which promotes endonucleolytic cleavage of the 5′ strand, releasing short oligonucleotides (Jazayeri et al., 2008; Mimitou and Symington, 2008). In the second stage, the partially resected DSB recruits helicases and nucleases, including BLM (Sgs1 in budding yeast; both are RecQ homologues), DNA2, and Exo1, which catalyze extensive and processive resection (Gravel et al., 2008; Liao et al., 2008; Mimitou and Symington, 2008; Zhu et al., 2008; Budd and Campbell, 2009; Cejka et al., 2010; Niu et al., 2010). These pathways, however, are not independent: MRX (Mre11–Rad50–Xrs2) recruits Dna2 to budding yeast DSBs independent of its nuclease activity (Shim et al., 2010),

Correspondence to Jean Gautier: jg130@columbia.edu

Abbreviations used in this paper: Alt-NHEJ, alternative nonhomologous end joining; C-NHEJ, classical nonhomologous end joining; CSF, cytostatic factor; DSB, double-strand break; HDR, homology-directed repair; HR, homologous recombination; HSS, high-speed supernatant; LSS, low speed supernatant; NHEJ, nonhomologous end joining; PKI, PKA inhibitor; ssDNA, single-stranded DNA; wt, wild type; xCtIP, *Xenopus* CtIP.

The Rockefeller University Press $30.00
J. Cell Biol. Vol. 194 No. 5 705–720
www.jcb.org/cgi/doi/10.1083/jcb.201103103

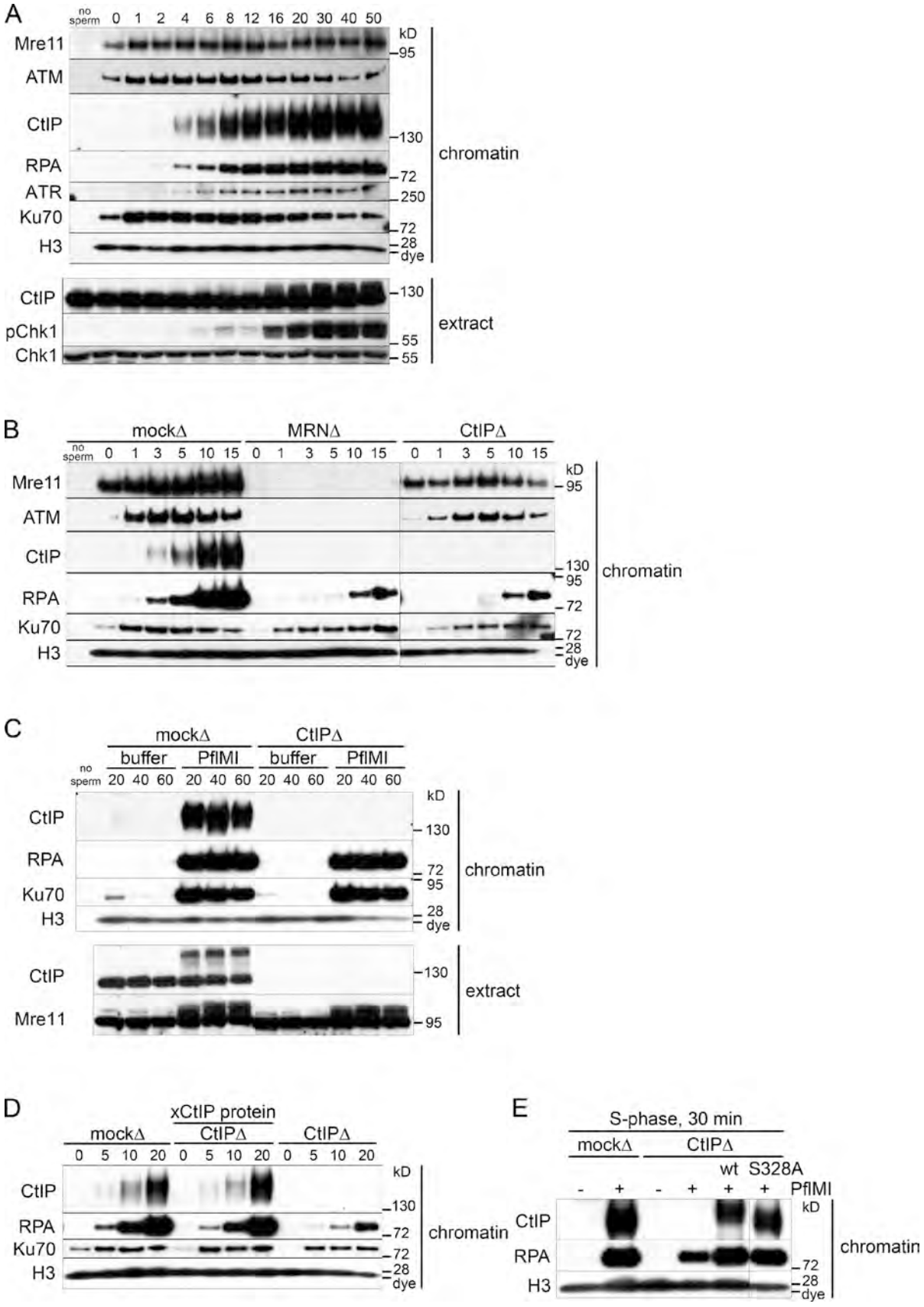

Figure 1. **DSB resection in S-phase *Xenopus* cell-free extract proceeds by CtIP-dependent and -independent pathways.** (A) Kinetics of recruitment of proteins to DSB-containing chromatin in S-phase extract. S-phase extract was preincubated with sperm chromatin (5,000 sperm/µl). Aliquots of the sample were taken before (0 min) and at the indicated time (minutes) after addition of 0.05 U/µl PflMI restriction endonuclease. At each time point, 0.5 µl of the

and human MRN stimulates resection of linear DNA by Exo1 in vitro (Nimonkar et al., 2011).

Whether resection is initiated on a DSB is a critical determinant of repair pathway choice (Shrivastav et al., 2008). Resection enables HDR and Alt-NHEJ and prevents repair by C-NHEJ, which requires near-blunt double-stranded DNA ends. The mode of DSB repair depends on cell cycle status such that C-NHEJ is predominant in G0 and G1 when Cdk activity is low and no homologous template is available for repair, whereas DSBs are repaired primarily through HDR mechanisms in S and G2. This switch to HDR in S phase is controlled in part by Cdk-dependent phosphorylation/activation of Sae2/CtIP (Limbo et al., 2007; Huertas et al., 2008; Huertas and Jackson, 2009).

The ssDNA-RPA intermediates formed by resection also promote activation of the ATR-dependent damage checkpoint that acts through the Chk1 kinase (Costanzo et al., 2003; Zou and Elledge, 2003). Activated Chk1 inhibits Cdk1 activity by down-regulating Cdc25 phosphatases, which counteract inhibitory phosphorylation of Cdk1 by Wee1 kinase (Karlsson-Rosenthal and Millar, 2006). This G2/M checkpoint prevents entry into mitosis.

In contrast to interphase, little is known about signaling from and repair of DSBs in mitosis, which occurs in the context of condensed chromosomes and high Cdk activity. Chromosomes damaged at the onset of mitosis proceed through to anaphase without repair (Zirkle and Bloom, 1953). Therefore, canonical damage checkpoints that down-regulate Cdk1 are not fully operational after prophase (Morrison and Rieder, 2004). Indeed, Wee1 becomes inactive upon entry into mitosis, and damage-induced inactivation of Cdk1 does not occur (Okamoto and Sagata, 2007). However, more profound perturbation of chromatin structure or disruption of kinetochore–spindle attachments trigger the spindle assembly checkpoint (Rieder and Khodjakov, 1997), which significantly retards mitotic progression in an ATM-independent manner (Iwai et al., 1997; Mikhailov et al., 2002). Despite attenuated DNA damage checkpoints, phosphatidylinositol 3-kinase–like kinase family members are activated during mitosis, as indicated by ATM- and DNA-PK–dependent phosphorylation of histone H2AX (Giunta et al., 2010; Nakamura et al., 2010a). ATM-dependent phosphorylation also induces CEP63 dissociation from centrosomes and aberrant spindle assemblies (Smith et al., 2009).

In this paper, we (a) ask whether resection of DSBs occurs during vertebrate M phase, (b) assess the impact of Cdk1 activity on resection, and (c) characterize the consequences of resection in mitosis. We used cell-free extracts to monitor recruitment of signaling and repair proteins to restriction endonuclease–induced DSBs in a chromosomal context. We confirm that the two-step mechanism of S-phase resection in yeast is evolutionarily conserved in vertebrates, with one pathway dependent on MRN-CtIP and other, later pathways, independent of these factors. In addition, we report that DSB resection also occurs during mitosis, both in the condensed chromosomes of M-phase *Xenopus laevis* cell-free extracts and in cultured human cells. M-phase resection requires MRN-CtIP and phosphorylation of CtIP at a conserved Cdk consensus site. Remarkably, ssDNA-RPA generated by CtIP in M phase does not activate the ATR-Chk1 checkpoint or support Rad51 chromatin recruitment. Moreover, by showing that Cdk1 is responsible for the failure to recruit Rad51 to resected ssDNA-RPA in M-phase extracts, our experiments uncover a critical role for Cdk1 in regulating DSB repair during mitosis. Thus, by promoting CtIP-dependent resection of DSB ends while preventing Rad51 chromatin assembly, Cdk1 inhibits both the nonhomologous and homologous modes of DSB repair during mitosis. In this manner, Cdk1 can postpone DSB repair until chromosomes have been segregated and decondensed in the next cell cycle.

Results

Recruitment of proteins in response to chromosomal DSBs in S-phase *Xenopus* extract

We used cell-free extracts derived from the eggs of *Xenopus* to study the DNA damage response. These DNA-free extracts, which can be prepared as M-phase or interphase (S phase) extracts, contain all nuclear and cytoplasmic proteins and membrane lipids. When supplemented with demembranated sperm chromatin, S-phase extracts assemble nuclear envelopes and undergo DNA replication (Blow and Laskey, 1986; Hutchison et al., 1988). In contrast, chromatin added to M-phase extract remains highly condensed and supports formation of mitotic spindles (Verde et al., 1990). Significantly, upon exposure to endonuclease-generated chromosomal DSBs (Yoo et al., 2006), these extracts recapitulate many aspects of the cellular response to DSBs (Costanzo et al., 2000, 2001; Di Virgilio and Gautier, 2005; Dupré et al., 2006; You et al., 2007; Jazayeri et al., 2008).

We have induced DSBs with restriction endonuclease added to extracts supplemented with sperm chromatin. To monitor recruitment of proteins that respond to DSBs, aliquots of the treated samples were centrifuged through a dense sucrose cushion, which effectively separates soluble cytosolic and nuclear proteins from the insoluble chromatin fraction.

In S-phase extract, the response to chromosomal DSBs was extremely rapid (Fig. 1 A). Although basal levels of Mre11,

sample was removed and processed for Western blotting (extract), and 15 µl of the sample was removed and processed for chromatin isolation followed by Western blotting with the indicated antibodies (chromatin). A sample with no chromatin added (no sperm) serves as a chromatin purification control in A–C. (B) Early resection is dependent on MRN and CtIP in S-phase extract. Short kinetics of protein recruitment to chromatin in response to DSBs in mock-depleted, Mre11-depleted, and CtIP-depleted S-phase extracts as in A. (C) An MRN-CtIP–independent resection pathway operates in S-phase extract. Mock-depleted or CtIP-depleted S-phase extract was incubated with sperm chromatin and either buffer or PflMI restriction endonuclease for extended time points as in A. (D) Addition of recombinant xCtIP protein to CtIP-depleted S-phase extract restores resection activity to control levels. Experiment performed as in A but with an S-phase extract that was mock depleted, CtIP depleted supplemented with 110 nM recombinant xCtIP protein, or CtIP depleted as indicated. (E) The CtIP–BRCA1 interaction is not required for resection of endonuclease-induced chromosomal DSBs. Sperm chromatin was incubated in S-phase extract that was mock depleted, CtIP depleted, or CtIP depleted supplemented with 75 nM wt or S328A-xCtIP and was treated with buffer (−) or PflMI (+) for 30 min. Samples were processed for chromatin isolation as in A. The black line indicates that intervening lanes have been spliced out.

ATM, and Ku70 bound to chromatin before treatment, these proteins were significantly enriched in the chromatin fraction by 1 min after addition of the restriction enzyme. CtIP and RPA bound to DSB-containing chromatin by 4 min followed by ATR (Fig. 1 A). Because RPA binds selectively to ssDNA, chromatin-associated RPA was used as a measure of the amount of ssDNA generated by DSB resection. Phosphorylation of the ATR substrate Chk1 was seen in the soluble extract 16 min after DSB induction, simultaneous with phosphorylation of soluble CtIP (Fig. 1 A, extract). In all chromatin-binding experiments, total histone H3 was used as a chromatin-loading control.

DSB resection occurs by CtIP-dependent and -independent pathways in S-phase extract

We next asked whether CtIP and MRN were required for resection in S phase. To this end, we immunodepleted CtIP or Mre11 (which removes the entire MRN complex) from S-phase extracts (Costanzo et al., 2001). Total mouse IgG was used in a mock depletion control. Depletion of MRN did not significantly codeplete CtIP or vice versa (Fig. S1 A). We determined that >98% of CtIP was depleted (Fig. S1 B) and that no residual protein was detected on damaged chromatin (Fig. S1 C). CtIP depletion was equally efficient in both S-phase and M-phase extracts (Fig. S1 B).

As expected, depletion of MRN abrogated ATM and CtIP recruitment to damaged chromatin (Fig. 1 B; Limbo et al., 2007; You et al., 2009). In contrast, ATM and Mre11 recruitment did not depend on CtIP. These data, along with the slower kinetics of CtIP recruitment compared with MRN and ATM (Fig. 1 A), suggests that MRN recognition of DSBs and ATM activation occur before and independently of CtIP recruitment. Importantly, depletion of either MRN or CtIP delayed but did not abolish DSB resection in S-phase extract (Fig. 1 B). This result reveals multiple distinct resection pathways in S phase, an MRN-CtIP–dependent pathway, and one or more pathways independent of the initial resection step. Initiation of resection was delayed by ∼7 min in the absence of CtIP-MRN. However, at later time points, similar amounts of ssDNA were formed in CtIP-depleted and control extract, suggesting that CtIP-independent mechanisms are able to initiate resection and continue to generate substantial amounts of ssDNA (Fig. 1 C).

Addition of excess purified *Xenopus* CtIP (xCtIP) protein to CtIP-depleted extracts (Fig. S1, D and E) restored CtIP chromatin binding to endogenous levels and reestablished resection kinetics to control rates (Fig. 1 D). This confirms that the resection defect in CtIP-depleted extract is caused by the specific removal of endogenous CtIP.

CtIP can interact with the BRCA1 tumor suppressor in a phosphodependent manner that requires Cdk-dependent phosphorylation of CtIP at Ser327 (in humans; S328 in *Xenopus*; Yu and Chen, 2004; Varma et al., 2005; Chen et al., 2008). Upon DNA damage, MRN is assembled into a larger protein complex that includes both CtIP and BRCA1 (Greenberg et al., 2006). To assess whether the CtIP–BRCA1 interaction influences DNA resection, we expressed and purified an xCtIP polypeptide (xCtIP-S328A) bearing a missense mutation known to abolish the CtIP–BRCA1 interaction in mammalian (Yu and Chen, 2004) and in chicken DT40 (Nakamura et al., 2010b) cells. As shown in Fig. 1 E, the xCtIP-S328A protein was as effective as the wild-type (wt) CtIP protein in stimulating resection when added to a CtIP-depleted S-phase extract. These results suggest that BRCA1 is not required for CtIP-dependent resection of nuclease-induced DSBs in the *Xenopus* extract.

Characteristics of CtIP-independent resection

To characterize further the CtIP-independent pathway, we monitored the binding of BLM and WRN RecQ helicases and of DNA2 helicase/nuclease to endonuclease-treated chromatin. All three factors, which have been implicated in vertebrate resection (Yan et al., 2005; Toczylowski and Yan, 2006; Gravel et al., 2008; Liao et al., 2008; Mimitou and Symington, 2008; Nimonkar et al., 2008; Zhu et al., 2008; Budd and Campbell, 2009), were enriched on damaged chromatin in mock-depleted S-phase extracts (Fig. 2 A). Both RecQ helicases bound chromatin in the CtIP-depleted extract, strongly suggesting their participation in the CtIP-independent resection. In contrast to BLM and WRN, DNA2 recruitment was largely CtIP dependent. Note that CtIP depletion did not codeplete DNA2 from extracts (Fig. 2 A, extract).

Crude cell-free extracts contain lipids that assemble into nuclear envelopes around added sperm chromatin. This compartmentalization allows the import and concentration of nuclear factors essential for origin firing and DNA replication. Membrane-free extract obtained by high-speed centrifugation of crude S-phase extract (high-speed supernatant [HSS]) cannot form nuclear envelopes and fails to replicate chromatin. To determine the role of nuclear envelopes, we assayed resection in mock- or CtIP-depleted membrane-free HSS. CtIP, RPA, and Ku70 all associated with damaged chromatin in the HSS extract (Fig. 2 B). Resection, as seen by RPA binding, was undetectable in the CtIP-depleted extract (Fig. 2 B). This implies that late pathway resection requires chromatin compartmentalization. Failure to resect DNA in CtIP-depleted HSS was not caused by the absence of BLM, WRN, DNA2, or Exo1 proteins because all are present in HSS (Fig. S2 A).

Because a nuclear envelope is required for both chromosomal DNA replication and late pathway resection, we asked whether the latter depends on DNA replication. To test this idea, we inhibited prereplication complex formation with geminin (McGarry and Kirschner, 1998) or Cdk2 with roscovitine (Bresnahan et al., 1997) to prevent origin firing. Both inhibitors completely blocked incorporation of radiolabeled nucleotides into genomic DNA (Fig. 2 C, bottom). However, neither inhibitor abrogated late pathway resection, as determined by RPA recruitment in CtIP-depleted S-phase extract (Fig. 2 C). DNA replication, therefore, is not required for CtIP-independent resection.

DSBs generated in M phase undergo CtIP-dependent resection

To determine whether DSB resection occurs in the context of highly condensed mitotic chromosomes, we induced DSBs in M-phase extract (cytostatic factor [CSF]–arrested extract in

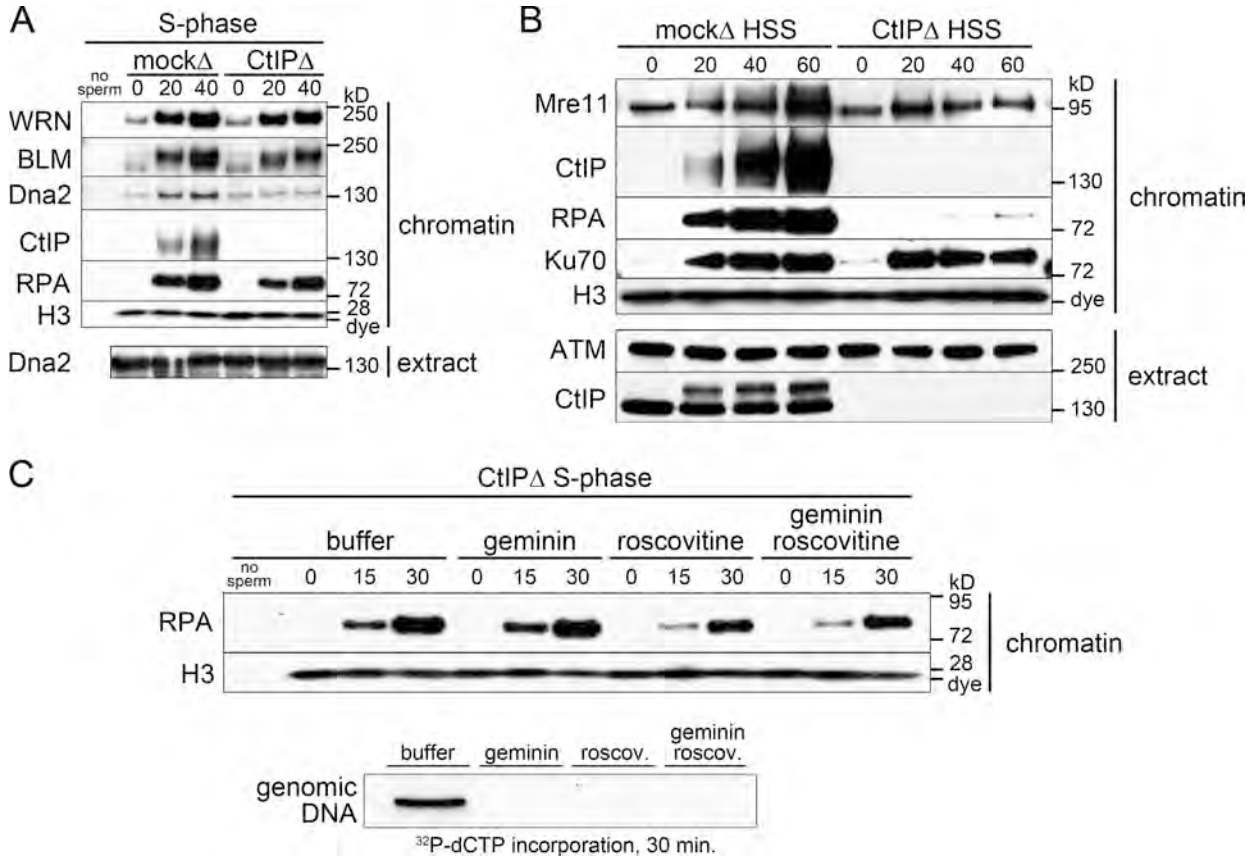

Figure 2. **Characteristics of CtIP-independent resection.** (A) Recruitment of late resection pathway components in the absence of CtIP. The mock- and CtIP-depleted S-phase extract was treated with PflMI restriction endonuclease, and chromatin was isolated at the indicated time points (minutes) followed by Western blotting with the indicated antibodies as in Fig. 1 A. (B) CtIP-independent resection does not occur in membrane-free HSS extract. Mock-depleted or CtIP-depleted membrane-free S-phase HSS extract was preincubated with sperm chromatin (5,000 sperm/μl). Aliquots were taken before (0 min) and at the indicated time after addition of PflMI restriction endonuclease (0.05 U/μl) and processed as in Fig. 1 A. (C) CtIP-independent resection does not require DNA replication. CtIP-depleted S-phase extract was supplemented with recombinant geminin protein, roscovitine (roscov.), both, or buffer and was preincubated with sperm chromatin. (top) 15-μl aliquots of the sample were taken before (0 min) and at the indicated times after addition of 0.05 U/μl PflMI restriction enzyme and processed for chromatin isolation followed by Western blotting. (bottom) In parallel, a 10-μl aliquot of each sample was taken before addition of the restriction enzyme supplemented with 0.1 μl [^{32}P]deoxy-CTP (dCTP) and incubated for 30 min to monitor DNA replication.

metaphase II of meiosis) and monitored recruitment of proteins to damaged chromatin. We confirmed that restriction endonuclease was able to generate DSBs in M-phase condensed chromosomes as indicated by (a) the rapid recruitment of Ku70 (a component of the Ku70/86 heterodimer that binds double-stranded DNA ends with high affinity; Fig. 3 B) and (b) TUNEL of endonuclease-treated chromatin isolated from M-phase extract (Fig. S2 B). ATM association with damaged chromatin peaked 1 min after endonuclease addition and then decreased (Fig. 3 A). A reduction in Mre11 gel mobility, indicating phosphorylation, and maximal histone H2AX phosphorylation was observed at 3 min. CtIP did not bind to undamaged M-phase chromatin but was recruited 3–5 min after damage. Chromatin-bound RPA was detected by 5 min, indicating that ssDNA is generated by DSB resection within M-phase chromatin (Fig. 3 A).

As in S phase, depletion of MRN in M phase abolished recruitment of ATM and, subsequently, CtIP to damaged chromatin (Fig. 3 B). Depletion of CtIP in M phase did not affect ATM or MRN recruitment and H2AX phosphorylation (Fig. 3 B and not depicted). Notably, M-phase extracts depleted of either MRN or CtIP were unable to resect DSBs. CtIP depletion did not affect ATM recruitment and, thus, MRN recognition of DSB; nevertheless, these breaks were not resected. Thus, MRN cannot support resection in the absence of CtIP.

In S phase, but not in M phase, we could detect resection by an MRN-CtIP–independent pathway by 10 min (compare Figs. 1 B and 3 B). However, even with prolonged incubation, we saw no resection in the absence of CtIP in M phase, despite the persistence of DSBs, as shown by Ku70 recruitment (Fig. 3 C). Furthermore, the amount of chromatin-bound RPA was proportional to the amount of endogenous CtIP in the extract, suggesting that CtIP is rate limiting for resection in M phase (Fig. S2 C). Rescue of CtIP-depleted M-phase extract with excess purified recombinant xCtIP protein (Figs. S1 D and S2 D) restored resection activity to mock-depleted levels (Fig. 3 D).

DSB resection also occurs in mitotic M-phase extract

We considered the possibility that resection in M-phase extract might be specific for CSF-arrested meiotic M-phase extract. To address this concern, we prepared a cycling mitotic extract that

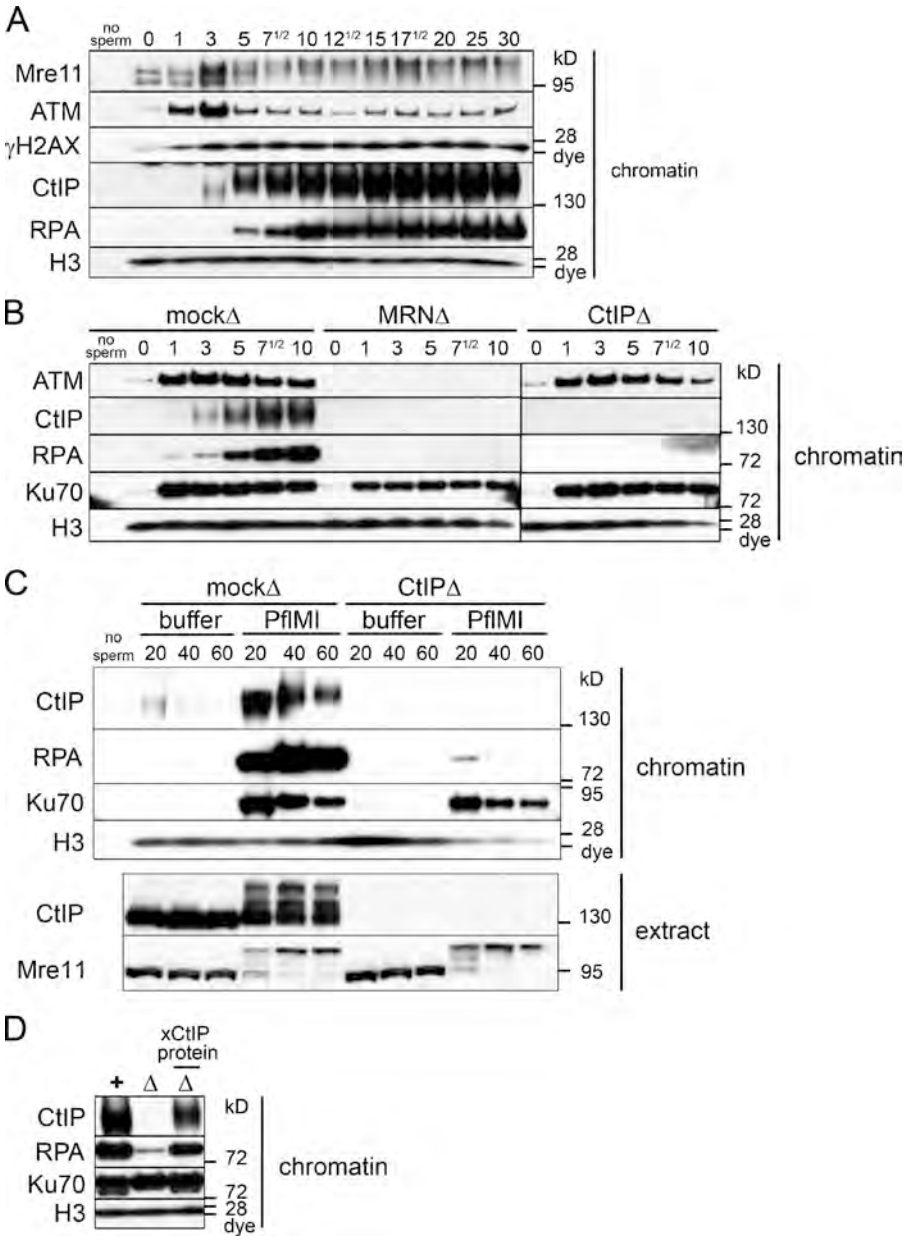

Figure 3. **DSBs generated in M phase undergo only CtIP-dependent resection.** (A) Kinetics of recruitment of proteins to DSB-containing chromatin in M-phase extract. M-phase extract (meiotic and CSF arrested) was preincubated with sperm chromatin (5,000 sperm/µl). 15-µl aliquots of the sample were taken before (0 min) and at the indicated times (minutes) after addition of PflMI restriction endonuclease (0.05 U/µl) and processed for chromatin isolation followed by Western blotting with the indicated antibodies as in Fig. 1 A. (B) All resection is dependent on MRN and CtIP in M-phase extract. Short kinetics of protein recruitment to chromatin in response to DSBs in mock-depleted, Mre11-depleted, and CtIP-depleted M-phase extracts as in Fig. 1 B. (C) No resection occurs in the absence of CtIP in the M-phase extract. Long kinetics of protein recruitment to chromatin in response to DSBs. The mock-depleted or CtIP-depleted M-phase extract was incubated with sperm chromatin and either buffer or PflMI restriction endonuclease for extended time points as in Fig. 1 C. (D) Addition of recombinant xCtIP protein to CtIP-depleted M-phase extract restores resection activity to control levels. Experiment performed as in Fig. 1 D but with the M-phase extract that was mock depleted (+), CtIP depleted (Δ), or CtIP depleted supplemented with 50 nM recombinant xCtIP protein (Δ with xCtIP protein above) as indicated for a 30-min time point. The black line indicates that intervening lanes have been spliced out.

was allowed to complete DNA replication. Nocodazole was then added to arrest the extract in mitosis, after which chromosomal DSBs were induced by restriction endonuclease (Fig. 4 A). Nuclear morphology was monitored by fluorescence microscopy to confirm cell cycle phase (unpublished data). Like CSF-arrested extract, mitotic extract supported CtIP binding to chromatin and DSB resection (Fig. 4 B). This confirms that resection can occur in both meiotic and mitotic M phases. We will continue to refer to CSF-arrested extract as M-phase extract for simplicity.

As an independent means to monitor ssDNA formation directly, we adapted a BrdU detection assay in cycling extract. Chromosomal DNA was replicated in the cycling extract in the presence of BrdU and arrested in the subsequent mitosis. After generation of DSBs, chromatin was isolated, and ssDNA was detected using the anti-BrdU antibody on DNA isolated under nondenaturing conditions (Fig. S3 A). Detection of ssDNA in this way requires replication-dependent incorporation of BrdU (Fig. S3 A, first and second lanes). Notably, consistent with results obtained by monitoring RPA chromatin binding, generation of ssDNA as seen by BrdU staining in M phase is dependent on CtIP (Fig. S3 B, compare mock- or CtIP-depleted extracts).

Human cells undergo resection within mitotic chromosomes

Our finding that resection takes place in the M-phase extract was rather surprising because evidence for mitotic resection in mammalian cells has not been reported. To ascertain whether resection also occurs during mammalian mitosis, we used a focused high-power UV laser to generate discrete regions of DSBs within HeLa cell nuclei. Asynchronous cultures were irradiated and stained for both RPA and the mitotic marker pH3 (phosphorylated histone H3). A fraction of undamaged control cells showed highly condensed mitotic chromosomes that

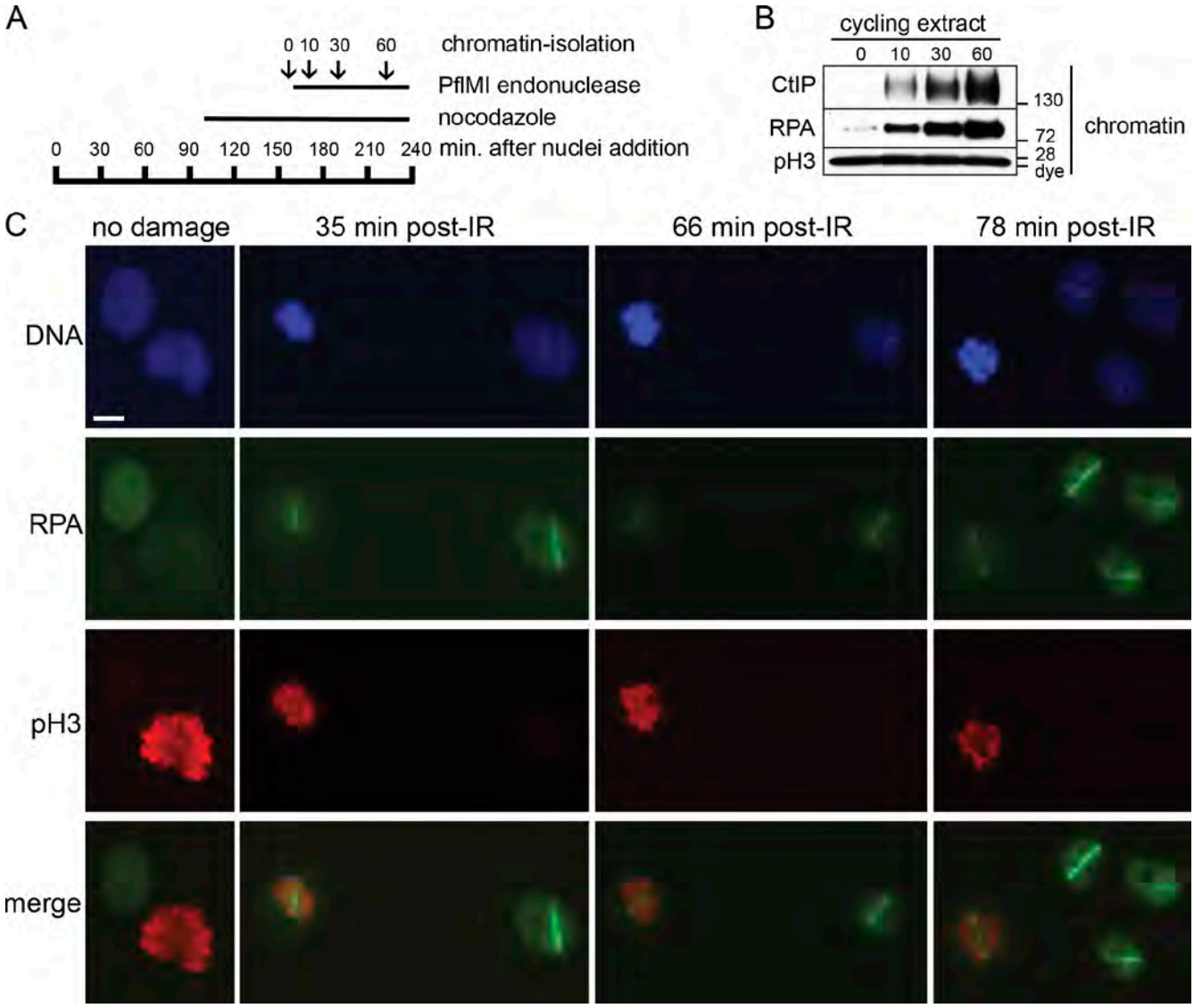

Figure 4. **DSB resection occurs in cycling mitotic *Xenopus* extract and mitosis of human cells.** (A) Schematic timeline of the cycling mitotic extract experiment. Cycling extract was incubated with sperm chromatin (5,000 sperm/µl). Nocodazole was added at 96 min to trap the nuclei in the subsequent mitosis. Microscopy analysis 34 min later confirmed that the chromatin was in a highly condensed state indicative of mitosis. An aliquot was taken before addition of 0.05 U/µl PflMI restriction endonuclease at 163 min (time 0). Aliquots were also taken at 10, 30, and 60 min after addition of PflMI and processed for chromatin isolation and Western blotting. (B) Resection of DSBs occurs in nocodazole-arrested mitotic extract. After arrest with nocodazole, DSBs were induced in the mitotic chromatin, and aliquots were taken before and at the indicated time points (minutes) after addition of PflMI and processed for chromatin isolation and Western blotting with the indicated antibodies. The mitotic status of the extract was also confirmed by the presence of pSer10–histone H3. (C) Resection of DSBs occurs in mitosis of human cells. Asynchronous HeLa cells were grown on 8-well chamber slides and mock irradiated (no damage) or microirradiated using a high-energy UV laser microscope (PALM MicroBeam IV). After the indicated time (±4 min), slides were processed and stained with antibodies against human RPA34 and phospho–Ser10-histone H3. Bar, 10 µm.

stained strongly for pH3 (Fig. 4 C, no damage). Distinct and persistent stripes of RPA were seen after irradiation in both interphase and mitotic cells (Fig. 4 C). 98% of cells irradiated in mitosis scored positive for γ-H2AX (98/100), and 80% scored positive for RPA (80/100). 98% of the RPA-positive cells were also positive for γ-H2AX (78/80; unpublished data). Because the G2/M damage checkpoint prevents irradiated G2 cells from entering mitosis, our data indicate that cells damaged during mitosis resect DSBs. Moreover, because undamaged HeLa cells proceed through mitosis in ∼45 min, cells that persist in metaphase at 66 and 78 min have presumably sustained kinetochore damage, causing arrest because of the spindle assembly checkpoint. We could not determine whether CtIP is required for resection in mammalian mitosis because CtIP is essential for cellular viability (Chen et al., 2005; Nakamura et al., 2010b) and because inactivation of CtIP induces rapid cell cycle arrest (unpublished data).

Phosphorylation of CtIP by Cdk1 is required for M-phase resection

CtIP is phosphorylated by Cdc28 (in budding yeast) and Cdk2 (in mammals) at residues equivalent to T806 of xCtIP. This phosphorylation occurs at the onset of S phase and constitutes a critical switch from C-NHEJ to HDR (Limbo et al., 2007;

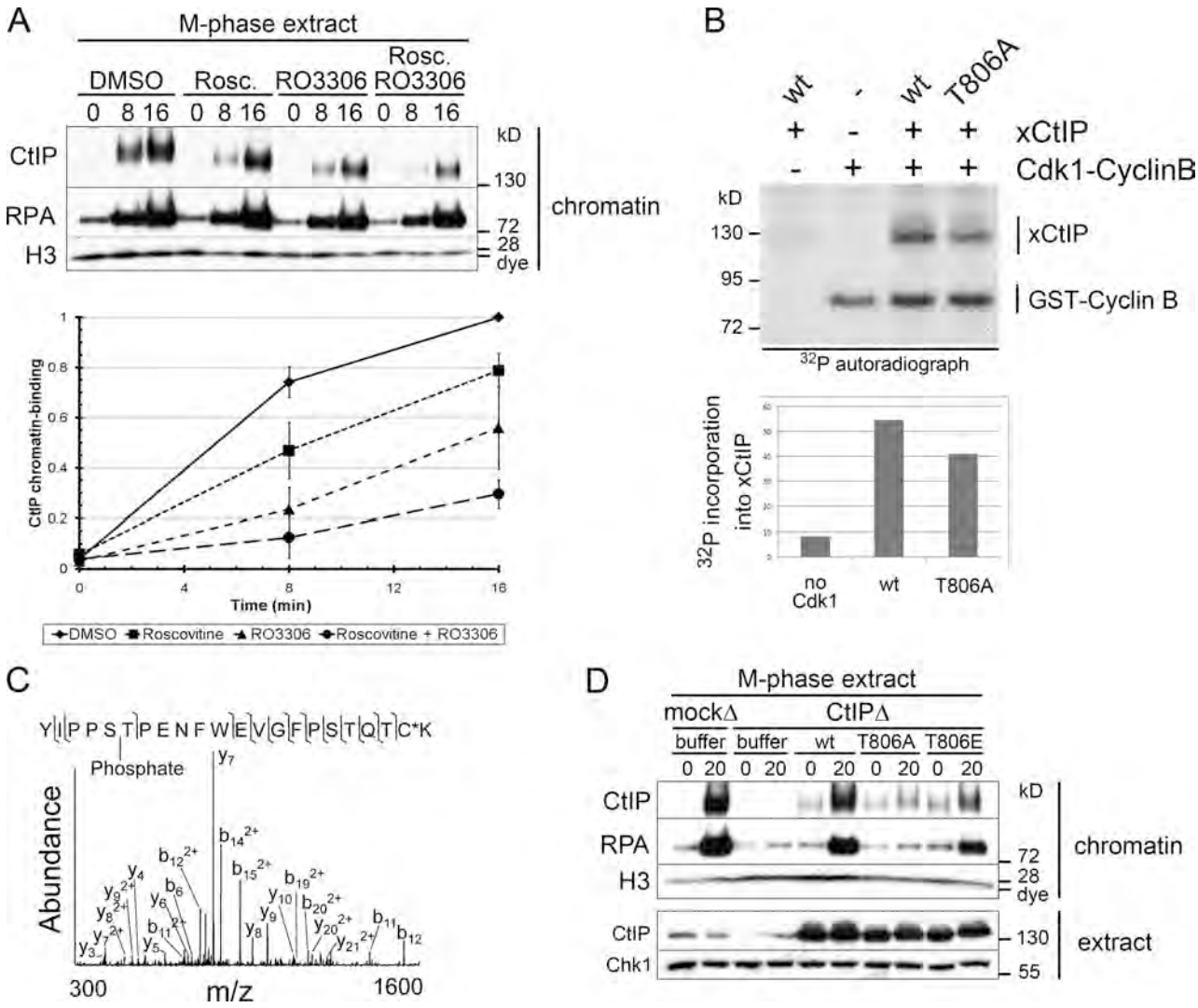

Figure 5. **Phosphorylation of CtIP by Cdk1 is required for M-phase resection.** (A) Cdk activity is required for CtIP function and M-phase resection. M-phase extract was treated with DMSO, 200 µM roscovitine (Rosc.), 200 µM RO-3306, or both, and chromatin was isolated at the indicated time points (minutes) after addition of PflMI restriction endonuclease. Quantification of relative CtIP chromatin binding from three independent experiments is shown on the bottom, with error bars representing one standard deviation. (B) Cdk1–cyclin B kinase phosphorylates recombinant xCtIP in vitro. Recombinant Cdk1–cyclin B was incubated with recombinant xCtIP (wt or T806A) as indicated in the presence of γ-[^{32}P]ATP. Samples were analyzed by SDS-PAGE and autoradiography. Quantification of the autoradiograph signal for xCtIP in this experiment is graphed on the bottom. Note that xCtIP-T806A incorporation is reduced by ∼25% because of the presence of multiple Cdk phosphorylation sites. (C) Tandem mass spectrometry of endogenous M-phase CtIP reveals phosphorylation at S805/T806. Tandem mass spectrum of phosphopeptide spanning residues 801–822. The experimental molecular mass of the intact precursor ion (2664.1613 D) closely matches the theoretical mass of the tryptic peptide 801–822 plus a phosphate group (2664.1607 D; mass difference = 0.0006 D). The fragmentation pattern confirms the identity of this phosphopeptide and narrows the localization of the phosphate group to either S805 or T806. The asterisk indicates that the cysteine residue was alkylated using iodoacetamide. (D) Conserved residue T806 is required for CtIP activity and resection in M phase. M-phase extract was mock depleted or CtIP depleted. CtIP-depleted extract was supplemented with buffer (−), wt xCtIP (wt), xCtIP-T806A (T806A), or xCtIP-T806E (T806E). PflMI restriction endonuclease (+) or buffer (−) was added, and chromatin was isolated after 15 min. Time points above are in minutes. m/z, mass to charge ratio.

Huertas et al., 2008; Huertas and Jackson, 2009). Cdk1–cyclin B is the prominent Cdk activity in M phase. To determine the role of Cdk in M-phase resection, we inhibited Cdk2 with roscovitine and Cdk1 with the highly specific small molecule RO-3306 (Vassilev et al., 2006). Treatment with both inhibitors simultaneously decreased CtIP binding to chromatin by ∼70% (Fig. 5 A). We next established that CtIP is an in vitro substrate for Cdk1–cyclin B (Fig. 5 B). We generated a nonphosphorylatable mutant of CtIP (CtIP-T806A) and purified the recombinant protein from baculovirus-infected insect cells (Fig. S4 A). Phosphorylation of xCtIP-T806A by Cdk1 was reduced relative to wt but not abolished because xCtIP contains several other Cdk sites, including the BRCA1 interaction site S328 (Fig. 5 B). To test whether CtIP was phosphorylated at T806 in M phase, we affinity purified endogenous CtIP from M-phase extract using the CtIP 11–1 mAb and subjected it to mass spectrometry. These results confirmed phosphorylation of CtIP at S805/T806 in M phase (Fig. 5 C).

To address the consequence of T806 phosphorylation on M-phase resection, we rescued CtIP-depleted M-phase extract with purified recombinant wt CtIP, CtIP-T806A, or CtIP-T806E (Fig. S4 B). Importantly, CtIP-T806A failed to bind chromatin

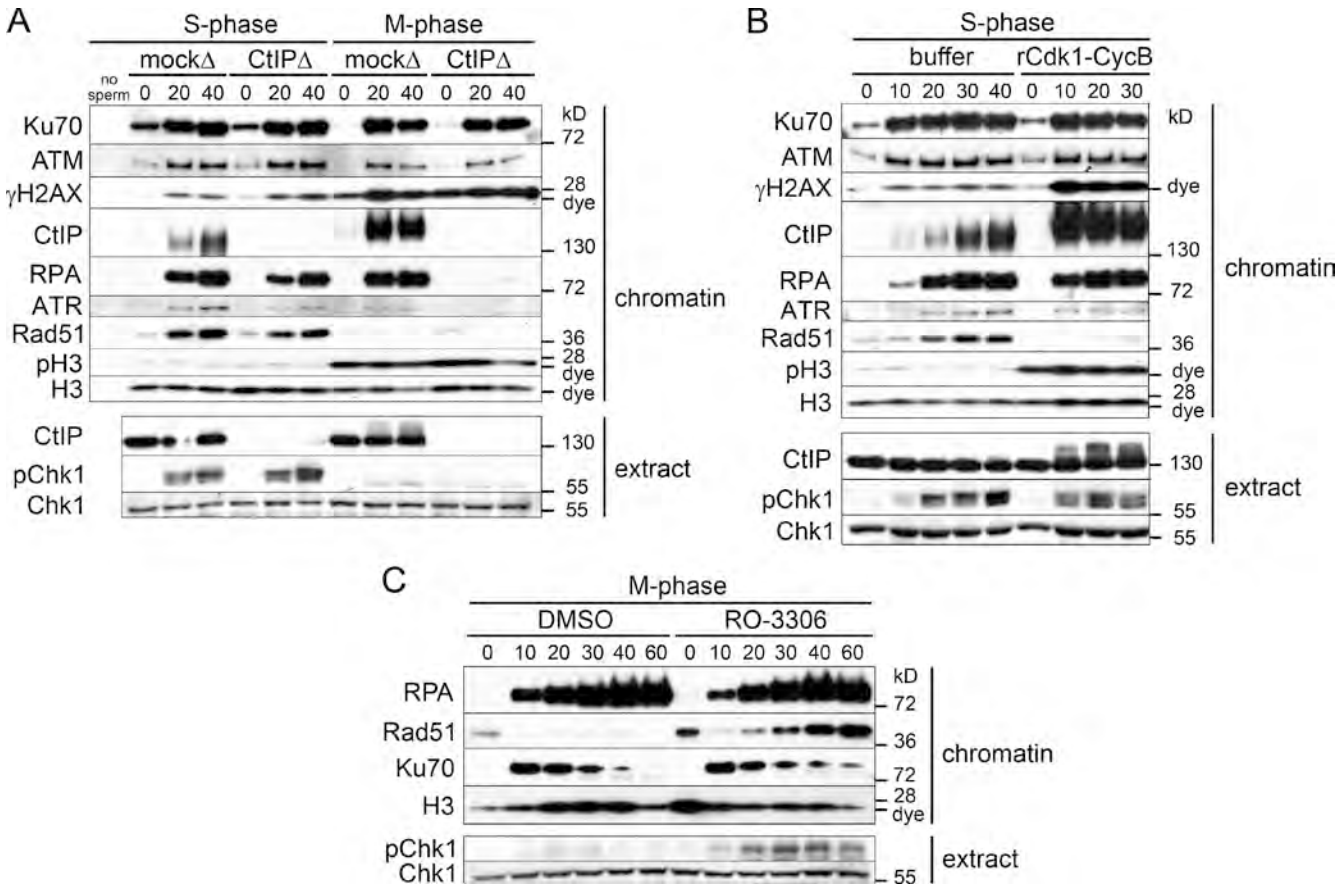

Figure 6. **M-phase Cdk1 activity inhibits Rad51 loading on ssDNA-RPA.** (A) Rad51 accumulates on resected chromatin, and Chk1 becomes activated in S- but not in M-phase extract. S- and M-phase extracts prepared from the same batch of eggs were either mock or CtIP depleted. Chromatin-binding time course in response to DSBs was performed as in Fig. 1 A. (B) Treatment of S-phase extract with Cdk1 inhibits Rad51 chromatin binding but not Chk1 activation. S-phase extract was supplemented with 100 nM recombinant Cdk1–cyclin B protein complex or buffer, and a chromatin-binding time course in response to DSBs was performed as in Fig. 1 A. (C) Inhibition of Cdk1 activity in M phase restores Rad51 accumulation in response to chromosomal DSBs. M-phase extract was supplemented with the specific Cdk1 inhibitor RO-3306 (200 μM) or DMSO, and a chromatin-binding time course in response to DSBs was performed as in Fig. 1 A. Time points above the blots are in minutes.

or to restore resection (Fig. 5 D). In contrast, the phosphomimic T806E mutant supported recruitment to damaged chromatin and resection (Fig. 5 D). This demonstrates that phosphorylation of CtIP by Cdk1 at T806 is required for resection of mitotic chromosomes. Phosphorylation of this same site is also required for CtIP-dependent resection in S-phase extract (Fig. S4, C and D).

M-phase resection does not lead to Rad51 chromatin recruitment or Chk1 activation

ssDNA generated in S-G2 sequentially activates ATR and Chk1, leading to inhibition of Cdk (Löbrich and Jeggo, 2007). Additionally, formation of ssDNA is the first step of the HDR pathway. Both of these outcomes pose problems to M-phase cells. Down-regulation of the mitotic kinase Cdk1, when chromosomes are highly condensed and under tension from spindles, could induce spontaneous exit from mitosis, with devastating consequences to genome integrity. In addition, condensed sister chromatids should not be available for homology search and HDR. To compare the consequences of DSB resection in S and M phase, we monitored Chk1 activation (phosphorylation on S344 in extract) and Rad51 chromatin binding in mock- or CtIP-depleted S- and M-phase extracts prepared from the same batch of eggs (Fig. 6 A). As also shown in Figs. 1 and 3, CtIP depletion delayed resection in S phase and abolished resection in M phase. As anticipated, ATR associated with chromatin, and Chk1 was activated in S phase after resection (Fig. 6 A). In contrast, despite generation of ssDNA-RPA, little chromatin-bound ATR was observed, and we failed to detect Chk1 activation in M phase. Consistent with this finding, damaged chromatin did not significantly reduce Cdk1 activity in M-phase extracts (Fig. S5 A). Chromatin-bound Rad51 was detected in control and CtIP-depleted S-phase extracts treated with a restriction enzyme, indicating that CtIP-independent resection can support Rad51 loading. In contrast, no chromatin-bound Rad51 was observed in M phase (Fig. 6 A).

Cdk1 activity inhibits Rad51 chromatin assembly on RPA-ssDNA intermediates

We then asked whether Cdk1 inhibits Rad51 loading and/or Chk1 activation. In the S-phase extract, levels of chromatin-associated Rad51 increased with time after induction of DSBs (Fig. 6 B, buffer). Addition of recombinant Cdk1–cyclin B (Fig. S5 B) to endogenous levels (Fig. S5 C) abrogated Rad51 filament assembly on resected DNA (Fig. 6 B). S-phase extract

incubated with Cdk1 resembled a mitotic extract, as indicated by robust H3 phosphorylation and damage-induced hyperphosphorylation of CtIP and H2AX (Fig. 6 B). Notably, Cdk1 activity abrogated Rad51 filament formation but did not prevent Chk1 activation.

Next, we examined the effect of Cdk1 inhibition in M phase by RO-3306 (Vassilev et al., 2006). As before, endonuclease treatment of M-phase extract induced robust resection and RPA binding but no Chk1 activation or Rad51 chromatin accumulation (Fig. 6 C, DMSO). Importantly, Cdk1 inhibition permitted Rad51 binding to damaged chromatin and partial activation of Chk1 (Fig. 6 C). Together, these data confirm that Rad51 chromatin loading is inhibited in a Cdk1-dependent manner downstream of the formation of ssDNA-RPA.

Discussion

Here, we show that vertebrate resection proceeds via distinct pathways in S phase (Fig. 1). We observe an early pathway that is dependent on both the MRN complex and CtIP. We also demonstrate robust but delayed resection in the absence of MRN-CtIP, which we denote as the late resection pathway. In *Saccharomyces cerevisiae*, resection also occurs by two distinct pathways (Mimitou and Symington, 2009). An initiating MRX- and Sae2-dependent endonucleolytic cleavage of 50–100-nt oligonucleotides from the 5′ strand is followed by a highly processive resection step involving helicases and nucleases, including Sgs1 (RecQ homologue), Dna2, and Exo1. In vertebrates, several factors have been implicated in resection of DSBs, including DNA2 (Liao et al., 2008), Exo1 (Bolderson et al., 2010), and the two RecQ homologues BLM (Gravel et al., 2008; Nimonkar et al., 2008) and WRN (Yan et al., 2005; Toczylowski and Yan, 2006). In our experiments, we show that both the BLM and WRN helicases are recruited independently of CtIP in S phase (Fig. 2 A) and are good candidates for late vertebrate resection factors. In contrast to WRN and BLM, recruitment of DNA2 to damaged chromatin was CtIP dependent. This is reminiscent of results obtained in *S. cerevisiae*, which show that Dna2 recruitment to DSBs is dependent on Mre11 (Shim et al., 2010). Our data indicate that the multistep process of DNA resection at DSBs is evolutionarily and functionally conserved from yeast and vertebrates.

Recent work by You et al. (2009) demonstrated that all resection in the *Xenopus* S-phase extract is exclusively dependent on CtIP. However, those experiments were performed in membrane-free HSS extracts. Our work shows that CtIP-independent resection does not occur in HSS extracts (Fig. 2 B) and that these investigators were, therefore, unable to detect late pathway resection, which is recapitulated only in complete extracts containing membranes.

Whether the BRCA1–CtIP interaction plays a significant role in DSB resection is presently unclear. A recent study using chicken lymphoblastoid DT40 cells reported that, although CtIP was dispensable for cell viability, the BRCA1–CtIP interaction was essential for DSB resection and subsequent HDR (Yun and Hiom, 2009). In contrast, Nakamura et al. (2010b) reported that CtIP was required for viability and that the BRCA1–CtIP interaction was dispensable for DSB resection and HDR in DT40 cells. We find that xCtIP-S328A, a point mutant that is defective for the BRCA1–CtIP interaction, is able to support resection of restriction endonuclease–induced DSBs when added to a CtIP-depleted extract (Fig. 1 E). Whereas our results suggest that BRCA1 is dispensable for resection of simple DSB ends, it is possible that BRCA1 is required to resect complex DNA ends. For example, cells harboring mutant CtIP defective in the BRCA1 interaction are sensitive to camptothecin, a topoisomerase inhibitor that creates DSBs with covalently attached protein adducts (Nakamura et al., 2010b). Additionally, Sae2/CtIP has been shown to process DNA ends containing adducts, including Spo11 and topoisomerase adducts (Keeney and Kleckner, 1995; Penkner et al., 2007; Hartsuiker et al., 2009; Nakamura et al., 2010b).

The fate of DSBs sustained during vertebrate mitosis is largely unknown. During this dynamic cell cycle phase, chromatin is highly condensed and may be relatively inaccessible to DNA metabolic enzymes. However, we show that DSBs are readily generated by restriction endonucleases in M phase and that resection of DSBs does indeed occur in *Xenopus* meiotic and mitotic M-phase extracts, as well as during mitosis in cultured human cells (Figs. 3 and 4). Previously, RPA was shown to relocalize in mitotic mammalian cells in response to ionizing radiation (Stephan et al., 2009).

Despite CtIP-dependent generation of ssDNA-RPA in M phase, we show that ATR does not accumulate to S-phase levels on damaged chromatin, and Chk1 is not activated, suggesting a defect in assembly of signaling complexes on ssDNA-RPA (Fig. 6 A). This is in agreement with a recent study showing that Chk1 was not phosphorylated in response to ionizing radiation in nocodazole-arrested human cells (Giunta et al., 2010). The mechanism of Chk1 repression in M phase is distinct from inhibition of Rad51. Thus, Cdk1 does not block Chk1 activation, whereas it completely prevents association of Rad51 with damaged DNA (Fig. 6 B). We propose that assembly of ATR-signaling complexes is inhibited during M phase because of a lack of an S-phase kinase activity, rather than Cdk1 activity itself.

Our experiments reveal a critical role for the mitotic kinase Cdk1 in regulating DSB repair in M phase. We establish that Cdk1–cyclin B phosphorylates CtIP at T806 and that the T806A phosphomutation completely abrogated resection in M phase (Fig. 5 D). T806 is also the target for Cdk2 phosphorylation at the onset of S phase, and phosphorylation of this site is required for S-phase resection in budding yeast and mammalian cells (Limbo et al., 2007; Huertas et al., 2008; Huertas and Jackson, 2009), as well as *Xenopus* extracts (Fig. S4, C and D). Moreover, we find that repression of Rad51 chromatin accumulation in M phase is caused by Cdk1 activity because addition of the recombinant Cdk1–cyclin B protein to S-phase extract abolished Rad51 binding (Fig. 6 B). In vitro and structural studies have shown that Cdk1-dependent phosphorylation of the C terminus of BRCA2 disrupts the interaction of that domain with Rad51, causing destabilization of Rad51 filaments and inhibition of HDR repair assays (Esashi et al., 2005, 2007). Moreover, human cells that have entered mitosis with DNA damage display γ-H2AX but not Rad51 foci (Ayoub et al., 2009). Our data

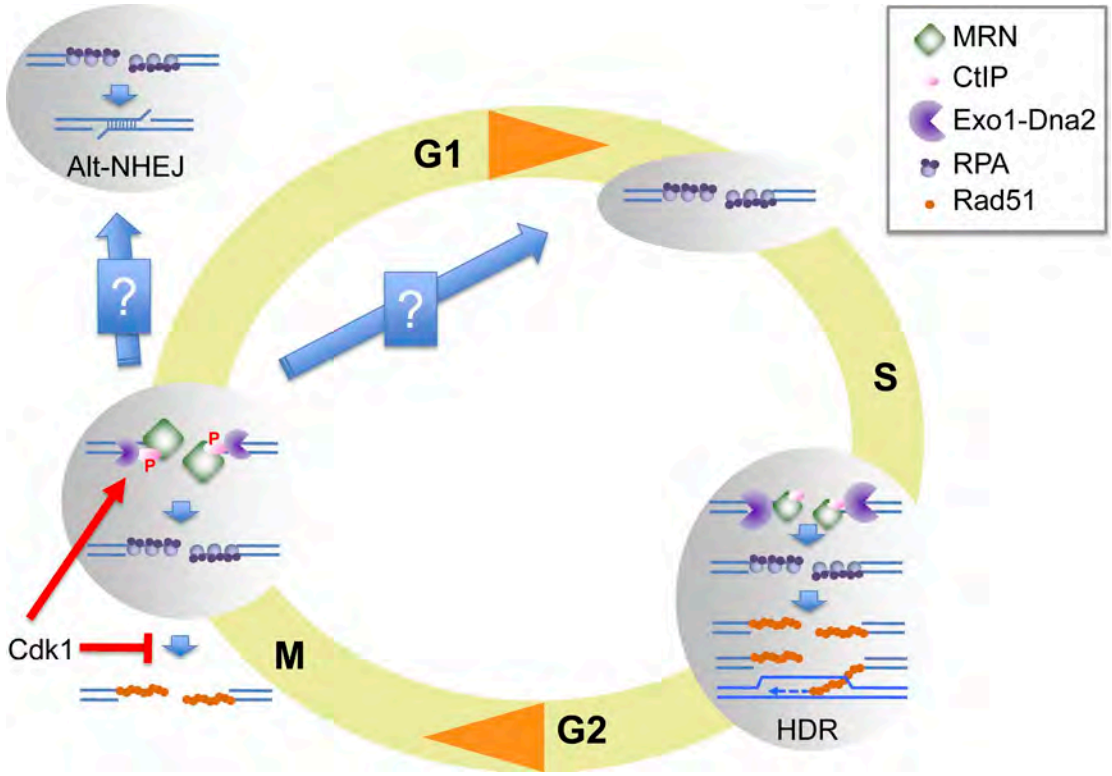

Figure 7. **Chromosomal DNA DSB resection in M phase.** DNA DSBs generated in S phase are resected via the concerted action of MRN-CtIP and two additional pathways represented here as a single Exo1-DNA2 entity. S-phase resection generates ssDNA-RPA, which is competent for Rad51 filament assembly, a necessary step for HR. In contrast, DSBs generated in M phase are processed into ssDNA-RPA intermediates that do not support Rad51 chromatin assembly. Cdk1 promotes resection by phosphorylating CtIP while at the same time inhibiting Rad51 chromatin assembly. Resection initiation is dependent on MRN-CtIP in M phase as reflected by the relative size of the resection machinery components. M-phase resection generates ends that are not compatible for repair by NHEJ or by HR. These ends could be substrates for microhomology-mediated end joining in M or G1 phase. Alternatively, they could be transmitted to the next S phase and repaired by HR. P, phosphorylation.

support these findings by showing that Rad51 association with ssDNA generated from DSB resection was inhibited by Cdk1. It is also possible that Cdk1-dependent phosphorylation of RPA32 prevents exchange of RPA for Rad51 on ssDNA. In support of this hypothesis, serines 23 and 29 of RPA32 are phosphorylated specifically in mitosis (Oakley et al., 2003; Anantha et al., 2008). Together, our study reveals a role for Cdk1 in the DNA damage response to DSBs.

Our results demonstrate that Cdk1 promotes the initiation of DSB resection and accumulation of ssDNA-RPA while at the same time inhibiting Rad51, thus uncoupling resection from downstream high-fidelity HDR (Fig. 7). Chromosome condensation and dynamic chromosome movement may prevent strand invasion and homology search in M phase. Repression of Rad51 association with ssDNA, therefore, may prevent potentially abortive homologous recombination (HR) attempts. Additionally, by disrupting the double-stranded nature of DNA ends, resection inhibits Ku and thereby prevents C-NHEJ. However, short-range resection in the absence of Rad51 assembly may promote toxic, CtIP-dependent Alt-NHEJ, a repair pathway recently shown to be responsible for a majority of chromosomal translocations (Fig. 7; Lee-Theilen et al., 2011; Zhang and Jasin, 2011).

Although we cannot directly assess the consequences of this CtIP- and M phase–dependent mode of resection, we posit that, if not immediately repaired by Alt-NHEJ, repair of DSBs incurred in M phase is delayed until the next cell cycle, at which point repair can proceed by high-fidelity mechanisms to preserve genome stability. In budding yeast, repair of a portion of DSBs sustained in G1 phase is delayed until HDR is possible in the following S phase (Lee and Petes, 2010). Moreover, budding yeast mitotic chromosomes harboring a DSB do not missegregate the chromosome fragment. Instead, the MRN complex facilitates maintenance of the broken DNA within a functional chromosome (Lobachev et al., 2004). Therefore, the same protein complex that is responsible for processing the DSB also ensures that the broken chromosome arm distal from the centromere is properly segregated.

In agreement with this notion, damaged DNA generated during mitosis in mammalian cells is marked by γ-H2AX, but these breaks persist and do not recruit repair factor 53BP1 until the cells exit mitosis (Giunta et al., 2010). Similarly, underreplicated DNA that escapes the G2/M damage checkpoint can form ultrafine bridges and chromosome breakage during mitosis (Chan et al., 2009). These breaks persist into the daughter cells, marked by 53BP1 after mitotic exit, until the subsequent S phase (Lukas et al., 2011). Together, these findings support a model in which damage is transmitted through mitosis to be repaired in the subsequent cell cycle after chromatin decondensation (Giunta and Jackson, 2011). A better understanding of how

cells handle and process DSBs occurring in mitosis has important implications for evaluating the impact of ionizing radiation and radiomimetic drugs on genome integrity.

Materials and methods

Chemicals and reagents

Caffeine, roscovitine, and nocodazole were obtained from Sigma-Aldrich. Ku55933 was obtained from KuDOS Pharmaceuticals. RO-3306 was obtained from Enzo Life Sciences. PflMI and terminal transferase were obtained from New England Biolabs, Inc. Histone H1 (382150) was obtained from EMD. PKA inhibitor (PKI) peptide (TTYADFIASGRTGRRNAIH) was obtained from Sigma-Aldrich.

Extract and sperm chromatin preparation

For preparation of all types of extracts, adult female *Xenopus* frogs (Nasco) were injected subcutaneously with 50 U pregnant mare serum gonadotropin (EMD) 4–7 d before extract preparation. To induce ovulation, 800 U human chorionic gonadotropin (Sigma-Aldrich) was injected subcutaneously 16–20 h before extract preparation.

Mitochondria-free crude S-phase and M-phase egg extract (freezable extract) was originally described by Kubota and Takisawa (1993) and subsequently modified by Trenz et al. (2008). Accordingly, eggs were collected and rinsed in 0.25× MMR solution (20 mM Hepes-KOH, pH 7.5, 400 mM NaCl, 1 mM $MgSO_4$, 2 mM $CaCl_2$, and 0.1 mM EDTA). After dejellying with 5 mM DTT, 20 mM Tris, pH 8.5, and 110 mM NaCl, eggs were washed with 0.25× MMR. For S-phase extracts, eggs were activated with 1 µg/ml calcium ionophore A23187 (Sigma-Aldrich) and then washed several times with S buffer (50 mM Hepes-KOH, pH 7.5, 50 mM KCl, 2.5 mM $MgCl_2$, and 250 mM sucrose) and once with S buffer plus 2 mM β-mercaptoethanol and 15 µg/ml leupeptin. For M-phase extracts, activation with A23187 was omitted, and S buffer was supplemented with 5 mM EGTA. Eggs were then spun at 160 *g* for 1 min in a swing-bucket Sorval rotor (HB-6; Thermo Fisher Scientific) to pack, and excess buffer was aspirated. Eggs were crushed at 16,500 *g* for 15 min at 4°C. The crude extract between the yolk top layer and pigmented granules was transferred to new tubes, supplemented with 20 µg/ml cytochalasin B (Sigma-Aldrich), and homogenized by rotation for 5 min at 4°C. The extract was then subjected to a high-speed spin in an ultracentrifuge (L8-80; Beckman Coulter) in a swing-bucket rotor (SW50.1; Beckman Coulter) for 15 min at 200,000 *g* at 4°C. The cytosolic and lipid membrane fractions were collected (excluding mitochondria directly below the membrane layer) and supplemented with 30 mM creatine phosphate, 150 µg/ml phosphocreatine kinase, and 20 µg/ml cycloheximide. Finally, extracts were mixed well with glycerol to 3% and were either immediately immunodepleted (see Immunodepletions) or flash frozen in 20-µl drops into liquid nitrogen to be later thawed and used for experiments and/or immunodepletion.

The membrane-free HSS extract was prepared as previously described (Smythe and Newport, 1991). In brief, eggs are washed, dejellied, packed, and crushed as in the previous paragraph. The crude extract was then spun at 46,000 rpm in a swing-bucket rotor (SW50.1) for 2.5 h. The clear, membrane-free HSS extract (top layer) was recovered, carefully excluding the cloudy membrane layer below. The HSS was either immediately immunodepleted or aliquoted to 100 µl into microcentrifuge tubes, flash frozen in liquid nitrogen, and stored at −80°C.

Cycling extract was prepared as previously described (Murray, 1991). Crude M-phase (CSF arrested) extract was activated with 0.4 mM $CaCl_2$ for 15 min at 21°C in the absence of cycloheximide. Note that it is important that the CSF-arrested extract is not clarified, either by high-speed centrifugation (as with preparation of mitochondria-free crude low speed supernatant [LSS]) or by centrifugation in a table-top Eppendorf centrifuge, as the clarified CSF extract is unable to be "activated" by calcium and will remain CSF arrested.

Demembranated sperm nuclei (chromatin) were isolated as previously described (Murray, 1991). In brief, male frogs were injected with 25 U pregnant mare serum gonadotropin 3 d before and with 125 U human chorionic gonadotropin 16 h before sperm preparation. The testes were removed from anesthetized frogs, trimmed of fat and blood vessels, and placed in a dish with cold 0.25× MMR. Testes were washed three times in NPB (250 mM sucrose, 15 mM Hepes, pH 7.7, 1 mM EDTA, 0.5 mM spermidine, 0.2 mM spermine, and 1 mM DTT). Excess NPB was removed, and testes were macerated with a razor for 20 min. The material was diluted in 10 ml NPB, filtered through cheesecloth, and spun in a swing-bucket rotor (HB-6) at 6,000 *g* for 15 min. The supernatant was discarded, and the sperm pellet was washed and spun twice more. Sperm were demembranated by incubation in NPB with 0.2% Triton X-100 for 15 min at RT with gentle agitation. Demembranated sperm chromatin was then washed and recovered by spinning at 6,000 *g* in cold NPB + 3% BSA (with protease inhibitors) and then twice in cold NPB + 0.3% BSA and finally resuspended in NPB + 0.3% BSA + 30% glycerol. Small aliquots of 10 µl were flash frozen in liquid nitrogen and stored at −80°C.

Antibodies

Anti-CtIP mouse monoclonal antibody (11–1) was raised against a GST fusion protein containing the C-terminal 278 amino acids of human CtIP (residues 620–897) as described previously (Yu and Baer, 2000). The following rabbit antisera were generated in our laboratory as previously described: *Xenopus* Mre11 (Di Virgilio and Gautier, 2005), *Xenopus* ATM (Dupré et al., 2008), *Xenopus* ATR (Costanzo and Gautier, 2003), and *Xenopus* Cdk1 (Gautier et al., 1989).

The following antibodies were obtained from commercial sources: antiphospho–histone H2AX Ser139 (05-636; Millipore), anti–histone H3 (9715; Cell Signaling Technology), anti-Ku70 (SC-56129; Santa Cruz Biotechnology, Inc.), antiphospho-Chk1 Ser345 (2341; Cell Signaling Technology), anti–human RPA32 (MS-691-PO; NeoMarkers), antiphospho–histone H3 Ser10 (05-817; Millipore), and anti-Exo1 (NBP1-19709; Novus Biologicals). The following antibodies were received as gifts: RPA70 (P. Jackson, Genentech, South San Francisco, CA), *Xenopus* Rad51 (K. Maeshima, National Institute of Genetics, Shizuoka, Japan), total *Xenopus* Chk1 (J. Sible, Virginia Polytechnic Institute, Blacksburg, VA), *Xenopus* BLM (W. Dunphy, California Institute of Technology, Pasadena, CA), *Xenopus* DNA2, and *Xenopus* WRN (H. Yan, Fox Chase Cancer Center, Philadelphia, PA).

Immunodepletions

Immunodepletions were performed by prebinding washed protein–A Sepharose CL-4B beads (GE Healthcare) with serum or hybridoma supernatant overnight with constant rotation at 4°C in compact reaction columns (United States Biochemicals). The antibody beads were then washed extensively and resuspended in extract, rotated at 4°C for 40 min, and collected for a second round of depletion. A 3:1 ratio of extract/beads (bed volume) was used for all immunodepletions. The amount of antibody used for each depletion (extract/antibody volume per round) was as follows: mouse IgG (015-000-002; Jackson ImmunoResearch Laboratories, Inc.) for mock depletions (1:0.044), *Xenopus* Mre11 rabbit serum (1:1), CtIP 11–1 monoclonal hybridoma supernatant (1:1.5), and *Xenopus* Cdk1 rabbit serum (1:1).

Assay to monitor the response to chromosomal DSBs

Extracts were preincubated with demembranated sperm nuclei (5,000 sperm/µl) for 10 min at 21°C to allow the DNA to become chromatinized. Aliquots of the sample were taken before (0 min) and at time points (minutes) after addition of the PflMI restriction enzyme (0.05 U/µl; New England Biolabs, Inc.). As indicated, at each time point, 0.5 µl extract/chromatin was removed from the sample and diluted in 9.5 µl Laemmli buffer. Samples (extract) were fractionated on 7% SDS-PAGE minigels and processed for Western blotting according to standard procedures. In parallel, at each time point, chromatin was isolated. 15-µl aliquots were diluted with 800 µl ice-cold chromatin isolation buffer (50 mM Hepes-KOH, pH 7.8, 100 mM KCl, and 2.5 mM $MgCl_2$) with 0.125% Triton X-100 and kept on ice for 10 min. 320 µl chromatin isolation buffer plus 30% sucrose (wt/vol) was added to low-retention microcentrifuge tubes (Thermo Fisher Scientific), and the diluted extract/chromatin was carefully layered on top of the sucrose cushion. Samples were spun at 8,500 *g* for 30 min at 4°C in a swing-bucket Sorval rotor (HB-6). The chromatin pellet was mixed with 15 µl Laemmli buffer, boiled, and fractionated on 3–8% Tris-acetate minigels (NuPAGE; Invitrogen) and processed for Western blotting according to standard procedures.

Cloning of xCtIP

xCtIP cDNA was acquired from Thermo Fisher Scientific (IMAGE [Integrated Molecular Analysis of Genomes and their Expression] ID 5514434; available from GenBank/EMBL/DDBJ under accession no. BC073395). The full-length cDNA was PCR amplified using cloning oligonucleotides encoding a 5′ 3×FLAG tag and a 3′ 6×His tag as well as unique restriction sites for subcloning: 5′ sense cloning oligonucleotide (3×FLAG; SalI), 5′-CGAGCTGTCGACCACCATGGACTACAAAGACCATGACGGTGATTATAAAGATCATGATATCGATTACAAGGATGACGATGACAAGGGAAGCATCACAGCATCCACTTGTGGCAGC-3′; and 3′ antisense cloning oligonucleotide (6×His; NotI), 5′-GCAGTGCGGCCGCCTAGTGGTGATGGTGATGATGTCCGGTCTTCTGCTCTTTAATCTTCG-3′.

The resulting PCR product was purified and digested with the engineered restriction sites and subcloned into pFastBac1. The xCtIP-pFastBac1 clone underwent transposition in host DH10Bac bacterial cells. The bacmid DNA was isolated and transfected into *Sf9* insect cells to generate recombinant baculovirus following the manufacturer's instructions (Bac-to-Bac; Invitrogen).

Site-directed mutagenesis of xCtIP

xCtIP mutants were generated by two-step PCR. In brief, wt xCtIP cDNA was used as a template for two separate PCR reactions, left and right. The left reaction contains the NotI-xCtIP forward oligonucleotide and the specific mutagenic sense oligonucleotide, which harbors the point mutation and also creates a novel restriction site for verification. The right reaction contains the xCtIP-EcoRI reverse oligonucleotide complementary to a naturally occurring EcoRI site in the middle of the xCtIP reading frame and the specific mutagenic antisense oligonucleotide, which harbors the point mutation and also creates a novel restriction site for verification. The PCR products are gel purified to remove parental template and mixed for use in a final PCR reaction containing only the NotI-xCtIP forward and xCtIP-EcoRI reverse oligonucleotide, to give a truncated mutant product. Digestion of the full-length wt clone with EcoRI and SalI and the truncated mutant PCR product with EcoRI and NotI, gel purification of the appropriate bands, and ligation yield the full-length mutant xCtIP coding sequence. The full-length coding sequence is then cloned into pBluescript (NotI and SalI sites) and sequenced for verification. The xCtIP sequence is then subcloned into pFastBac1, and the mutations were again verified by digestion with restriction enzymes corresponding to the novel sites introduced into the mutants.

The sequences for these primers were as follows: NotI-xCtIP forward, 5′-GCGGTGGCGGCCGCCTAGTGGTG-3′; xCtIP-EcoRI reverse, 5′-GTTGAATTCACTGAAGGTTCTATGG-3′; S328A sense (creates the AgeI site), 5′-GGAATAGAAGGGAAGCAGCACCGGTTTTTGGAGAACCTGTG-3′; S328A antisense (creates the AgeI site), 5′-CACAGGTTCTCCAAAAACCGGTGCTGCTTCCCTTCTATTCC-3′; T806A sense (creates the AfeI site) 5′-CGATACATTCCACCAAGCGCTCCTGAGAATTTTTGGGAG-3′; T806A antisense (creates the AfeI site), 5′-CTCCCAAAAATTCTCAGGAGCGCTTGGTGGAATGTATCG-3′; T806E sense (creates the BseYI site), 5′-GATTCCGATACATTCCACCCAGCGAGCCTGAGAATTTTTGGGAG-3′; and T806E antisense (creates the BseYI site) 5′-CTCCCAAAAATTCTCAGGCTCGCTGGGTGGAATGTATCGGAATC-3′.

Recombinant protein purification

3 d after infection with wt or mutant xCtIP baculovirus, *Sf9* cells were harvested, and lysates were subjected to affinity purification. In brief, cells were washed in PBS and lysed in wash buffer (50 mM Tris-Cl, pH 7.5, 200 mM NaCl, 0.5% Triton X-100, and 10% glycerol) with protease inhibitor cocktail (Sigma-Aldrich) and phosphatase inhibitors (250 mM NaF, 50 mM sodium vanadate, 50 mM β-glycerophosphate, and 50 mM sodium pyrophosphate decahydrate). Lysate was dounced, cleared by centrifugation at 17,000 *g*, and incubated with equilibrated anti-FLAG M2 antibody-conjugated beads (Sigma-Aldrich) for 3 h at 4°C. Beads were then washed extensively in wash buffer and twice with elution buffer (25 mM Tris-Cl, pH 7.5, 50 mM NaCl, 0.01% Triton X-100, 20% glycerol, protease inhibitor cocktail, and 10 mM β-glycerophosphate). Protein was eluted with elution buffer plus 300 µg/ml 3×FLAG peptide (Sigma-Aldrich). Small aliquots were flash frozen in liquid nitrogen and stored at −80°C.

The Cdk1–cyclin B-GST complex was purified using glutathione beads (GE Healthcare) according to the manufacturer's instructions. Kinase activity of the recombinant complex was verified and calibrated to endogenous Cdk1–cyclin B activity of M-phase extracts by performing the histone H1 kinase assay as described previously (Smythe and Newport, 1991).

DNA replication assay

10-µl aliquots of extract/chromatin were removed from the reaction, and 0.1 µl [^{32}P]deoxy-CTP was added and incubated for 30 min at 21°C. DNA was then isolated by proteinase K digestion at 60°C for 1 h before phenol/chloroform extraction and ethanol precipitation. The DNA pellet was then resuspended in 20 µl water and run on a 0.8% agarose gel. The bottom third of the gel containing unincorporated radioactive nucleotide was cut off and discarded, and the remainder was fixed in 30% trichloroacetic acid, dried by pressing between Whatman paper and paper towels overnight, and exposed to x-ray film (Costanzo et al., 2000).

Immunofluorescence of UV laser-irradiated HeLa cells

HeLa cells were cultured on 8-well chamber slides (Thermo Fisher Scientific) and sensitized overnight with 10 µM BrdU (Sigma-Aldrich). Cells were microirradiated with a 355-nm solid-state UV laser using a microscope (PALM MicroBeam IV; Carl Zeiss). Slides were fixed in 4% paraformaldehyde for 5 min at RT, permeabilized with 0.1% Triton X-100 for 10 min, and blocked in a 50% FBS/5% milk solution. Slides were then stained with antibodies at a 1:1,000 dilution in 3% BSA overnight at 4°C, washed thoroughly with 0.2% PBS-Tween, and then incubated with the appropriately labeled secondary antibodies for 1 h at RT. Antibodies used were rabbit antiphospho-Ser10 histone H3 (05-817) with goat anti–rabbit Alexa Fluor 568 secondary fluorescent antibody and mouse anti-RPA34 (Ab-1 MS-691-PO; NeoMarkers) with goat anti–rabbit Alexa Fluor 488 secondary fluorescent antibody. After thorough washing with 0.2% PBS-Tween, cells were mounted with Vectashield medium with DAPI (Vector Laboratories). Slides were imaged on a microscope (Eclipse E400; Nikon) using a Plan Fluor 40× objective lens (0.75 numerical aperture, 0.72-mm working distance; Nikon) at RT. Images were captured with a camera (CoolSNAP EZ; Photometrics) and NIS-Elements software (F package, version 2.20; Nikon). Red (A568), green (A488), and blue (DAPI) images of the same cells were merged and assigned to R, G, or B channel in Photoshop CS (version 8.0; Adobe). Final images were produced in Photoshop CS by showing all three channels (merge) or turning down the output (levels) of two channels to show only one.

Histone H1 kinase assay (endogenous Cdk1 activity) and in vitro kinase assay of Cdk1–cyclin B and xCtIP

The assay to measure activity of endogenous (or added recombinant) Cdk1–cyclin B in extract was modified from Smythe and Newport (1991). 1 µl extract was diluted in 119 µl elution buffer (80 mM glycerol-2-phosphate, 10 mM $MgCl_2$, and 5 mM EGTA) and flash frozen in liquid nitrogen until all samples were collected. Samples were thawed on ice, 10 µl diluted extract was mixed with 10 µl kinase mix (20 mM Hepes, pH 7.5, 5 mM EGTA, 10 mM $MgCl_2$, 0.4 mg/ml histone H1, 20 µM PKI peptide, 350 µM ATP, and 0.25 µl γ-[^{32}P]ATP) and incubated for 10 min at 21°C, and the reaction was stopped by mixing with 20 µl of 2× Laemmli buffer. Samples were fractionated by 12% SDS-PAGE, dried, and autoradiographed. For the in vitro kinase assay of recombinant xCtIP with Cdk1–cyclin B, 30 nM recombinant xCtIP was mixed with 6 nM recombinant Cdk1–cyclin B complex in a 20-µl reaction containing 10 µM PKI peptide, 0.25 mM ATP, 0.5 µl γ-[^{32}P]ATP, 20 mM Hepes, pH 7.5, 5 mM EGTA, 10 mM $MgCl_2$, and 40 mM glycerol-2-phosphate. This reaction was incubated for 90 min at 21°C and then fractionated on 7% SDS-PAGE, dried, and autoradiographed.

Isolation of endogenous M-phase xCtIP

Monoclonal anti–human CtIP 11–1 supernatant was purified using protein A–Sepharose beads in a high salt buffer (Harlow and Lane, 1988) and dialyzed into 0.1 M sodium phosphate buffer, pH 7.4. 60 µg antibody was conjugated to 6 mg paramagnetic M270 epoxy beads (Invitrogen) in 1 M ammonium sulfate in 1 ml total volume overnight at 30°C. The beads were extensively washed, blocked in 5% BSA, and used to isolate endogenous xCtIP from 3.5 ml freshly prepared M-phase extract for 3 h at 4°C. The beads were extensively washed and eluted with 0.5 N aqueous ammonium hydroxide and 0.5 mM EDTA, snap frozen in liquid nitrogen, and sublimated overnight in SpeedVac, and the dried pellet was resuspended in alkylating sample buffer (2% SDS, 10% glycerol, 100 mM DTT, 100 mM Tris, pH 8.8, 500 mM iodoacetamide [dissolved in 200 mM ammonium bicarbonate], and 0.05% bromophenol blue), heated to 70°C for 10 min, boiled briefly, run on 7% Tris-acetate gel (NuPAGE), and stained by colloidal Coomassie.

Tandem mass spectrometry analysis of endogenous M-phase xCtIP

The gel section corresponding to the expected size of CtIP was excised and subjected to in-gel digestion with proteomic-grade trypsin (Promega). The resulting digestion products were cleaned with a STAGE (stop and go extraction) tip (Rappsilber et al., 2003) and loaded onto a home-packed reverse-phase C18 column (75-µm internal diameter). The peptides were separated using a linear gradient (0–42% acetonitrile and 0.5% acetic acid for 120 min at 150 nl/min) and directly sprayed into a mass spectrometer (LTQ Orbitrap; Thermo Fisher Scientific) for analysis. The repetitive analytical cycle incorporated a high resolution mass scan in the Orbitrap (resolution = 60,000) followed by tandem mass spectrometry scans in the ion trap of the 10 most intense peaks observed in each Orbitrap mass spectrum. The raw mass spectral files were converted into the mzXML format, and CtIP peptides were identified with the X!tandem engine (The Global Proteome Machine Organization; Craig and Beavis, 2004). The spectra of the putative phosphopeptides were verified manually.

BrdU-based resection assay

The crude cycling extract (cycloheximide free) was activated with calcium and then briefly clarified by centrifugation at 4°C for 5 min at 14,000 rpm

in a bench-top Eppendorf centrifuge. The extract was then incubated with 50 µM BrdU and 5,000 sperm nuclei per microliter for 60 min. Nocodazole was added to 12 µg/ml, and DNA was allowed to finish replication for an additional 2 h. Extract/nuclei were examined by fluorescence microscopy at intervals to monitor nuclear morphology and nuclear envelope breakdown. 30-µl samples were taken immediately before and at the indicated time points after addition of 0.05 U/µl PflMI restriction enzyme. DNA was isolated from the samples by proteinase K digestion for 30 min at 50°C, phenol/chloroform extraction, and ethanol precipitation. 50 µg DNA was spotted onto N+ charged nylon membranes (GE Healthcare), baked for 2 h at 60°C, and processed for Western blotting using the anti-BrdU antibody (B35128; Invitrogen). Immunodepletion requires clarified extract (microcentrifuge at 14,000 rpm for 5 min), which caused inefficient entry into mitosis and nuclear envelope breakdown (also see note under Extract and sperm chromatin preparation). To overcome this, recombinant Cdk1–cyclin B was added to 150 nM to force entry into mitosis at 3 h. 1 h later, samples were taken before and at the time points after PflMI addition.

Online supplemental material

Fig. S1 shows CtIP immunodepletion and recombinant protein purification. Fig. S2 shows that DSBs are generated in M-phase chromatin, and CtIP is rate limiting for their resection. Fig. S3 shows BrdU-based physical resection assay. Fig. S4 shows purification and assay of recombinant CtIP-T808A and -T806E. Fig. S5 shows endogenous and recombinant Cdk1–cyclin B kinase activity. Online supplemental material is available at http://www.jcb.org/cgi/content/full/jcb.201103103/DC1.

We gratefully acknowledge Dr. Theresa Swayne of the Herbert Irving Comprehensive Cancer Center Microscopy Shared Resource Center for assistance with UV laser microirradiation experiments. We thank Dr. Rebecca Burgess and Dr. Lorraine Symington for critical reading of the manuscript. We thank Drs. W. Dunphy, H. Yan, and K. Maeshima for antibodies.

This work was supported by grants RO1CA092245 and RO1GM077495 to J. Gautier and RR00862 and RR022220 to B.T. Chait.

Submitted: 18 March 2011
Accepted: 2 August 2011

References

Anantha, R.W., E. Sokolova, and J.A. Borowiec. 2008. RPA phosphorylation facilitates mitotic exit in response to mitotic DNA damage. *Proc. Natl. Acad. Sci. USA*. 105:12903–12908. doi:10.1073/pnas.0803001105

Ayoub, N., E. Rajendra, X. Su, A.D. Jeyasekharan, R. Mahen, and A.R. Venkitaraman. 2009. The carboxyl terminus of Brca2 links the disassembly of Rad51 complexes to mitotic entry. *Curr. Biol.* 19:1075–1085. doi:10.1016/j.cub.2009.05.057

Blow, J.J., and R.A. Laskey. 1986. Initiation of DNA replication in nuclei and purified DNA by a cell-free extract of *Xenopus* eggs. *Cell*. 47:577–587. doi:10.1016/0092-8674(86)90622-7

Bolderson, E., N. Tomimatsu, D.J. Richard, D. Boucher, R. Kumar, T.K. Pandita, S. Burma, and K.K. Khanna. 2010. Phosphorylation of Exo1 modulates homologous recombination repair of DNA double-strand breaks. *Nucleic Acids Res.* 38:1821–1831. doi:10.1093/nar/gkp1164

Bresnahan, W.A., I. Boldogh, P. Chi, E.A. Thompson, and T. Albrecht. 1997. Inhibition of cellular Cdk2 activity blocks human cytomegalovirus replication. *Virology*. 231:239–247. doi:10.1006/viro.1997.8489

Budd, M.E., and J.L. Campbell. 2009. Interplay of Mre11 nuclease with Dna2 plus Sgs1 in Rad51-dependent recombinational repair. *PLoS ONE*. 4:e4267. doi:10.1371/journal.pone.0004267

Cejka, P., E. Cannavo, P. Polaczek, T. Masuda-Sasa, S. Pokharel, J.L. Campbell, and S.C. Kowalczykowski. 2010. DNA end resection by Dna2-Sgs1-RPA and its stimulation by Top3-Rmi1 and Mre11-Rad50-Xrs2. *Nature*. 467:112–116. doi:10.1038/nature09355

Chan, K.L., T. Palmai-Pallag, S. Ying, and I.D. Hickson. 2009. Replication stress induces sister-chromatid bridging at fragile site loci in mitosis. *Nat. Cell Biol.* 11:753–760. doi:10.1038/ncb1882

Chen, L., C.J. Nievera, A.Y. Lee, and X. Wu. 2008. Cell cycle-dependent complex formation of BRCA1.CtIP.MRN is important for DNA double-strand break repair. *J. Biol. Chem.* 283:7713–7720. doi:10.1074/jbc.M710245200

Chen, P.L., F. Liu, S. Cai, X. Lin, A. Li, Y. Chen, B. Gu, E.Y. Lee, and W.H. Lee. 2005. Inactivation of CtIP leads to early embryonic lethality mediated by G1 restraint and to tumorigenesis by haploid insufficiency. *Mol. Cell. Biol.* 25:3535–3542. doi:10.1128/MCB.25.9.3535-3542.2005

Costanzo, V., and J. Gautier. 2003. Single-strand DNA gaps trigger an ATR- and Cdc7-dependent checkpoint. *Cell Cycle*. 2:17. doi:10.4161/cc.2.1.290

Costanzo, V., K. Robertson, C.Y. Ying, E. Kim, E. Avvedimento, M. Gottesman, D. Grieco, and J. Gautier. 2000. Reconstitution of an ATM-dependent checkpoint that inhibits chromosomal DNA replication following DNA damage. *Mol. Cell*. 6:649–659. doi:10.1016/S1097-2765(00)00063-0

Costanzo, V., K. Robertson, M. Bibikova, E. Kim, D. Grieco, M. Gottesman, D. Carroll, and J. Gautier. 2001. Mre11 protein complex prevents double-strand break accumulation during chromosomal DNA replication. *Mol. Cell*. 8:137–147. doi:10.1016/S1097-2765(01)00294-5

Costanzo, V., D. Shechter, P.J. Lupardus, K.A. Cimprich, M. Gottesman, and J. Gautier. 2003. An ATR- and Cdc7-dependent DNA damage checkpoint that inhibits initiation of DNA replication. *Mol. Cell*. 11:203–213. doi:10.1016/S1097-2765(02)00799-2

Craig, R., and R.C. Beavis. 2004. TANDEM: matching proteins with tandem mass spectra. *Bioinformatics*. 20:1466–1467. doi:10.1093/bioinformatics/bth092

Di Virgilio, M., and J. Gautier. 2005. Repair of double-strand breaks by nonhomologous end joining in the absence of Mre11. *J. Cell Biol.* 171:765–771. doi:10.1083/jcb.200506029

Dupré, A., L. Boyer-Chatenet, and J. Gautier. 2006. Two-step activation of ATM by DNA and the Mre11-Rad50-Nbs1 complex. *Nat. Struct. Mol. Biol.* 13:451–457. doi:10.1038/nsmb1090

Dupré, A., L. Boyer-Chatenet, R.M. Sattler, A.P. Modi, J.H. Lee, M.L. Nicolette, L. Kopelovich, M. Jasin, R. Baer, T.T. Paull, and J. Gautier. 2008. A forward chemical genetic screen reveals an inhibitor of the Mre11-Rad50-Nbs1 complex. *Nat. Chem. Biol.* 4:119–125. doi:10.1038/nchembio.63

Esashi, F., N. Christ, J. Gannon, Y. Liu, T. Hunt, M. Jasin, and S.C. West. 2005. CDK-dependent phosphorylation of BRCA2 as a regulatory mechanism for recombinational repair. *Nature*. 434:598–604. doi:10.1038/nature03404

Esashi, F., V.E. Galkin, X. Yu, E.H. Egelman, and S.C. West. 2007. Stabilization of RAD51 nucleoprotein filaments by the C-terminal region of BRCA2. *Nat. Struct. Mol. Biol.* 14:468–474. doi:10.1038/nsmb1245

Gautier, J., T. Matsukawa, P. Nurse, and J. Maller. 1989. Dephosphorylation and activation of *Xenopus* p34cdc2 protein kinase during the cell cycle. *Nature*. 339:626–629. doi:10.1038/339626a0

Giunta, S., and S.P. Jackson. 2011. Give me a break, but not in mitosis: the mitotic DNA damage response marks DNA double-strand breaks with early signaling events. *Cell Cycle*. 10:1215–1221. doi:10.4161/cc.10.8.15334

Giunta, S., R. Belotserkovskaya, and S.P. Jackson. 2010. DNA damage signaling in response to double-strand breaks during mitosis. *J. Cell Biol.* 190:197–207. doi:10.1083/jcb.200911156

Gravel, S., J.R. Chapman, C. Magill, and S.P. Jackson. 2008. DNA helicases Sgs1 and BLM promote DNA double-strand break resection. *Genes Dev.* 22:2767–2772. doi:10.1101/gad.503108

Greenberg, R.A., B. Sobhian, S. Pathania, S.B. Cantor, Y. Nakatani, and D.M. Livingston. 2006. Multifactorial contributions to an acute DNA damage response by BRCA1/BARD1-containing complexes. *Genes Dev.* 20:34–46. doi:10.1101/gad.1381306

Harlow, E., and D. Lane. 1988. Antibodies: A Laboratory Manual. Cold Spring Harbor Laboratory, Cold Spring Harbor, NY. 726 pp.

Hartsuiker, E., M.J. Neale, and A.M. Carr. 2009. Distinct requirements for the Rad32(Mre11) nuclease and Ctp1(CtIP) in the removal of covalently bound topoisomerase I and II from DNA. *Mol. Cell*. 33:117–123. doi:10.1016/j.molcel.2008.11.021

Huertas, P., and S.P. Jackson. 2009. Human CtIP mediates cell cycle control of DNA end resection and double strand break repair. *J. Biol. Chem.* 284:9558–9565. doi:10.1074/jbc.M808906200

Huertas, P., F. Cortés-Ledesma, A.A. Sartori, A. Aguilera, and S.P. Jackson. 2008. CDK targets Sae2 to control DNA-end resection and homologous recombination. *Nature*. 455:689–692. doi:10.1038/nature07215

Hutchison, C.J., R. Cox, and C.C. Ford. 1988. The control of DNA replication in a cell-free extract that recapitulates a basic cell cycle in vitro. *Development*. 103:553–566.

Iwai, M., A. Hara, T. Andoh, and R. Ishida. 1997. ICRF-193, a catalytic inhibitor of DNA topoisomerase II, delays the cell cycle progression from metaphase, but not from anaphase to the G1 phase in mammalian cells. *FEBS Lett.* 406:267–270. doi:10.1016/S0014-5793(97)00282-2

Jazayeri, A., A. Balestrini, E. Garner, J.E. Haber, and V. Costanzo. 2008. Mre11-Rad50-Nbs1-dependent processing of DNA breaks generates oligonucleotides that stimulate ATM activity. *EMBO J.* 27:1953–1962. doi:10.1038/emboj.2008.128

Karlsson-Rosenthal, C., and J.B. Millar. 2006. Cdc25: mechanisms of checkpoint inhibition and recovery. *Trends Cell Biol.* 16:285–292. doi:10.1016/j.tcb.2006.04.002

Keeney, S., and N. Kleckner. 1995. Covalent protein-DNA complexes at the 5′ strand termini of meiosis-specific double-strand breaks in yeast. *Proc. Natl. Acad. Sci. USA*. 92:11274–11278. doi:10.1073/pnas.92.24.11274

Kubota, Y., and H. Takisawa. 1993. Determination of initiation of DNA replication before and after nuclear formation in *Xenopus* egg cell free extracts. *J. Cell Biol.* 123:1321–1331. doi:10.1083/jcb.123.6.1321

Lee, P.S., and T.D. Petes. 2010. From the Cover: mitotic gene conversion events induced in G1-synchronized yeast cells by gamma rays are similar to spontaneous conversion events. *Proc. Natl. Acad. Sci. USA*. 107:7383–7388. doi:10.1073/pnas.1001940107

Lee-Theilen, M., A.J. Matthews, D. Kelly, S. Zheng, and J. Chaudhuri. 2011. CtIP promotes microhomology-mediated alternative end joining during class-switch recombination. *Nat. Struct. Mol. Biol.* 18:75–79. doi:10.1038/nsmb.1942

Liao, S., T. Toczylowski, and H. Yan. 2008. Identification of the *Xenopus* DNA2 protein as a major nuclease for the 5′->3′ strand-specific processing of DNA ends. *Nucleic Acids Res.* 36:6091–6100. doi:10.1093/nar/gkn616

Limbo, O., C. Chahwan, Y. Yamada, R.A. de Bruin, C. Wittenberg, and P. Russell. 2007. Ctp1 is a cell-cycle-regulated protein that functions with Mre11 complex to control double-strand break repair by homologous recombination. *Mol. Cell*. 28:134–146. doi:10.1016/j.molcel.2007.09.009

Lisby, M., J.H. Barlow, R.C. Burgess, and R. Rothstein. 2004. Choreography of the DNA damage response: spatiotemporal relationships among checkpoint and repair proteins. *Cell*. 118:699–713. doi:10.1016/j.cell.2004.08.015

Lobachev, K., E. Vitriol, J. Stemple, M.A. Resnick, and K. Bloom. 2004. Chromosome fragmentation after induction of a double-strand break is an active process prevented by the RMX repair complex. *Curr. Biol.* 14:2107–2112. doi:10.1016/j.cub.2004.11.051

Löbrich, M., and P.A. Jeggo. 2007. The impact of a negligent G2/M checkpoint on genomic instability and cancer induction. *Nat. Rev. Cancer*. 7:861–869. doi:10.1038/nrc2248

Lukas, C., V. Savic, S. Bekker-Jensen, C. Doil, B. Neumann, R.S. Pedersen, M. Grøfte, K.L. Chan, I.D. Hickson, J. Bartek, and J. Lukas. 2011. 53BP1 nuclear bodies form around DNA lesions generated by mitotic transmission of chromosomes under replication stress. *Nat. Cell Biol.* 13:243–253. doi:10.1038/ncb2201

McGarry, T.J., and M.W. Kirschner. 1998. Geminin, an inhibitor of DNA replication, is degraded during mitosis. *Cell*. 93:1043–1053. doi:10.1016/S0092-8674(00)81209-X

Mikhailov, A., R.W. Cole, and C.L. Rieder. 2002. DNA damage during mitosis in human cells delays the metaphase/anaphase transition via the spindle-assembly checkpoint. *Curr. Biol.* 12:1797–1806. doi:10.1016/S0960-9822(02)01226-5

Mimitou, E.P., and L.S. Symington. 2008. Sae2, Exo1 and Sgs1 collaborate in DNA double-strand break processing. *Nature*. 455:770–774. doi:10.1038/nature07312

Mimitou, E.P., and L.S. Symington. 2009. DNA end resection: many nucleases make light work. *DNA Repair (Amst.)*. 8:983–995. doi:10.1016/j.dnarep.2009.04.017

Morrison, C., and C.L. Rieder. 2004. Chromosome damage and progression into and through mitosis in vertebrates. *DNA Repair (Amst.)*. 3:1133–1139. doi:10.1016/j.dnarep.2004.03.005

Murray, A.W. 1991. Cell cycle extracts. *Methods Cell Biol.* 36:581–605. doi:10.1016/S0091-679X(08)60298-8

Nakamura, A.J., V.A. Rao, Y. Pommier, and W.M. Bonner. 2010a. The complexity of phosphorylated H2AX foci formation and DNA repair assembly at DNA double-strand breaks. *Cell Cycle*. 9:389–397. doi:10.4161/cc.9.2.10475

Nakamura, K., T. Kogame, H. Oshiumi, A. Shinohara, Y. Sumitomo, K. Agama, Y. Pommier, K.M. Tsutsui, K. Tsutsui, E. Hartsuiker, et al. 2010b. Collaborative action of Brca1 and CtIP in elimination of covalent modifications from double-strand breaks to facilitate subsequent break repair. *PLoS Genet.* 6:e1000828. doi:10.1371/journal.pgen.1000828

Nimonkar, A.V., A.Z. Ozsoy, J. Genschel, P. Modrich, and S.C. Kowalczykowski. 2008. Human exonuclease 1 and BLM helicase interact to resect DNA and initiate DNA repair. *Proc. Natl. Acad. Sci. USA*. 105:16906–16911. doi:10.1073/pnas.0809380105

Nimonkar, A.V., J. Genschel, E. Kinoshita, P. Polaczek, J.L. Campbell, C. Wyman, P. Modrich, and S.C. Kowalczykowski. 2011. BLM-DNA2-RPA-MRN and EXO1-BLM-RPA-MRN constitute two DNA end resection machineries for human DNA break repair. *Genes Dev.* 25:350–362. doi:10.1101/gad.2003811

Niu, H., W.H. Chung, Z. Zhu, Y. Kwon, W. Zhao, P. Chi, R. Prakash, C. Seong, D. Liu, L. Lu, et al. 2010. Mechanism of the ATP-dependent DNA end-resection machinery from *Saccharomyces cerevisiae*. *Nature*. 467:108–111. doi:10.1038/nature09318

Oakley, G.G., S.M. Patrick, J. Yao, M.P. Carty, J.J. Turchi, and K. Dixon. 2003. RPA phosphorylation in mitosis alters DNA binding and protein-protein interactions. *Biochemistry*. 42:3255–3264. doi:10.1021/bi026377u

Okamoto, K., and N. Sagata. 2007. Mechanism for inactivation of the mitotic inhibitory kinase Wee1 at M phase. *Proc. Natl. Acad. Sci. USA*. 104:3753–3758. doi:10.1073/pnas.0607357104

Penkner, A., Z. Portik-Dobos, L. Tang, R. Schnabel, M. Novatchkova, V. Jantsch, and J. Loidl. 2007. A conserved function for a *Caenorhabditis elegans* Com1/Sae2/CtIP protein homolog in meiotic recombination. *EMBO J.* 26:5071–5082. doi:10.1038/sj.emboj.7601916

Rappsilber, J., Y. Ishihama, and M. Mann. 2003. Stop and go extraction tips for matrix-assisted laser desorption/ionization, nanoelectrospray, and LC/MS sample pretreatment in proteomics. *Anal. Chem.* 75:663–670. doi:10.1021/ac026117i

Rieder, C.L., and A. Khodjakov. 1997. Mitosis and checkpoints that control progression through mitosis in vertebrate somatic cells. *Prog. Cell Cycle Res.* 3:301–312. doi:10.1007/978-1-4615-5371-7_24

Shim, E.Y., W.H. Chung, M.L. Nicolette, Y. Zhang, M. Davis, Z. Zhu, T.T. Paull, G. Ira, and S.E. Lee. 2010. *Saccharomyces cerevisiae* Mre11/Rad50/Xrs2 and Ku proteins regulate association of Exo1 and Dna2 with DNA breaks. *EMBO J.* 29:3370–3380. doi:10.1038/emboj.2010.219

Shrivastav, M., L.P. De Haro, and J.A. Nickoloff. 2008. Regulation of DNA double-strand break repair pathway choice. *Cell Res.* 18:134–147. doi:10.1038/cr.2007.111

Smith, E., D. Dejsuphong, A. Balestrini, M. Hampel, C. Lenz, S. Takeda, A. Vindigni, and V. Costanzo. 2009. An ATM- and ATR-dependent checkpoint inactivates spindle assembly by targeting CEP63. *Nat. Cell Biol.* 11:278–285. doi:10.1038/ncb1835

Smythe, C., and J.W. Newport. 1991. Systems for the study of nuclear assembly, DNA replication, and nuclear breakdown in *Xenopus laevis* egg extracts. *Methods Cell Biol.* 35:449–468. doi:10.1016/S0091-679X(08)60583-X

Stephan, H., C. Concannon, E. Kremmer, M.P. Carty, and H.P. Nasheuer. 2009. Ionizing radiation-dependent and independent phosphorylation of the 32-kDa subunit of replication protein A during mitosis. *Nucleic Acids Res.* 37:6028–6041. doi:10.1093/nar/gkp605

Symington, L.S. 2002. Role of RAD52 epistasis group genes in homologous recombination and double-strand break repair. *Microbiol. Mol. Biol. Rev.* 66:630–670. doi:10.1128/MMBR.66.4.630-670.2002

Toczylowski, T., and H. Yan. 2006. Mechanistic analysis of a DNA end processing pathway mediated by the *Xenopus* Werner syndrome protein. *J. Biol. Chem.* 281:33198–33205. doi:10.1074/jbc.M605044200

Trenz, K., A. Errico, and V. Costanzo. 2008. Plx1 is required for chromosomal DNA replication under stressful conditions. *EMBO J.* 27:876–885. doi:10.1038/emboj.2008.29

Varma, A.K., R.S. Brown, G. Birrane, and J.A. Ladias. 2005. Structural basis for cell cycle checkpoint control by the BRCA1-CtIP complex. *Biochemistry*. 44:10941–10946. doi:10.1021/bi0509651

Vassilev, L.T., C. Tovar, S. Chen, D. Knezevic, X. Zhao, H. Sun, D.C. Heimbrook, and L. Chen. 2006. Selective small-molecule inhibitor reveals critical mitotic functions of human CDK1. *Proc. Natl. Acad. Sci. USA*. 103:10660–10665. doi:10.1073/pnas.0600447103

Verde, F., J.C. Labbé, M. Dorée, and E. Karsenti. 1990. Regulation of microtubule dynamics by cdc2 protein kinase in cell-free extracts of *Xenopus* eggs. *Nature*. 343:233–238. doi:10.1038/343233a0

Yan, H., J. McCane, T. Toczylowski, and C. Chen. 2005. Analysis of the *Xenopus* Werner syndrome protein in DNA double-strand break repair. *J. Cell Biol.* 171:217–227. doi:10.1083/jcb.200502077

Yoo, H.Y., S.Y. Jeong, and W.G. Dunphy. 2006. Site-specific phosphorylation of a checkpoint mediator protein controls its responses to different DNA structures. *Genes Dev.* 20:772–783. doi:10.1101/gad.1398806

You, Z., J.M. Bailis, S.A. Johnson, S.M. Dilworth, and T. Hunter. 2007. Rapid activation of ATM on DNA flanking double-strand breaks. *Nat. Cell Biol.* 9:1311–1318. doi:10.1038/ncb1651

You, Z., L.Z. Shi, Q. Zhu, P. Wu, Y.W. Zhang, A. Basilio, N. Tonnu, I.M. Verma, M.W. Berns, and T. Hunter. 2009. CtIP links DNA double-strand break sensing to resection. *Mol. Cell*. 36:954–969. doi:10.1016/j.molcel.2009.12.002

Yu, X., and R. Baer. 2000. Nuclear localization and cell cycle-specific expression of CtIP, a protein that associates with the BRCA1 tumor suppressor. *J. Biol. Chem.* 275:18541–18549. doi:10.1074/jbc.M909494199

Yu, X., and J. Chen. 2004. DNA damage-induced cell cycle checkpoint control requires CtIP, a phosphorylation-dependent binding partner of BRCA1 C-terminal domains. *Mol. Cell. Biol.* 24:9478–9486. doi:10.1128/MCB.24.21.9478-9486.2004

Yun, M.H., and K. Hiom. 2009. CtIP-BRCA1 modulates the choice of DNA double-strand-break repair pathway throughout the cell cycle. *Nature*. 459:460–463. doi:10.1038/nature07955

Zhang, Y., and M. Jasin. 2011. An essential role for CtIP in chromosomal translocation formation through an alternative end-joining pathway. *Nat. Struct. Mol. Biol.* 18:80–84. doi:10.1038/nsmb.1940

Zhang, Y., M. Gostissa, D.G. Hildebrand, M.S. Becker, C. Boboila, R. Chiarle, S. Lewis, and F.W. Alt. 2010. The role of mechanistic factors in promoting chromosomal translocations found in lymphoid and other cancers. *Adv. Immunol.* 106:93–133. doi:10.1016/S0065-2776(10)06004-9

Zhu, Z., W.H. Chung, E.Y. Shim, S.E. Lee, and G. Ira. 2008. Sgs1 helicase and two nucleases Dna2 and Exo1 resect DNA double-strand break ends. *Cell*. 134:981–994. doi:10.1016/j.cell.2008.08.037

Zirkle, R.E., and W. Bloom. 1953. Irradiation of parts of individual cells. *Science*. 117:487–493. doi:10.1126/science.117.3045.487

Zou, L., and S.J. Elledge. 2003. Sensing DNA damage through ATRIP recognition of RPA-ssDNA complexes. *Science*. 300:1542–1548. doi:10.1126/science.1083430